UNIVERSIDADE DA BEIRA INTERIOR

Ciências

Improvement of STEAP 1 Biosynthesis from *Pichia pastoris* X33 cells under an optimized feeding strategy

Diana Rute Tavares Duarte

Dissertação para obtenção do Grau de Mestre em

Biotecnologia

(2º ciclo de estudos)

Orientador: Prof. Doutor Luís António Paulino Passarinha
Coorientador: Prof. Doutor Cláudio Jorge Maia Baptista

Covilhã, outubro de 2017

Acknowledgments

Firstly, I would like to make special thanks to my supervisors, Professor Luís Passarinha and Professor Claúdio Maia for the opportunity to let me develop this work, for helping and guiding me through this year.

To my colleagues and friends at CICS, the biggest thanks for all the patience, friendship, laughs, support, and encouragement. Special thanks to Margarida Gonçalves, Fátima Santos, and Augusto Pedro for the biggest help, companionship, and teachings during the past year.

To my friends that have always been with me and believe in me. I thank you for your friendship and kind words that make me forget a bad day and give me hope in the future.

My forever thankfulness goes to my dad and my little brother Ivo, for your support, love and believing. To my mom special thanks, I hope that you are proud of me. I can never repay what you have done for me.

Resumo

O cancro da próstata é uma das patologias com maior incidência em todo o mundo. Atualmente, os meios de diagnóstico e terapêuticos existentes são invasivos e apresentam uma eficácia limitada sobretudo em estágios mais avançados da doença. Desta forma, torna-se necessário o estudo de proteínas específicas cuja expressão esteja relacionada com o seu desenvolvimento e progressão. Diversos estudos têm sugerido a proteína Six-transmembrane Epithelial Antigen of the Prostate 1 (STEAP1) como um possível biomarcador e/ou alvo imunoterapêutico para o cancro da próstata. A STEAP1 é constituída por 6 domínios transmembranares e encontra-se presente na membrana plasmática das células epiteliais, nomeadamente nas junções que promovem a comunicação célula-célula. Alguns estudos suportam a hipótese que a STEAP 1 assume um papel preponderante na comunicação entre células tumorais, estando desta forma envolvida na progressão do cancro. No entanto, estudos complementares são ainda necessários para resolver a sua estrutura tridimensional de forma a melhor compreender as suas funções na carcinogénese assim como delinear novas estratégias terapêuticas. Deste modo, elevadas quantidades de STEAP1 são requeridas a partir de tecnologias emergentes de DNA recombinante. Nestes domínios, a levedura *Pichia pastoris* tem-se revelado um hospedeiro adequado na expressão de proteínas recombinantes. Em particular, a sua capacidade para realizar modificações pós-tradução torna-a num sistema microbiano ideal para a produção recombinante de proteínas membranares. Assim, os principais objetivos do presente trabalho são: 1) Aumentar a escala de produção da proteína STEAP1 para bioreator em culturas de *Pichia pastoris* X33 testando diferentes feeds de glicerol e metanol; 2) Avaliar a adição de diferentes chaperones químicos que contribuam para a estabilização conformacional da STEAP1; 3) Estudar a influência dos diferentes feeds de glicerol em eventuais processos de *N*-glicosilação. Os resultados obtidos demonstraram que - através um feed por gradiente de glicerol e constante de metanol - houve um aumento da produção de STEAP1, para cerca do dobro, aquando a suplementação do meio com 1M de Prolina. Observa-se que na aplicação de um feed exponencial de glicerol e constante de metanol, a quantidade de STEAP1 produzida encontra-se no peso molecular correto (~35kDa), embora se tivesse verificado níveis de produção reduzidos. Adicionalmente, denotou-se através da digestão dos lisados com a enzima PNGase F que um feed constante de glicerol e metanol parece produzir STEAP1 com *N*-glicosilação. Como trabalho futuro serão desenvolvidas estratégias de purificação da proteína STEAP1.

Palavras-chave:

Biossíntese, Cancro da próstata, *Pichia pastoris*, Proteínas recombinantes, STEAP1.

Resumo alargado

O cancro da próstata é uma das patologias com maior incidência nas sociedades modernas, principalmente em homens com idade superior a 50 anos. Os meios de diagnóstico e de terapia existentes são invasivos e com eficácia limitada. Assim, é necessário encontrar e estudar genes específicos que codifiquem proteínas específicas neste grupo de patologias. Ao longo dos últimos anos, inúmeras biomoléculas têm sido identificadas como biomarcadores para o cancro da próstata, dos quais a proteína Six-transmembrane epithelial antigen of the prostate 1 (STEAP1). Esta encontra-se maioritariamente presente na membrana plasmática das células epiteliais, nomeadamente nas junções que promovem a comunicação célula-célula. É constituída por seis domínios transmembranares interligados por três loops extracelulares e 2 intracelulares. De acordo com a literatura, é sugerido o seu papel na comunicação entre células tumorais, estando envolvida em processos de carcinogénese e invasão tumoral. No entanto, estudos adicionais são necessários para resolver a sua estrutura 3D de forma a compreender o papel da STEAP1 no desenvolvimento e progressão tumoral assim como desenvolver moléculas terapêuticas que diminuam a sua função oncogénica. De uma forma geral para a realização de estudos cristalográficos são requeridas elevadas quantidades de proteína alvo. Nas últimas décadas a tecnologia de DNA recombinante emergiu e otimizou exponencialmente a obtenção de níveis de expressão, consideráveis, de proteínas membranares para o desenvolvimento de estudos de bio-interação e estruturais. Neste domínio cientifico, a levedura Pichia pastoris tem-se revelado o hospedeiro ideal na expressão recombinante de proteínas membranares, destacando-se a sua capacidade de realizar modificações pós-tradução similares às identificadas em eucariotas superiores. Assim, os principais objetivos do presente trabalho são: 1) Aumentar a escala de produção da proteína STEAP1 em biorreator com culturas de Pichia pastoris X33 testando diferentes feeds de glicerol e metanol; 2) Avaliar a adição de diferentes chaperones químicos que contribuam para a estabilização conformacional da STEAP1; 3) Estudar a influência dos diferentes feeds de glicerol em eventuais processos de *N*-glicosilação. Relativamente à estratégia desenvolvida, o processo fermentativo compreendeu três fases: o batch em glicerol, fed-batch (2 horas de feed de glicerol e 1 hora de mistura glicerol/metanol) e por último a etapa de indução com metanol. Tendo como primeiro objetivo o incremento da biossíntese recombinante da proteína STEAP1 foram testados diferentes feeds de glicerol e metanol, durante a fase de fed-batch e de indução, respetivamente. Especificamente, analisaram-se três feeds de glicerol distintos - constante, gradiente e exponencial - e dois feeds de metanol - constante e exponencial. As concentrações de glicerol e metanol no meio extracelular foram quantificadas ao longo do processo fermentativo por HPLC com um índice de refração acoplado. Devido à existência de dímeros e/ou bandas de maior peso molecular em análises efetuadas por Western blot (WB), comparando a densitometria das bandas, usou-se a enzima PNGase F para compreender se as alterações de peso molecular observadas seriam

devido a diferentes padrões de *N*-glicosilação da proteína em estudo. Deste modo, obteve-se para um feed constante de glicerol e metanol um pico de produção de STEAP1 às 2 horas de indução, sendo produzida com um peso molecular superior (~48KDa). A realização de ensaios complementares com a enzima PNGase F demonstraram que as diferenças no peso molecular podem estar relacionadas com a existência de *N*-glicosilações na estrutura 3D da biomolécula alvo. Relativamente ao feed de glicerol por gradiente e constante de metanol obteve-se um pico de produção às 10 horas de indução. No entanto, por WB denotou-se a existência de bandas com elevado peso molecular (~63 kDa), sugerindo a formação de agregados proteicos: dímeros. Consequentemente, testaram-se diferentes concentrações de prolina (0,2, 0,5 e 1M), trealose (0,1, 0,25 e 0,5 M) e histidina (0,04 e 0,08 mg/mL) no meio de cultura, de forma a avaliar se as moléculas adicionadas poderiam funcionar como chaperones químicos, promovendo a consequente estabilização da STEAP1 durante a sua expressão e diminuindo a concentração de dímeros. Os resultados obtidos demonstraram que - através um feed por gradiente de glicerol e constante de metanol - houve um aumento da produção da STEAP1, para cerca do dobro, aquando a suplementação do meio com 1M de Prolina. Do tratamento dos lisados obtidos, nesta estratégia com a enzima PNGase F, observa-se que não há alteração nos padrões de glicosilação, mesmo para diferentes concentrações de enzima durante os vários tempos de reação testados. Para complemento dos resultados obtidos, efetuaram-se ensaios adicionais por eletroforese bidimensional, de forma a averiguar se os diferentes padrões de *N*-glicosilação conduzem a uma alteração do ponto isoelétrico da STEAP1 (pI teórico ~ 9,28). Os resultados obtidos reforçam que os dímeros de STEAP1 formados durante o feed de glicerol por gradiente e constante de metanol, podem não estar relacionados com interações que originem modificações pós-tradução. Adicionalmente, denota-se que a aplicação do feed exponencial de glicerol e constante de metanol, embora decresça a quantidade de STEAP1 obtida, toda a proteína produzida encontra-se no peso molecular correto e descrito na literatura (~35kDa). Observou-se também que os níveis de metanol (< 8.3 g/L nas primeiras horas de indução) e glicerol (entre 0.7- 7.0 g/L) permanecem em níveis tolerantes e inócuos para as culturas de P. pastoris, não impedindo desta forma a expressão da STEAP1. Finalmente foi ainda testado um feed exponencial de metanol durante a etapa de indução tendo por base os feed exponencial e gradiente de glicerol anteriormente referenciados. Com a estratégia descrita obteve-se um incremento basal na biossíntese da STEAP1, prevalecendo a formação de dímeros e degradações de baixo peso molecular. Concluindo, foi otimizada com sucesso uma nova estratégia que visa ao aumento da biossíntese da proteína STEAP1 de forma recombinante em biorreactor. Este incremento foi alcançado pela combinação de diferentes perfis de alimentação de fonte de carbono e de indutor com o uso de diferentes chaperones químicos. Em suma, a estratégia ideal é através da aplicação de um feed de glicerol por gradiente combinado um feed constante de metanol durante 10 horas e suplementado com 1M de Prolina. Como trabalho futuro serão desenvolvidas novas estratégias de purificação da proteína STEAP1.

Abstract

Prostate cancer (PCa) is the most common type of cancer in aged men. Actually, the main problem arises from the fact that both PCa diagnosis and therapy are still invasive and limited in advanced stages of this disease. Thus, it is necessary to identify, study and characterize specific proteins whose expression correlates with these pathologies. Concerning this, it has been suggested that the Six-transmembrane epithelial antigen of the prostate 1 (STEAP1) protein as a good biomarker and/or immunotherapeutic target for PCa. It is located in the plasma membrane of epithelial cells, in both tight and gap junctions. STEAP1 is composed of six transmembrane domains, connected by three extracellular and two intracellular loops. Therefore, it has been suggested that this protein plays an important role in intracellular communication between cancer cells, contributing to the cancer process and tumor invasiveness. The characterization of STEAP1 structure and function might allow the development of specific inhibitors, envisaging a decrease of its oncogenic role. However, the techniques used for protein structural and functional characterization demand for high quantities of the target protein, which may be achieved through the recombinant DNA technology. Therefore, the aim of this work was to improve STEAP1 biosynthesis from mini-bioreactor *Pichia pastoris* X33 methanol induced cultures. This was achieved through the study of different glycerol and methanol feeding profiles during the fed-batch phases. Briefly, the medium supplementation with Proline 1M in a gradient glycerol and constant methanol feed, leads to high quantities of STEAP1 (increase for the double). An exponential glycerol and constant methanol feed produces fewer amounts of the protein but in the correct molecular weight (~35kDa). The influence of the fermentation conditions on STEAP1 molecular weight and *N*-glycosylation was studied using the enzyme PNGase F. The results showed that a constant glycerol feed seems to produce STEAP1 with *N*-glycosylation. However, the dimers produced in the gradient glycerol feed are not due *N*-glycosylation process. Two-dimensional electrophoresis proves this, and it was demonstrated that they correspond to different *N*-glycosylation patterns. Overall, it was successfully optimized a new strategy for recombinant STEAP1 biosynthesis, through the study of different feeding profiles. Future work encompassing will be developed an alternative strategy to perform the purification on the target protein.

Keywords:

Biosynthesis, Prostate cancer, *Pichia pastoris, Recombinant proteins,* STEAP1.

Table of Contents

List of Figures

List of Tables

List of Acronyms

2-DE	Two-dimensional electrophoresis
μ	Specific growth rate (h^{-1})
AOX1	Alcohol Oxidase
AR	Androgen Receptor
BMGH	Buffered Minimal Medium Containing Glycerol
BSA	Bovine Serum Albumin
BSM	Basal Salt Medium
DMSO	Dimethyl Sulfoxide
DO	Dissolved oxygen
DTT	Dithiothreitol
E. coli	*Escherichia coli*
HPLC	High-performance liquid chromatography
OD_{600nm}	Optical Density at 600nm
PCa	Prostate Cancer
pI	Isoelectric point
PIA	Proliferative Inflammatory Atrophy
P. pastoris	*Pichia pastoris* X33
PSA	Prostate Specific Antigen
SDS	Sodium Dodecyl Sulphate
SDS-PAGE	Sodium dodecyl sulphate-polyacrylamide gel electrophoresis
STEAP	Six-Transmembrane epithelial antigen of the prostate
WB	Western Blot
YNB	Yeast Nitrogen Base

Work presented in this thesis has resulted in:

Oral communication in the XII Annual CICS-UBI Symposium, Covilhã (2017): **Duarte DR**, Pedro AQ, Maia CJ, Passarinha LA, Improvement of STEAP1 biosynthesis from mini-bioreactors *Pichia pastoris* X33 cultures.

Poster presentation at the II International Congress on Health Sciences Research towards Innovation and entrepreneurship: Trends in Biotechnology for Biomedical Application, Covilhã (2017): **Duarte DR**, Pedro AQ, Maia CJ, Passarinha LA, Improvement of STEAP1 biosynthesis from *Pichia Pastoris* X33 cells under an optimized strategy.

Poster presentation at the 9th Conference on Recombinant Protein Production, Croatia (2017): Barroca-Ferreira J, Pais JP, Santos MM, **Duarte DR**, Pedro AQ, Maia CJ, Passarinha LA, Evaluation of *Escherichia coli* and *Pichia pastoris* host in the biosynthesis of STEAP1: a membrane therapeutic target for prostate cancer.

Chapter I – Introduction

1. Human Prostate

1.1. Anatomy and Physiology

The prostate is the main gland in male reproductive and urinary system. It is oval shaped with a rounded tip. The size varies from man to man, but generally, it has approximately 4 cm wide and 3 cm thickness. It possesses two lobes that bring urine from the bladder, through the prostate, to the penis. The main function is the production of the fluid that protects and nourish the sperm in the semen [1–3]. It is composed of two main compartments, the stroma and the epithelium. Both structures influence each other reciprocally via different signaling pathways to the normal prostate development and homeostasis. According to the general anatomical and microscopical structure of the prostate depicted in Figure 1, the prostate gland is covered by a layer of connective tissue called the prostatic capsule. Anatomically, it is composed of three main zones: the central, the transition, and the peripheral zone [2,4]. The peripheral zone is the predominant zone, comprising almost 70% of glandular tissue and covers the posterior and lateral features of the gland. This peripheral zone is the most associated with adenocarcinoma development. The transition and the central zone accounts for 5-10% and 20-25% of the total glandular tissue, respectively. The transition zone has an important clinical significance once it is the main region where benign prostatic hyperplasia (BPH) are diagnosed [1,2].

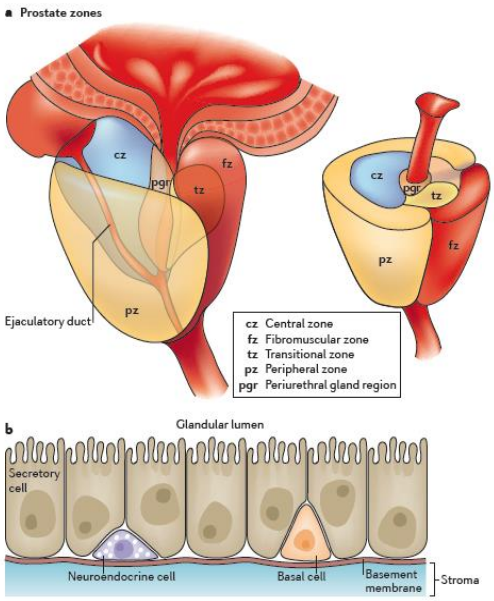

Figure 1. General anatomical and microscopical structure of the prostate, from [1,2].

In relation to the microscopic structure, the prostate is composed by a glandular epithelium embedded in a fibromuscular stroma. The main function of the stromal compartment is to maintain the correct microenvironment of the epithelial cells. Also, it helps to maintain or restore the homeostasis of the prostate [1,5,6]. The epithelial compartment has the main glandular function, once it secrets the prostatic fluid that contributes to the most volume of the entire ejaculate. Some factors control the ejaculation and regulate the proteins involved in sperm maturation, they have mechanistically and functionally linked to each other. The accumulation of zinc (Zn^{2+}) and citrate play an important physiological role in prostate. Also, the loss of this ability may be related to the development and progression of prostate malignancy [5,7–9].The epithelium is divided into several types of cells such as columnar luminal, basal, and neuroendocrine cells. The main function of the columnar cells is the production of prostatic secretions. These cells express high levels of androgen receptors (AR) and require androgens for its survival and secretory activity. On the other hand, the basal cells are undifferentiated cells, with a distinct morphology, that can originate all types of epithelial cells. Their differentiation and growth only occur in the presence of androgens, despite its survival and maintenance are androgen independent [1,4,10,11]. The neuroendocrine cells have regulatory functions that seem to be involved in the proliferation of adjacent cells. They produce neuropeptides such as, chromogranin A (Cg A), neuron-specific enolase (NSE), somatostatin or calcitonin, which has been described as biological markers for cancer [12,13].

Prostate development and function are dependent on AR signaling, particularly from 5α-dihydrotestosterone (DHT). The intracellular reduction of testosterone into DHT by 5- α-reductase in the prostatic epithelium is necessary to complete prostate morphogenesis. After the development of the prostate, androgens are involved in the survival promotion of the secretory epithelium. Besides that, it is described that the AR is differentially expressed in the stroma and epithelium compartments, with a paracrine and autocrine control, respectively. Alterations in these pathways may promote tumorigenesis [5,11,14].

1.2. Prostate Cancer

Carcinogenesis is a process characterized by changes in the cellular phenotype of some cells, that are based on genome changes [15,16]. Typically, the cancer cells have the ability to grow into several environments and fail the response to the usual controls on such proliferation. Contrary to normal cells, cancer cells replication is not limited beyond the limits imposed by telomere length [16,17].

They also present the ability to stimulate new blood vessel formation, thus ensuring the oxygen and nutrients required for their survival and proliferation. Also promote angiogenesis, vessel co-option, and vascular mimicry to create an extracellular matrix rich in growth factors with a

specific pH that makes difficult the anticancer-drug proliferation [16–19]. Moreover, the cancer cells display specific characteristics, namely: unlimited proliferation, self-sufficiency in growth signals, resistance to antiproliferative and apoptotic stimuli, tissue invasion and metastasis [15,20]. Typically, the cancer environment is composed of stromal cells, acting as support cells for the tumor itself, which is responsible to attract new blood vessels to bring nutrients and oxygen, invade detection, and metastasizing to distal organs. The major problem in the currently available treatments is the lack of specificity of the drugs, once they should present a large therapeutic window to kill tumor cells while sparing normal cells [20,21].

From all the cancers studied in the literature, this work will focus on the prostate cancer (PCa). Concerning this, the PCa is one of the most frequently diagnosed cancer, more than 3.3 million men living with this pathology in the United States. It is the second leading cause of male cancer-related death in North America and the third one in Portugal [22–25]. The PCa incidence in Portugal has been increasing since 1998, and it was the most frequent cancer among men in 2009, with 5433 new cases. It is predicted the existence of new 8600 incident cases and 1700 deaths caused by PCa in 2020 [26].

Typically, it tends to develop in older men, aged 50 and over. In many clinical cases, PCa develops slowly, although in some patients it can be aggressive and metastasize to other parts of the body. The risk factors associated with the appearance of PCa include aging and ethnicity, family history and genetic factors, diet and lifestyle, hormonal levels, and also environmental factors [27–30].

The mechanisms involved in the prostate carcinoma are not well understood but, it seems that the PCa progression is down-regulated by androgen-responsive genes [31,32]. These critical factor contributes to the development of prostate tumors, through the inhibition of apoptosis rather than an enhanced cellular proliferation [33]. Furthermore, there is evidence for the formation of pre-cancerous lesions initiated by an inflammatory process that occurs during tissue injury. Indeed, it was described the existence of three different stages involved in PCa development and progression, namely prostatic intraepithelial neoplasia (PIN), proliferative inflammatory atrophy (PIA) and prostatic and metastatic carcinoma, as shown in Figure 2 [2,31,34].

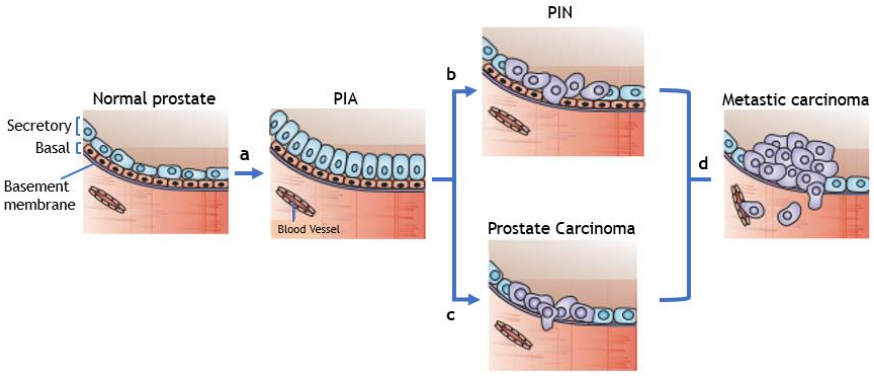

Figure 2. Cellular and molecular model of early prostate neoplasia progression. Formation of a) PIA lesions ; b) PIN lesions; c) Prostate carcinoma ; and d) Metastic carcinoma, adapted from [31], .

PIA seems to be a precursor of PCa, and these lesions occur mainly in stromal and epithelial cells, as described in Figure 2a. The PIN lesions are described as the most likely precursor to PCa progress, and involve an abnormal proliferation of basal and luminal cells, showing a dysplastic behavior, according to Figure 2b. When the PCa cells reach the blood, they progress through the bloodstream and metastasize into different organs, including liver, lung, and bones(Figure 2c and d) [3,10,34]. Changes of epithelial and stromal cells genes expression during the different development stages of PCa notably contribute to the enhancement of tumor growth, survival, migration, and invasiveness [3,35]. The PCa is androgen-dependent at initial stages. In the primary PCa development, only a few AR genes have been mutated and the androgen ablation therapies reveal that the tumor is in regression. However, in advanced stages of PCa, the prostate cells became AR-independent, as they are able to survive and proliferate without circulating androgens, thus restricting the use of androgen ablation therapies [36,37].

1.2.1. Diagnosis and Treatment

Current diagnosis of PCa can be achieved by prostate-specific antigen (PSA) test, digital rectal examination, and biopsies for histopathological staging [38–41]. Early detection of PCa has increased dramatically with a serum test for the PSA, which is a serine protease secreted by epithelial cells of the prostate and has an important role in seminal fluids liquefaction [38,41]. However, the PSA test may not distinguish PCa from benign disease such as BPH and prostatitis, leading to the detection of false positives [40,42]. Thus, the best way to perform a correct PCa diagnosis is a biopsy of the respective tissue, that is currently collected by ultrasound transrectal sampling. The main disadvantages of this procedure are the fact that it is an invasive test and offer a significant risk of posterior infection [39,40].

Thereby, the Gleason score grading is the method used to unify the PCa progression and aggressiveness. With this grading, it is possible to characterize and distinguish the different stages of PCa. This system was created by Dr. Donald F. Gleason and is based on the histological pattern of carcinoma cells in the prostatic tissue. The Gleason-score is ranged between 2 and 10, in agreement with the severity of the disease. An increasing of Gleason grade is directly related to tumor size and invasiveness [43,44]. Treatments for PCa depend on the stage of cancer and the age of the patient. For example, in men with the low-Gleason score (2-4), the main action is through the regular measurement of serum PSA levels and prostate biopsies as monitoring. In aggressive cancers, related with high-grade Gleason score (9-10) the most common treatment is the androgen receptor ablation therapy, radiation, prostatectomy, or a combination of both. Nevertheless, these therapies may be violent and can diminish the life quality of the patients [25,32,43,45]. As mentioned, therapies through the androgen receptor ablation have been reported as a possibility, but the loss of androgen-dependence for advanced cancer stages may preclude the application of these treatments. Most androgen-independent PCa still express the androgen receptor protein, suggesting the importance for androgen-refractory PCa [35,46,47]. Despite the many advances in PCa diagnosis and treatments, it is crucial to identify of novel markers and therapeutic targets to improve the diagnostic and treatment specificity.

1.2.2. Immunotherapeutic targets

Nowadays, there are several biomolecules that may be used as cancer biomarkers and allow a specificity both in the diagnosis and treatment. Proteins that are over-expressed in PCa can be considered as an ideal immunotherapeutic target. In general, these proteins are highly expressed in cancer disease, in comparison with normal cells and are accessible to therapeutic modalities at the cell surface [27,41]. The main biomarkers of PCa are the prostatic acid phosphatase (PAP), prostate-specific membrane antigen (PSMA), prostate stem cell antigen (PSCA), Gg A, NSE and, the six-transmembrane epithelial antigen of the prostate I (STEAP1), as will be described below [12,38,39,41,48,49] .

The PAP is a dimeric glycoprotein produced predominantly by the prostate, in spite of being identified in several organs, such as the liver, brain, and lungs. It is used as a serum biomarker for metastatic PCa detection. However, PAP reveals a low sensitivity to detect the local of the disease [38,41].

The PSMA is a transmembrane glycoprotein expressed on the surface of prostatic epithelial cells. It was identified in several prostate tissues, being suggested that is upregulated in carcinomas when compared with the benign tissue. Additionally, it was well described the correlation between high PSMA levels, high Gleason score values and a PCa invasive and aggressiveness stage [38,41,48].

The PSCA is a glycoprotein expressed on cell-surface of the prostate basal cells and detected in prostate tissues. Several studies suggest it might play an important role in carcinogenesis, being involved in cell adhesion, signaling, and prevention of apoptosis. Indeed, an increased PSCA expression is correlated with higher Gleason score values and consequently advanced PCa stage and metastasis [39,48,50,51].

As mentioned behind, CgA and NSE could be used as a PCa biomarker. Several studies suggest that some neuroendocrine peptides may increase the invasive potential of PCa cells. Thereby, it may lead to a rapid progression and aggressiveness of tumors rich in neuroendocrine elements [52–54]. Also, it was described the association between NSE expression with other biomarkers, namely CgA and PSA. Therefore, an increased expression of these biomolecules might be associated with the presence of a mixed epithelial-neuroendocrine tumor cell population [12,55,56]. The CgA is a peptide produced by neuroendocrine cells. It is commonly used to detect neuroendocrine features on tissues or serum. While its functions are still unknown, it is believed that CgA is involved in the regulation of protein secretion. Several studies suggest that CgA plays an important role in the initial PCa detection, eventually combined with free total PSA test [12,13,39,46]. The NSE is known to be a cell specific isoenzyme of glycolytic enzyme enolase. It is a specific marker for neuroendocrine prostatic cells and is associated with tumor differentiation and invasiveness. So, NSE can be a biomarker for the diagnosis, staging, and treatment of related neuroendocrine prostatic tumors [52,53,56].

Finally, STEAP1 is a transmembrane protein mostly expressed in the plasmatic membrane of epithelial prostate cells. Several studies in the literature suggest its relevance in cell-cell communication and tumor invasiveness, being associated with high Gleason score and Ewing tumors. Indeed, STEAP1 is pointed as a promising immunotherapeutic target as long as over-expressed in all stages of Pca in comparison with normal prostate cells [22,49,57].

2. General overview of STEAP family

The human Six-transmembrane epithelial antigen of the prostate (STEAP) proteins family are found in mammals and comprises at least five homologous members - STEAP1 to 4 and STEAP1B [49,58]. Typically, they act as metalloreductases, suggesting their role in metal homeostasis. Still, STEAP proteins family have great importance in responses to inflammation, oxidative stress response, cell-cell communication, proliferation and tumor invasiveness, fatty-acids and glucose metabolism as well as endoplasmic reticulum stress [22,49,58–61].

Regarding on the amino acids sequence of the STEAP1 proteins family, they share at least 60% similarity. It was described their capacity to form homo or hetero-oligomers each other's, although they seem to have different function and location in the cell [58,61,62].

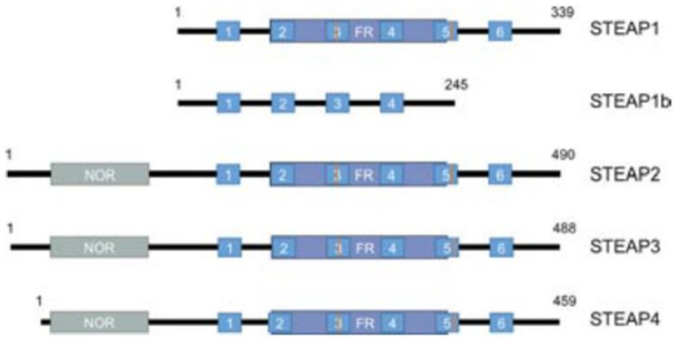

Figure 3. Schematic illustration of the domain organization of STEAPs proteins family, adapted from [60].

All members of the STEAP proteins family, unless STEAP1B, have six transmembrane domains and an intracellular *N*- and C-terminal groups [61]. Their *N*-terminal group has a structural GXGXXGA/A motif (Rossman-fold), which is typically found in proteins that bind nucleotides [58,61,63]. Also, their C-terminal group, share a great homology with FRE family of metalorredutases in yeasts. As suggested in Figure 3, all proteins, except STEAP1B, have an heme binding histidine group close to the transmembrane domain 3 and 5 [49,58,61].

The first member of this family identified was STEAP1, whose gene is located on the chromosome 7q21.13 near to STEAP1B gene located on 7q15.3. Also, the genes encoding STEAP2 (7q21.13) and STEAP4 (7q21.12) appears at the same place, just like other genes predicted to encode membrane proteins. Only the STEAP3 gene is located on chromosome 2q14.2 [49,58,61].

STEAP1B gene is transcribed into a mRNA of 1.2 kb that origins a protein of 245 amino acids, with 28.8 kDa. It shares 88% amino acids similarity to STEAP1 but, does not have the last two transmembrane domains. These two proteins lacks the FNO-like domain and the Rossman fold and therefore seem do not have the capacity to reduce metals [61].

STEAP2 is encoded by a mRNA of 2.2 kb and produces a protein of 490 amino acids, with 56.1 kDa. This protein is associated with the plasma membrane and Golgi complex, suggesting that it may be involved in the partial induction of cell cycle, as a receptor to bind exogenous and endogenous ligands [49,58,61,64,65].

In relation to STEAP3, this protein is weakly expressed in most human tissues, although it seems to be highly expressed in bone marrow and liver [61,66]. Encodes a mRNA of 4.3 kb which gives rise to a protein with 488 amino acids, 54.6 kDa and with a preferential localization in plasma and endosomal membranes. It was related the role of STEAP3 in secretory pathways as supporting important physiologic functions in iron metabolism [49,61,67].

Finally, STEAP4 is encoded by a mRNA of 4.5 kb and a protein with 459 amino acids, 52.0 kDa. It appears to be involved in secretory and endocytic pathways such as STEAP2 and 3 [61]. Therefore, its major location is in the plasma membrane, close to the Golgi complex and vesicular-tubular structures of the cytosol [49,68]. STEAP4 has abundant expression and a relevant physiological function into various organs such as placenta, heart, and lung [49,58,61].

2.1. Structure and Function of STEAP1

The STEAP1 protein was identified in 1999 by Hubert and coworkers as a novel marker and therapeutic target for PCa [22,49]. The STEAP1 gene is located close to the telomeric region of the chromosome and the size comprises 10.4 Kb, including 5 exons and 4 introns. It gene transcription gives rise to two different mRNA of 1.4 kb and 4.0 kb, which only the first is processed into a mature protein. The protein produced has 339 amino acids with a predicted molecular weight of 39 kDa [22,61]. STEAP1 predicted secondary structure has six transmembrane domains, an intracellular C- and N-terminal, three extracellular and two intracellular loops [49,58,61,64]. The STEAP1 is present in the plasma membrane of the epithelial cells, with lesser intensity on the cytoplasm. Thus, due to its location, several studies suggested the relevance of STEAP1 as an important play in cancer development and progression [49,58]. The predicted structure and location at cell-cell junctions suggest that STEAP1 could take part in intracellular cell communication and cell adhesion [69]. Indeed, it appears to act as an ion channel, by mediating the transport of some proteins in both tight and gap junctions. Also, it was reported that STEAP1 promote cell growth by raising the intracellular level of reactive oxygen species (ROS) as shown in Figure 4 [49,57,61,70].

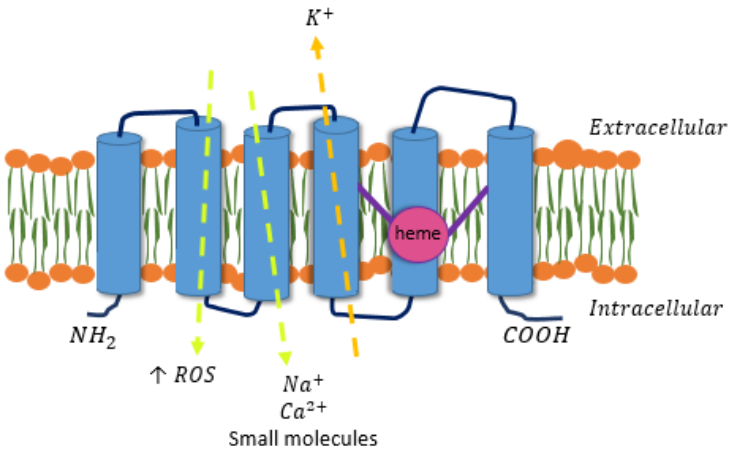

Figure 4. Schematic STEAP1 protein structure, cellular localization, and physiologic functions, adapted from *[49]*.

Several research groups comproves that STEAP1 may promote cancer cell proliferation and invasion, perhaps through modulation of sodium (Na^+), calcium (Ca^{2+}), potassium (K^+) and also small molecules [49,71]. Interestingly, it was described that higher levels of Na^+ promote an invasive phenotype in PCa cells [72]. Also, the modulation of Ca^{2+} and K^+ seems to have a prevalent role in PCa progression. The presence of these channels appears to be linked with the loss of androgen receptor expression and function, and consequently, the cancer development [22,61,71,73]. In addition, STEAP1 is overexpressed in PCa but it was also detected in other human cancer cell lines, such as pancreas, colon, breast, prostate, testicular, cervical, bladder and ovarian carcinoma, severe lymphocytic leukemia, and Ewing sarcoma [22,57,70,73].

Gomes and coworkers reported the positive association between STEAP1 expression and, high Gleason score, suggesting its role in PCa progression and aggressiveness. Concerning its role as a biomarker, STEAP1 seems to be highly reliable for distinguishing malignant PCa from BPH [73]. In another study, it was reported the correlation between STEAP1 expression, the invasive behavior, and the oxidative stress of Ewing tumors. This comprises the second most common type of bone-associated cancer in children and is characterized by the fusion of oncogenic proteins and early metastasis [57]. Also, it was denoted by RT-PCR the presence of high quantities of STEAP1 in solid tumors compared with normal tissues. This finding provides evidence that this gene is associated with the deregulation of normal cell growth [70].

It was reported that 17b-Estradiol (E2) downregulates STEAP1 gene regulation in both rat mammary glands and MCF-7 breast cancer cells [74]. Another study related that STEAP1 is down regulated by sex hormones. This group describes that neoplastic prostate cells (LNCaP) treated with DHT, and E2 for different periods induces a down-regulation of STEAP1 expression. Additionally, using inhibitors of androgen and estrogen receptor (AR and ER) it was showed that the down-regulation of STEAP1 is AR-dependent, but ER-independent [74,75].

2.2. STEAP 1 as an immunotherapeutic target

Nowadays, STEAP1 is a promising candidate to be imposed as a therapeutic and diagnosis target, due its location and over-expression in several cancers. Hereupon, during the last years several strategies have been developed for targeting STEAP1, including antibody-drug conjugates, DNA cancer-vaccines, small-molecule therapy [22,61,69,76,77].

In the last years it has become recurrent the use and commercialization of antibodies as treatment for several pathologies. Owing to its specificity, has highlighting the need to identification novel cell surface targets suitable for cancer therapies. Furthermore, it was described the use of monoclonal antibodies (mAb) that have a higher specificity to bind STEAP1

extracellular loops leading to a decrease of it oncogenic function following the mAb administration [69]. Recently, some studies have shown STEAP1 as a suitable antigen for T-cell-based immunotherapy in prostate, colon, pancreas, bladder, Ewing sarcoma, breast, testicular cancer. The results show that $STEAP1_{86-94}$ and $STEAP1_{262-270}$ are specific stimulators for $CD8^{+}$T cells acting as HLA-A*0201 restricted epitopes [59,67]. Also, the vaccination with $STEAP1_{262-270}$ peptides encapsulated into PLGA microspheres in HLA-A*0201 transgenic mice, revealing a new approach in PCa immunotherapy [76].

The deep knowledge of STEAP1 structure and function is crucial for the development of new molecules with therapeutic and clinical applications. Thereby, several modifications in the STEAP1 structure were reported and supported through in silico analysis, such as *N*-glycosylation, *N*-Glycation, Phosphorylation and *O*-linked ß-*N*-acetyl glucosamine [78]. So, different mechanisms of post-translational modification (PTM) could be involved in the differential expression of STEAP1 between non-neoplastic (PNT1A) and LNCaP cells. It was denoted the presence of two consensus motifs Asn-X-Thr/Ser (X may be any amino acid except proline) in protein sequence, but just a single potential N-glycosylation site was identified in Asn143. The potential score of another Asparagine was below the threshold line, as shown in Figure 5A. Based on the potential score, several Lysines are suggested as potential glycation sites, at positions Lys5, 15, 17, 30, 108, 148, 149, 156, depicted in Figure 5B. Some amino acids could be phosphorylated, such as Serine, Threonine, and Tyrosine. It was predicted that four Serines (Ser3, 187, 240 and 244), two Threonines (Thr160 and 246) and four Tyrosines (Tyr27, 147, 219 and 252) are potentially phosphorylated on STEAP1, as showed in Figure 5C. *O*-linked ß-*N*-acetyl glucosamine (GlcNAcylation) is usually associated with phosphorylation. The potential *O*-ß-GlcNAc anchor sites can be found on Thr236 and 333, Ser237 and 242 of the STEAP1 sequence, much close to phosphorylation predicted sites, as shown in Figure 5D [62,78-80].

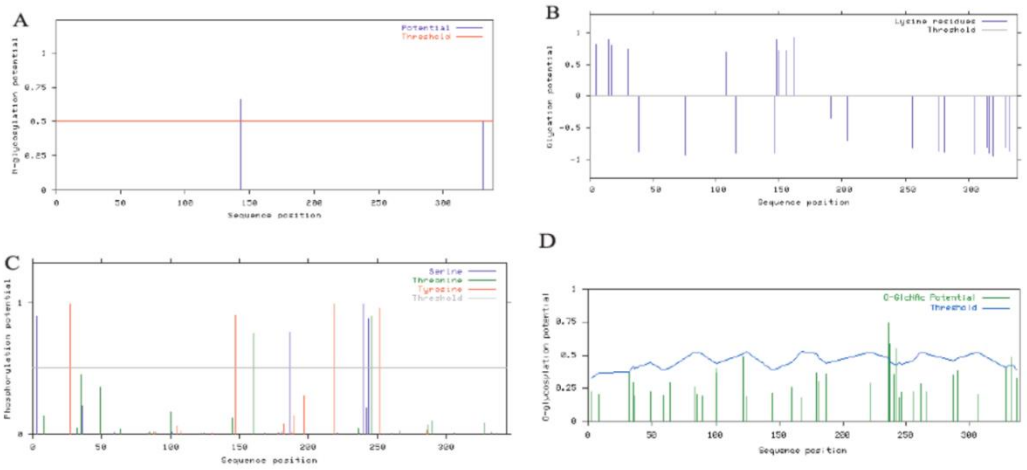

Figure 5. Prediction of the several *N*-glycosylation, glycation, phosphorylation and *O*-ß-GlcNAc sites of STEAP1 using: A) NetNGlyc 1.0; B) NetGlycate 1.0; C) NetPhos 2.0 and D) YinOyang 1.2, respectively, adapted from *[78]*.

Curiously it was demonstrated that STEAP1 mRNA and the native protein are highly stable in LNCaP cells in comparison with the PNT1A cells. So, the differences reported in PTM could contribute for STEAP1 overexpression and stabilization in PCa cells [78] . It is well documented that these modifications tend to confer higher stability to proteins and are often implicated in the development and pathogenesis of several diseases, including cancer [81]. Furthermore, certain PTM's may even be used as diagnostic targets and are known to enhance tumor cell proliferation and invasion, as in PCa. Hence, more specific studies related with these particular PTM are required to evaluate the role of these modifications in tumorigenesis [62,78,81–83].

3. Recombinant protein biosynthesis

The major bottleneck for the characterization of membrane proteins is the production of sufficient amounts of high-quality samples. For this reason, the use of recombinant technology has revolutionized the strategies for protein production. It is possible to obtain high quantities of different human recombinant proteins when compared with the natural source. The selection of an ideal expression system, as well as the appropriated growth conditions, the characteristics of the target protein and its posterior application, are specific examples of factors to be considered when producing proteins.

3.1. Host strain and promoter selection

There are several systems that allow overproduction of recombinant proteins such as prokaryotic and eukaryotic. The ideal expression system should combine a wide range of features, namely low-cost, safety, rapid growth and if necessary the capacity to perform secretion-linked protein modification steps, as glycosylation [84,85]. As mentioned below, the most widely system used to express recombinant proteins, both on a laboratory and industrial scale, is the Prokaryotic system. While, if the target protein needs some posttranslational modifications the Eukaryotic cells are preferable [85,86].

3.1.1. Prokaryotic system

Prokaryotic cell cultures are cheap and allow the production of large amounts of recombinant proteins in a short period of time. Due to the well-known transcription and translational mechanism, bacterial cells are frequently used to produce heterologous proteins. Noteworthy

is the wide availability of promoters and mutant host strains. However, the disadvantages of bacteria cells are the inability to perform PTM in target synthesized protein [85,86].

Escherichia coli (E. coli) is a Gram-negative bacterium and a useful system for recombinant protein expression. The ease to perform genetic manipulation and the well-characterized genome are the greatest advantage of its use. Moreover, these bacteria are capable grow rapidly in order to achieve high cell densities onto fermentation media with inexpensive substrates. A great disadvantage of *E. coli* is the inability to perform post-translational modifications, as well the lack of efficient secretion systems into the extracellular medium. An additional problem is the presence of recombinant lipopolysaccharide (LPS) anchored into the bacteria membrane surface. For therapeutic proteins, it is necessary the complete removal of LPS, once they can promote, in humans, a strong immune responses [85–88].

Besides, others prokaryotic systems can be used in the upstream step, such as the gram-positive *Bacillus spp*. The most commonly used are *Bacillus megatherium*, *Bacillus subtitles* and *Bacillus brevis*. The *bacillus* strain used in biotechnology are not pathogenic and do not secrete toxic secondary metabolites. Their greatest advantage is the absence of LPS in the membrane and the efficient secretory system of heterologous proteins, which greatly facilitates their isolation and purification. However, the main disadvantages of these hosts are the requirement of complex media, high endogenous protease activity, structural instability of the plasmid and production of lower levels of heterologous protein when compared with *E.coli* [85,89,90].

3.1.2. Eukaryotic System

Distinct eukaryotic systems such as mammalian and insect cells, yeast, filamentous fungus, and microalgae are an interesting alternative for recombinant protein biosynthesis. Mammalian and insect cells allow obtaining catalytical active biomolecules, with the correct PTM [85,91–93] However, the culture of these cells is time-consuming, expensive and the amount of target product is usually low. Unlike, the yeast cells culture receives special attention. The hands-on is facilitated and produces large quantities of the recombinant protein in a short period of time. The common yeasts applied to biosynthesized heterologous protein are *Saccharomyces cerevisiae (S. cerevisiae)* and *Pichia pastoris (P.pastoris)* [85,94,95].

Saccharomyces cerevisiae was the first eukaryote to have its complete genome sequenced. Being commonly associated with the pharmaceutical, brewing and baking industries. It is the most widely employed species in the laboratory for the production of membrane proteins [94,96]. It might grow in an aerobic or anaerobic medium, in the presence of several carbon sources, such as glucose or glycerol. The switch from a respiratory to a fermentative metabolism occurs in response to a change in the external concentration of a carbon source

easily metabolized. The main advantages of *S. cerevisiae* are the tolerance to low pH and the ability to perform posttranslational modifications [94,97]. The major difference between *S. cerevisiae* and *P. pastoris* is the *N*-glycosylation performed. In *P. pastoris*, the oligosaccharides are a shorter chain length, no more than 20 residues, compared with 50-150 residues in *S. cerevisiae*. In addition, *P. pastoris* lacks the mannosyl-transferase which yields immunogenic α -1, 3-linked mannosyl terminal linkages in *S. cerevisiae* [94,98].

3.1.2.1. Pichia pastoris

Since the 1980 *Pichia pastoris (P. pastoris)* has been used as a host for heterologous protein expression, being described for the first time by Guillirmond in 1919. It is a methylotrophic yeast, this means that it is capable of metabolizing methanol as its sole carbon and energy source [84,99]. The most advantage of its application is the ability to perform the correct protein folding, the post-translational modifications inside the cell and, forward the heterologous protein into the extracellular medium. In addition, it has the genome completely sequenced which facilitate its manipulation in the laboratory [100–102].

P. pastoris can have different promotors consonant the product to express and the resources to be used, like the inducer. The promoter mostly used is AOX1, although there are others, GAP, FLDI, PEX8 or YPT7. In relation to the plasmids, the most used belongs to pPICZα (A, B, or C) plasmids family, that confer zeocin™ resistance.

This vector has multiple cloning sites and its pUC origin allows replication and maintenance of the plasmid in *E. coli* cells before *P. pastoris* transformation. The fragment 5'AOX1, containing the AOX1 promoter, permits methanol inducible high-level expression in *P. pastoris cells* [103–106].

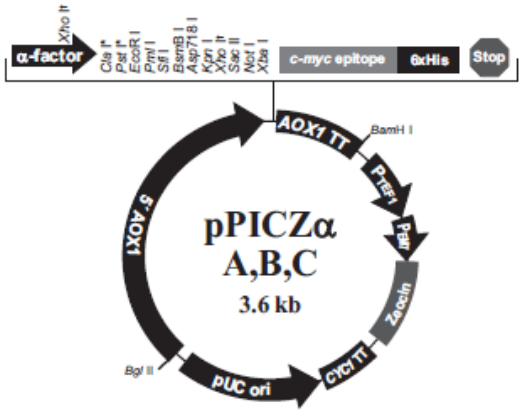

Figure 6. pPICZα (A, B, C) expression vector (Retrieved from Invitrogen, EasySelect™ *Pichia pastoris* Expression Kit no. 25, 2010).

Normally, the heterologous protein expression in *P. pastoris* is regulated using the strong and inducible AOX1 promoter, which synthesizes the enzyme alcohol oxidase 1 (AOX1), allowing to control the expression of genes required for methanol metabolism [100,107]. Depending on the ability to metabolize methanol, there are several phenotypes of *P. pastoris, including* Mut^S (methanol utilization slow), Mut (methanol utilization) and Mut^+ (methanol utilization plus) [101,104,108]. The main difference between each phenotype is the expression of the AOX1 or AOX2 proteins. The strain Mut^+ (e.g., *P. pastoris* X33 or GS115) express both AOX1 and AOX2, whereas Mut^S (e.g., *P. pastoris* KM71H or MC 100-3) only express the AOX2. Typically, the AOX1 gene is more strongly transcribed than AOX2 [102,104,108–110].

The most relevant metabolic pathways in *P. pastoris* are glycolysis, pentose phosphate pathway, citric acid cycle, methanol metabolism, gluconeogenesis, anapleurotic reactions depending on carbon sources [84,107]. All operational conditions, such as a carbon source, flow rates, pH, temperature, dissolved oxygen, might regulate the expression of genes involved in the metabolic pathways mentioned above, and consequently, the quantity and quality of the target protein may change [84,101,107]. The first reaction of methanol metabolism occurs in peroxisomes and is the oxidation of methanol to formaldehyde using molecular oxygen by AOX1 and AOX2 proteins. This reaction generates formaldehyde and hydrogen peroxide that are toxic to the cells. Its reduction to water and oxygen is made by the enzyme catalase in the peroxisomes. The followings metabolites will then go to the cytoplasm for more reaction, as demonstrated in Figure 7 [84,100,107].

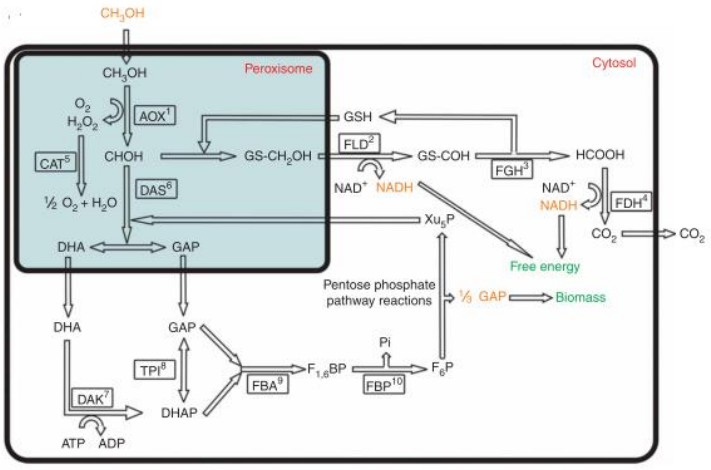

Figure 7. Methanol/Glycerol pathway in *Pichia pastoris* metabolism, adapted from [100].

It is well known that, *P. pastoris* can grow on several carbon and energy sources, where glycerol, glucose, and methanol are the most commonly used. Once the AOX1 expression is repressed by glycerol and glucose, is important to switch to less repressive carbon sources, such as sorbitol, trehalose, rhamnose and some amino acids [101,111]. Also, it was described that

mixed feeds often generate high cell expression profiles which can increase specific production rates, optical densities and decrease the induction time period [99,110,111].

One of the major inconvenient in the application of *P. pastoris* as an expression host, is the high-level expression of proteases during the fermentation and the hiper-glycosylation pattern of the mature protein [103,109,112]. The glycosylation is a very common post-translational modification (PTM) that occurs in the endoplasmic reticulum. *P. pastoris* can add both *N* and *O*-Glycosylation, that consist in the repetition of mannose (Man) and acetyl glucosamine (GlcNAc) attached to an amino acid. As mentioned, the *N*-glycosylation is when oligosaccharides are covalently attached to an asparagine residue on the consensus motif Asn-X-Thr/Ser (X may be any amino acid except proline). In *P. pastoris* this process, is characterized by hyper-mannosylation, 9-11 mannoses residues which may result in a short half-like or even immunogenicity of the target recombinant proteins. *O*-glycosylation is when an oligosaccharide is attached to Serine or Threonine. So, the modifications by oligosaccharides attachment are involved in the correct folding of proteins, stability, immunogenicity, and biological functions, that take part in many physiological processes [93,113,114]. Since the modification by glycosylation may be critical in the activity of therapeutic proteins, for instance enzymes and ion channels, is mandatory the study of protein glycosylation pattern of the newly-synthesized protein. In the last decades, few enzymes were available for carbohydrate analysis; endoglycosidase D, F, H, ß-galactosidase, Peptide *N*-Glycosidase F (PNGase F) and Neuraminidases [98,106,115]. The PNGase F is commonly applied and is involved in the most effective enzymatic method for removing all *N*-linked oligosaccharides attached to proteins [113,116,117]. This protein is a glycoamidase that cleaves a specific linkage between Asn and the GlcNAc, in which Asn is converted to aspartic acid [104,106,113].

3.2. Fermentation strategies and main conditions

A shake flask fermentation is considering an initial strategy to have some knowledge of the upstream conditions to be apply in the biosynthesis of human recombinant proteins. However, to obtain higher massic and volumetric productivities and to control all the fermentation parameters the bioreactors fermentations are the best option. A bioreactor system allows to control in a real-time mode different operating conditions such as pH, temperature, oxygen dissolved, STIRRER and aeration (directly related with mass transfer of oxygen) [118–120].

Pedro and coworkers have studied the best growth conditions to produce membrane proteins into *Pichia pastoris* X33, firstly in shake flask and then in bioreactor [108,121]. Typically, the procedure for expression of proteins in *P. pastoris* bioreactor cultures involves three main phases: a batch of glycerol, fed-batch phase, and methanol induction phase. The batch culture is generally started with an inoculum growing at the maximum specific growth rate in a semi-

defined media. Normally, it is extended until the full exhaustion of glycerol, in order to achieve a maximum cell growth. The second stage is a fed-batch, which complements a glycerol fed-batch phase with a mixed glycerol and methanol feed stage. The glycerol feed is to further increase cell concentration without repressing growth. The mixed feed is to prepare the cells for a secondary carbon source. In the third stage, methanol is added to the fermentation medium in a fed-batch mode, in order to start the induction phase [121,122].

The method of different carbon source/inductor or nutrient feeding is critical to the success of a fermentation process, as it affects both the maximum attainable cell concentration and productivity. Regarding this, three main types of feeding profiles can be considered: constant, exponential, and stepwise feeds. In constant feeding, a carbon source/inductor or nutrient is used to feed the bioreactor at a predetermined rate that does not change during the process. Due to the increase in culture volume and cell concentration, the specific growth rate continuously decreases [101,122]. In stepwise (or gradient) feeding, the carbon source/inductor or nutrient is added to the culture at successive increasing rates. Normally, the cell growth can be exponential during the entire culture period if the feed rate is increased in proportion to biomass levels. Several articles suggest a stepwise lowering of glycerol- rate [122,123]. Exponential feeding allows *P. pastoris* cells to grow at predetermined specific growth rates, which cause a slight increase in AOX1 activity due to the derepression of its and consequently enhance the productivity [109,122,124].

Usually, the specific growth rate is ranged between 0.001 h^{-1} and 0.14 h^{-1}, at low and high methanol cultivation, respectively, and close to 0.18 h^{-1} when wild type P. pastoris growing on glycerol [101,109,122]. Hereupon, the standard behavior of specific AOX1 activity during the fed-batch phase is depicted in the Figure 8 [109].

...

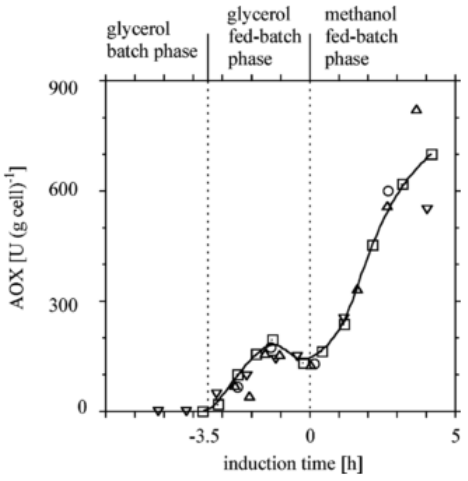

Figure 8. Specific AOX activity during the transition phase in *Pichia pastoris* high cell density fed-batch cultivations, from [109].

As an alternative to glycerol/methanol co-feeding strategy, several studies were developed with different feeding strategies, especially using sorbitol as co-substrate and a non-repressing carbon source [125]. A typical diauxic behavior is observed in mixed-substrates in batch cultures with glucose, or glycerol/methanol. Therefore, the applicattion of glucose or glycerol/methanol is used sequentially [105,108,125].

Finally, the study of different methanol feeding strategies are important to enhance heterologous protein production. The methanol induction phase also depends on the operational conditions, such as the temperature, pH, culture medium, medium molecules supplementation, on the target heterologous protein characteristics, host features [105,107].

Typically, the feeding rate can be calculated using some standard equations (1 and 2) below described [109,114] :

$$F(t)_0 = \frac{\mu \times V_0 \times X_0}{S_0 \times Y_{x/s}} \quad (1) \qquad F(t) = F(t)_0 \times e^{\mu t} \quad (2)$$

F(t)	feed flow-rate (h^{-1})
μ	specific growth rate (h^{-1})
V_0	Culture volume (L)
X_o	Cell concentration (g/L DCW)
S_o	Substrate concentration in the feeding solution (g/L), $S_{methanol}$ = 790 g/L
$Y_{x/s}$	Cell yield on carbon substrate, specific for each strain (Cmol/Cmol), *Pichia pastoris* in methanol, $Y_{x/s}$ =0.45 C_{mol}/C_{mol}
t	Fermentation time (hours)

Hereupon, several parameters control the fermentation process and contribute for the correct protein biosynthesis, such as the foam formed during the induction phase. It is formed due to gassing used to maintain an appropriate dissolved oxygen concentration in the medium. Foaming could promote a decrease in the productivity since the bursting bubbles may affect the protein stability. Also, the bubbles stimulate specific alterations on the oxygen transfer coefficient (KLa) or in the carbon source uptake [126–128].

The presence of some solutes in solution could interfere in osmolarity and consequently in the protein productivity. Some researchers described a relationship between the osmolarity, high/low salt or solute concentrations in the culture media, and the unfolded state of *P. pastoris* proteome. Certainly, salt environments, working as osmoprotectant, leads to the increase of proteins involved in glycolysis and down-regulate proteins in relevant metabolic pathways [129].

Still, the temperature and the pH may affect the normal *P. pastoris* metabolism and consequently promote significant differences on protein expression. Indeed, some works described that the falling of induction temperature enhances the protein productivity, through the decrease of homologous protease production. The proteases formed during the fermentation can damage the correct structure of the target protein [121,130].

It is well known that chemical chaperones may protect both prokaryotic and eukaryotic cells, acting mostly as osmolytes [131]. Also protect the proteins against extreme temperatures, dehydration, high salt, and/or solute concentration, helping in the folding and stabilization [131,132]. Several osmolytes, as amino acids or derivates, polyols, amines, sulphur analogs, peptides, are uncharged at neutral pH, favoring its solubilization. Nevertheless, these molecules may accumulate to high amounts in the cell due to uptake or synthesis, protecting the host against the stressful environment [133,134]. Until now, the chemical chaperone more used is the dimethyl sulfoxide (DMSO). Even through its toxicity to the cells, DMSO promote protein folding and stability. It was described its influence in the oxidative stress in *S. cerevisiae*. The interaction between the DMSO and the recombinant proteins is mostly based on hydrophobic interaction [133,135]. Pedro *and coworkers* studied different DMSO concentration and proved that 6% (v/v) DMSO is the most effective concentration that can be applied in *Pichia pastoris* reactor cell cultures without interfer in the cell viability [121].

Due to the above reasons, is extremely relevant the use of chemical chaperones with lower toxicity for the cells. Considering this, several chaperones may contribute to protein and cell protection, alone or combined with DMSO [131,136]. Some examples, histidine, proline, trehalose, Trimethylamine-*N*-Oxide (TMAO), cysteine, arginine, glycerol, and sorbitol could be used to mantain protein stability and decrease agregation, structures show in Figure 9 [133,137–139].

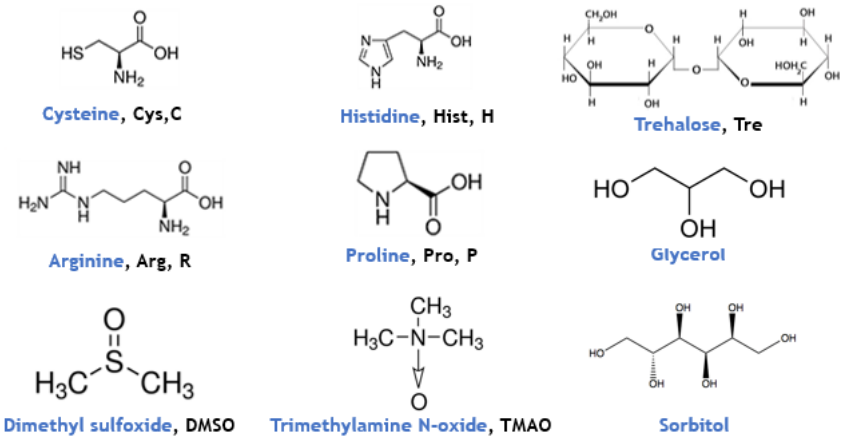

Figure 9. Chemical structure of several molecules used as chaperones.

Succinctly, arginine and histidine are basic amino acids. Arginine does not act as a protein-stabilizer but rather as a suppressor of protein aggregation. Its solubility leads to the improvement of native product yield [111,112]. Histidine could form coordination complexes with metal ions of the proteins, acting as a physiological effector in metabolic regulation. Cysteine is a polar charged amino acid, characterized by a thiol side chain, where the stabilization occurs through the disulfide bridge. Particularly it was described that histidine prevents the oxidative inactivation of AMP deaminase in yeast, but a lesser effect was denoted for cysteine [133,137].

Proline is a apolar amino acid, that solubilizes the protein through the interaction with its native state, preventing the formation of aggregates. The role of proline in osmoregulation needs to be considered when it is applied as a cultivation additive. Proline affects osmotic balance contributing to the homeostasis of cytoplasmic pH in *E. coli* cells. Although, for better results it is necessary to combined it with salts, such as K^+ and PO_4^{-3}, as they are crucial for salt-induced proline uptake. In *S. cerevisiae,* the uptake of proline is induced by the addition of solutes, as sorbitol or ethanol, to the fermentation medium [133,142,143].

The supplementation of sugar to the medium supplementation create osmotic stress that indirectly leads to the stabilization of the protein structure [133]. A great example of these is trehalose, a disaccharide with high affinity for water molecules. There are three theories to explain the protective effect of threhalose: It may form a protective barrier against abiotic stresses (vitrification theory); It may sequester the water molecules for the protein surface (preferential exclusion theory); or forms complexes with the target protein stabilizing its three-dimensional structure (water replacement theory) [144].

Glycerol and sorbitol are polyols that promote the solvent reorganization around the proteins, repealing the water molecules, enhancing the hydrophobic interactions [133,136]. TMAO modify the water- amide interactions, protecting the proteins against the denaturing effect of urea and inorganics ions. It also, stabilize both hydrophobic and hydrophilic proteins through the enhancement of the protein folding and binding to ligands [136,145].

Finally, metal ions act as co-factors for both recombinant and host proteins. Co-factors are essential for protein folding, as they bind to the unfolded polypeptide, accelerating the protein refolding and contributing to its stabilization [133].

Taking into account these compounds beneficial effects but also their negative side, namely their toxicity to the cells, it may be interesting to combined them and see if they can interact with one another in order to enhance their activity and lower the concentrations needed to have a positive effect [133,136].

Chapter II – Aims

The combination of STEAP1 over-expression in PCa cells and its main function as oncoprotein strongly encourage the possibility of using this protein as a potential therapeutic target for cancer. For this reason, it is important discover and resolve 3D structure of human STEAP1. Indeed, understanding its behavior in PCa development and invasiveness is crucial to perform the design of specific ligands that could decrease its oncogenic function.

However, it is essential to obtain high levels of purified and correctly processed protein. Since STEAP1 biosynthesis may requires PTM, such as *N*-glycosylation, it is highly desirable to perform the production stage in a eukaryotic system, such as *Pichia pastoris*. Therefore, the main aim of this master thesis was the scale up of STEAP1 biosynthesis in *Pichia pastoris* X33 onto a mini-bioreactors lab platform. This strategy can allow the control of all fermentation parameters that consequently leads to high amounts of recombinant human STEAP1. To achieve the main goal, the following intermediate objectives were defined to:

- Improve STEAP1 production in *Pichia pastoris* X33 methanol-induced cultures from mini-bioreactors;
- Study different feeding strategies of Glycerol and Methanol;
- Evaluate the effect of different chaperones on STEAP1 expression levels and conformational stabilization;
- Understand the effect of bioreactor feeding profiles in the *N*-glycosylation state of the target protein.

Chapter III – Materials and Methods

1. Materials

Ultrapure reagent-grade water was obtained from a Milli-Q system (Millipore/Waters). Calcium chloride dihydrate, dithiotreitol (DTT), sulfuric acid (H_2SO_4), Sodium dodecyl sulfate (SDS) and Phenylmethylsulphonyl fluoride (PMSF) were obtained from PancReac AppliChem (Darmstadt, Germany). ZeocinTM was purchased from InvivoGen (Toulouse, France). Deoxyribonuclease I (DNase), glass beads (500 µm) and proline were obtained from Sigma-Aldrich Co. (St Louis, MO, USA). Yeast nitrogen base(YNB) was obtained Pronadisa (Malaysia). Yeast extract and glycerol were acquired from HiMedia Laboratories (Mumbai, India). Glacial acetic acid and potassium hydroxide were obtained from CHEM-LAB N.V (Zedelgem). Peptone was bought from Becton, Dickinson Company (Sparks, MD). Magnesium sulfate heptahydrate was purchased from LabKem, (Barcelona, Spain). Agar, Glucose, Hydrochloric acid (for glass beads wash), Tris-base, Methanol, Dimethyl sulfoxide, phosphoric acid, Tween-20, bovine serum albumin (BSA) were obtained from Thermo Fisher Scientific UK (Loughborough, UK). Histidine, trehalose, and ammonium hydroxide were purchased from Thermo Fisher Scientific UK (Loughborough, UK), more specifically USB chemicals, ACROS Organics, JTBaker respectively. Biotin was obtained from Roche (Basileia, Swiss). The NZYColour protein marker II applied in the estimation of subunit molecular weight was purchased from NZYTech (Lisbon, Portugal). Antifoam A was obtained from Sigma-Aldrich (St. Louis, MO, USA), Bis-Acrylamide 30% was obtained from Grisp Research Solutions (Porto, Portugal). The enzyme Peptide *N*-Glycosidase F (PNGase F) was purchased from New England Biolabs® (EUA). A specific STEAP1 Elisa Kit was acquired from Abbexa Lda (Germany). All other chemicals were of analytical grade commercial available and used without further purification.

2. Methods

2.1. Strain, plasmids, and media

The plasmid pICZαB-STEAP1_His6 (Invitrogen Corporation, Carlsbad, CA, USA) was previously produced by our research group and used for recombinant STEAP1 production into *Pichia pastoris* X-33 Mut$^+$ strain (from Invitrogen, EasySelect™ Pichia Expression Kit no. 25, 2010). The *P. pastoris* transformants were selected on YPD plates (1% yeast extract, 2% peptone, 2% glucose and 2% Agar) supplemented with 200 µg/mL Zeocin™.

Pre-fermentation process was carried out in BMGH medium (2% YNB, $4x10^{-4}$ g/L biotin and 1% glycerol, 1M potassium phosphate buffer pH 6.0) supplemented with 200 µg/mL Zeocin™. The bioreactor fermentation was performed in BSM medium (20.3 mL/L H_3PO_4, 0.5g/L $CaCl_2$, 11.3 g/L $MgSO_4.7H_2O$, 3.1 g/L KOH, 40 g/L Glycerol)[146], supplemented with a trace elements solution, SMT (27 g/L $FeCl_3 \cdot 6H_2O$, 2 g/L $ZnCl_2$, 2 g/L $CoCl_2 \cdot 6H_2O$, 2 g/L $Na_2MoO_4 \cdot 2H_2O$, 1 g/L $CaCl_2 \cdot 2H_2O$, 1.2 g/L $CuSO_4$ and 0.5 g/L H_3BO_4, prepared in 1.2 M HCl) and 250 µg/mL Zeocin™.

2.2. STEAP1 biosynthesis

Pichia pastoris X33 transformed with the vector pPICZαB-STEAP1_6His was streaked and selected on YPD plates supplemented with 200 µg/mL Zeocin™, and grown at 30ºC for 3-5 days. Then, a single colony was picked and transferred to 100mL of BMGH medium in 500 mL shake flask supplemented with 200 µg/mL Zeocin™, and grown overnight at 30 ºC and 250 rpm until the optical density at 600 nm (OD_{600nm}) typically reached 5-6.

To estimate the pre-fermentation volume to collect, the next formula (3) was used:

$$OD_{pre-ferm.} \times V_{pre-ferm.} = \left(V_{pre-ferm.} + V_{ferm.}\right) \times OD_{ferm.} \quad (3)$$

The volume to be collected (under aseptic conditions) from the pre-cultivation were calculated with formula 3 in order to fix the initial OD_{600nm} at 0.5. The batch and fed-batch processes were carried out in 750mL bench-top parallel mini-bioreactors (Infors HT, Switzerland) with 250 mL of the BSM medium previously sterilized and supplemented with 250 µg/mL Zeocin and 4.35 mL/L of SMT solution. The pH and temperature were kept constant throughout the batch and fed-batch processes at 4.7 and 30ºC, respectively as demonstrated in Figure 10. The pH value was controlled by the automatic addition of 0.75 M H_2SO_4 and 12.5 % (v/v) NaOH through two peristaltic pumps. The DO (dissolved oxygen in solution) was controlled by a two-level cascade of stirring (between 500 and 950 rpm) and the air flow (between 0.2 and 2). The feed consisted of 50 % (v/v) glycerol and 100 % (v/v) methanol dissolved in MiliQ sterilized water. The different feeding profiles of methanol and glycerol, under study were maintained and controlled by the automated peristaltic pumps controlled by IRIS software (Infors HT, Switzerland).

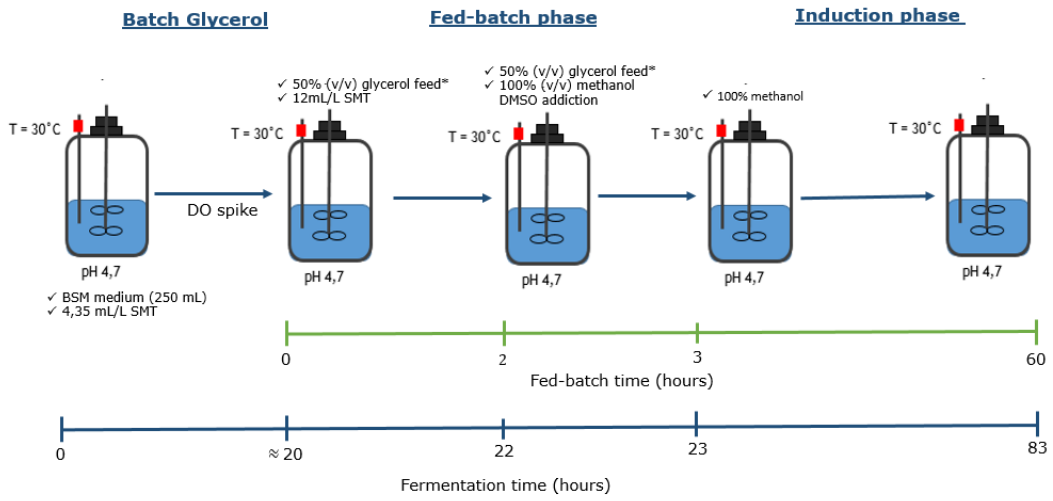

Figure 10. Structure of the production process implemented and developed for recombinant STEAP1 biosynthesis in *P. pastoris* bioreactor cultures, adapted from [121].

Unless otherwise stated, experiments were performed under three different glycerol feeding profiles -constant, exponential, and stepwise - during 3 hours of the fed-batch phase. Next, an induction phase was carried out during 60 hours with a constant methanol flow-rate. The culture was supplemented with 6% (v/v) DMSO and 12 mL/L of SMT solution at the beginning of methanol feeding [121,146]. During the fermentation process, foaming was controlled manually by the addition of the antifoam agent (Antifoam A) concentrated at 5% (v/v).

2.3. Cell lysis and Protein Recovery

The protocols for *Pichia pastoris* lysis and protein recovery were previously optimized by our research group [108]. Briefly, the cells were harvested by centrifugation for 5 minutes at 1500g, 4ºC and stored frozen at -20ºC until the samples were used. Prior to the cell lysis, a new centrifugation was performed. The cell lysis, it was performed by a combination of a mechanical and physical lysis, based on vortex-ice cycles. The *P. pastoris* suspensions were lysed in lysis buffer (50 mM Tris Base, 150 mM NaCl, 10 mM DTT, 1mM $MgCl_2$, pH 8.0), protease inhibitors (1 mM PMSF) and glass beads. The mixture was carried out in the proportion of 1:2:2 (for 1 g biomass, 2g glass beads, and 2 mL lysis buffer). It was vortexed 7 times for 1 minute with an interval of 1 minute on ice. For the removal of cell debris, a new centrifugation was done at 500g, for 5 minutes at 4ºC. A portion of lysis buffer was further added to improve the elimination of cells debris and glass beads. Subsequently, the supernatant was collected to a lysis tube, DNase (1 mg/mL) was added, and it was centrifugated at 16000g for 30 minutes at 4ºC. The pellet was resuspended in a solubilization buffer (lysis buffer plus 1% (v/v) SDS, pH 7.8) at 4ºC until full solubilization nearly 10-12 hours. The protein content on the lysate was then quantified and the samples were frozen at -20ºC for further analysis.

2.4. Total protein quantification

The total protein quantification in the lysates obtained after solubilization was quantified by Pierce BSA Protein Assay Kit (Thermo Fisher Scientific, Waltham, MA, USA). The use of bovine serum albumin (BSA) was required as standard, according to manufacturer instructions. Briefly, 10 µL of each sample, blank or standard (in triplicates) and 200 µL of WR (Reagent A and B were provided by the manufacturer) were added to each well and homogenized. The plate was then incubated at 37°C for 30 minutes (dark conditions). The 96 well plate was read in a xMark™ Microplate Absorbance Spectrophotometer (Bio-Rad) at 562nm.

For the calibration curves, several solutions of different BSA concentrations (ranged between 25-2000 µg/mL) were prepared in triplicates using the protein solubilization buffer (50 mM Tris Base, 150 mM NaCl,10 mM DTT, 1mM $MgCl_2$, pH 7.8), diluted in 1:10. Depending on sample concentration was required a sample dilution between 1:10 and 1:30. The following calibration curve was used to quantify the cell lysates:

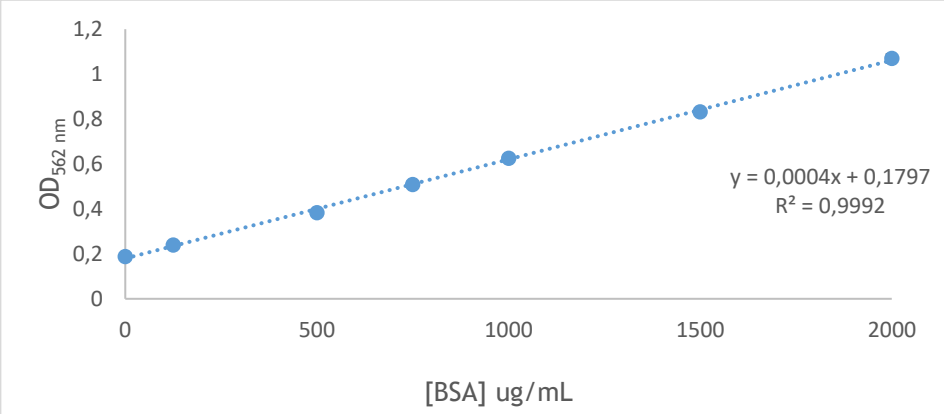

Figure 11. BSA calibration curve for total protein quantification (µg/mL) ranged between 25 – 2000 µg/mL.

2.5. SDS-PAGE and Western Blotting

The samples (50 µg of total protein) were prepared in a loading buffer [500 mM Tris-Cl (pH 6.8), 10 % (w/v) SDS, 0.02 % (w/v) bromophenol blue, 0.2 % (v/v) glycerol, 0.02 %(v/v) 2-mercaptoethanol] at a ratio of 3:1 (15 µL of sample to 5 µL of loading buffer) and denatured at 100ºC for 5 minutes. Total proteins were resolved by a 12% SDS-PAGE gel at 120 V during approximately 1 hour and 45 minutes at room temperature with a running buffer (25 mM Tris, 192 mM glycine, 0.1 % (w/v) SDS). Afterwards, the protein extracts were electrotransferred to a PVDF membrane (GE Healthcare, Buckinghamshire, UK, 6x9 cm) at 750 mA for 45 minutes in electrotransfer buffer (25mM Tris, 192 mM glycine, 10% (v/v) methanol and 10% (v/v) SDS).

Membranes were blocked during 1 hour in a 2.5% (w/v) milk solution and incubated overnight with a rabbit polyclonal antibody against human STEAP1 (sc-271872, diluted at 1:600; Santa Cruz Biotechnology, Dallas, Texas, U.S.A.) at 4ºC with a constant stirring. Then, the membranes were washed with a washing buffer (50 mM Tris, 155 mM NaCl, 0.1 % (w/v) Tween-20), and further incubated with a polyclonal antibody anti-rabbit (NIF 1317, diluted 1:40000; Santa Cruz Biotechnology, Dallas, Texas, U.S.A.) for 1 hour at room temperature with constant stirring. Finally, the membranes were washed again, exposed to ECL substrate (Biorad, Hercules, USA) for 5 minutes and visualized on the Molecular Imager FX (Biorad, Hercules, USA). When required, a gel was stained with the colloidal blue staining in a three-stage process: initially, the gel was fixed for 1 hour in a fixation solution [40%(v/v) of pure ethanol and 10%(v/v) acetic acid glacial 99%], stained by Coomassie brilliant blue overnight at room temperature over a constant stirring, and finally was incubated during 1 hour in a discoloration solution [1 %(v/v) of acetic acid glacial 99%].

2.6. Dry *Pichia pastoris* weight assessment

The relationship between the cell density (OD_{600nm}) and the dry biomass weight (g/L) of *P. pastoris* was a requirement for the calculation of the feed flow-rate (h^{-1}) applied in the exponential methanol feedings tested. The OD was measured spectrophotometrically at 600nm and the assessment of dry biomass weight was performed by adapting what was previously described by Silva and coworkers [147]. For biomass dry weight assay, aliquots (1 ml) of fermentation culture were centrifuged at 10,000 g for 10 minutes in pre-weighed tubes. The pellets were washed three times with an equal volume of 0.9% (w/v) NaCl solution. Then, the pellets were dried at 75ºC for at least 2 hours and dried slowly in a desiccator until constant weight. The dry cell weight was calculated from the average of three independent samples. A calibration curve was performed as shown in Figure 12. For *P. pastoris*, one unit of OD_{600nm} was found to correspond to 0.91 g/L of biomass dry weight.

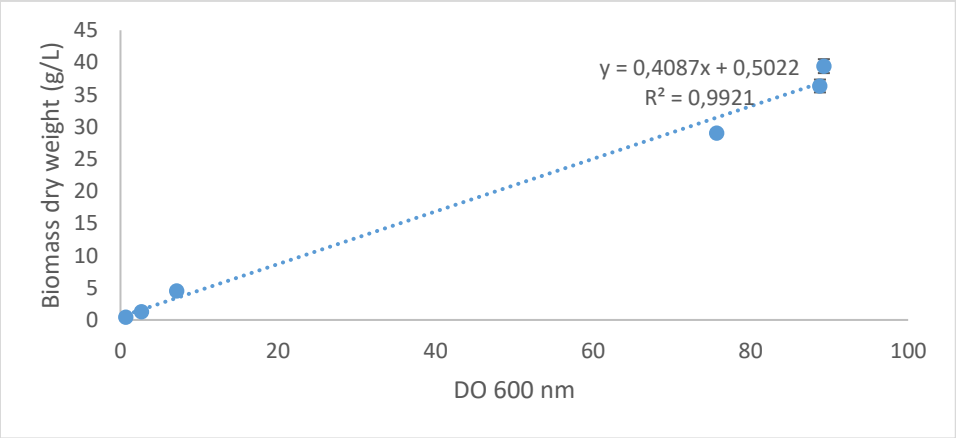

Figure 12. Relationship between $OD_{600\ nm}$ and *P. pastoris* dry weight (g/L).

2.7. Glycerol and Methanol assessment

The determination of glycerol and methanol levels in *P. pastoris* cultures supernatants were carried out in a High Performance Liquid Chromatography (HPLC) coupled with a refractive index detector (RID) [108]. The samples were previously withdrawn at specific times and centrifuged at 16000g for 5 minutes at 4ºC. The resulting supernatant was filtered on a 0.22µm filter prior to HPLC injection.

Briefly, the separation was achieved using a Hi-Plex H ion-exchange analytical column (Agilent, Santa Clara, CA, USA) with a 7.7x 300 mm and 8 µm pore size. The mobile phase consisted of a 5 mM H_2SO_4 solution prepared with MiliQ water, filtered through a 0.2 µm pore membrane and degassed for 15 minutes before use. The flow rate was set to 0.6 mL/min and column temperature at 65ºC, with an injection of 22 µL. The autosampler of RID was maintained at 4ºC to minimize the degradation of any compound in solutions.

The range of compounds detection was ranged between 0.125 to 62.5 g/L for glycerol and 0.395 to 237g/L for methanol, as show in Figure 13. The typical retention time for glycerol and methanol standards was estimated, respectively, in 13.380 and 18.331 min.

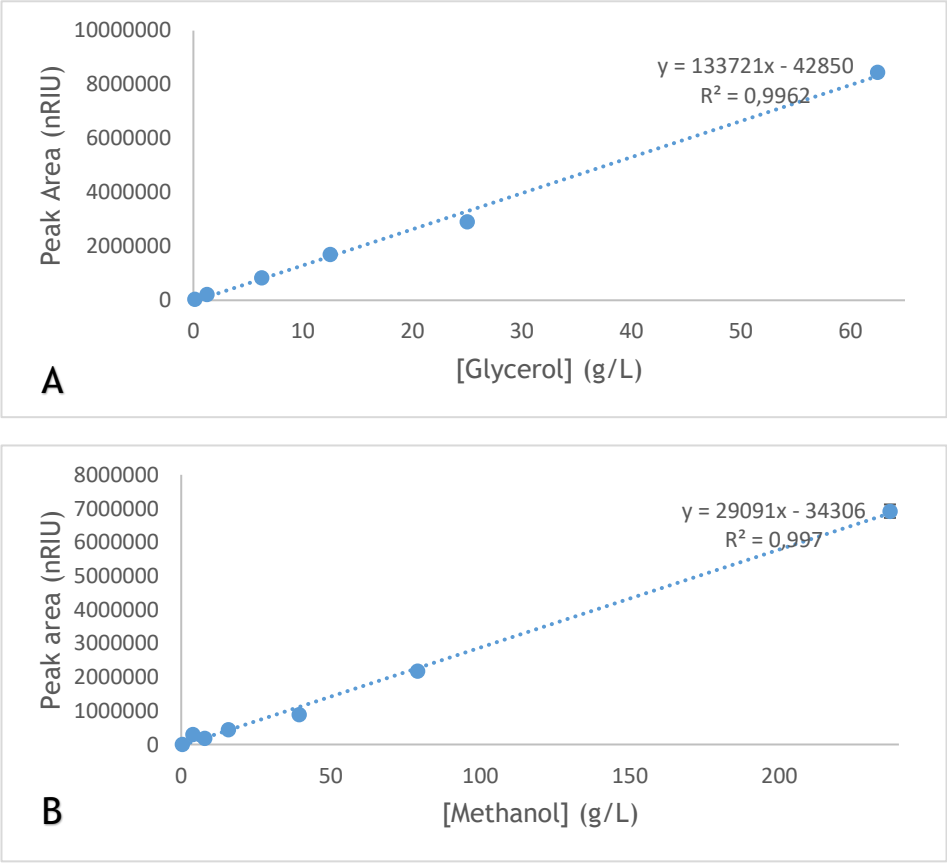

Figure 13. Calibration curves measured by HPLC-RID for A) Glycerol ranged between 0.125-62.5g/L;B) Methanol ranged between 0.395- 237 g/L.

2.8. Evaluation of *N*-glycosylation

As evidenced by the analysis using the CBS network tool NetNGlyc 1.0 (Server; http://www.cbs.dtu.dk/services/NetNGlyc/, consulted 2017/05/04 at 16:05 hours) there are two possible *N*-glycosylation sites in STEAP1 primary structure, suggesting possible PTM in Ans143, by the predicted probability. On the other hand, using the network tool NetOGlyc-3.1 (Server;http://www.cbs.dtu.dk/services/ NetOGlyc-3.1/, consulted 2017/05/04 at 16:00 hours), it was predicted several threonine residues as potential *O*-glycosylation sites but with low probability to occur. It is well described the capacity of *P. pastoris* to perform PTM, namely *N*-glycosylation. While, and based on network tool, to evaluate these PTM in STEAP1 it was used PNGase F, because this protein has specificity to react with *N*-linked glycosylation [78,113].

2.8.1. PNGase F assay

The *N*-glycosylation assay was previously adapted from the protocol manufacturer (PNGase F, 500.000 units/ml, 174P0704S, New England BioLabs®). The assay was performed under denaturing conditions. Initially, 50 µg of total protein (lysate) were added to 1 µl of Glycoprotein Denaturing Buffer (10X) and H_2O (to perform a 10 µl total reaction volume). Then, the proteins were denatured by a heating reaction at 100°C for 10 minutes, were chilled on ice and centrifuged for 10 seconds. Subsequently, was added 2 µl GlycoBuffer 2 (10X), 2 µl 10% NP-40 and 6 µl H_2O to make a total reaction volume of 20 µl. Finally, for the enzymatic reaction was added 1 µl PNGase F, and mixed gently. The mixture was incubated at 37°C for 1 hour. The reaction was stopped by heating at 100ºC for 5 minutes. The de-glycosylated proteins were resolved on a 12% SDS-PAGE gel and analyzed by SDS-PAGE and Western-Blot.

In terms of optimization, it was tested different concentrations of lysate (20 or 50 µg), the total volume used (20 or 30 µL), the amount of PNGase F (1, 3 or 5 µL) and enzymatic reaction time (1 or 2 hours).

2.8.2. Bi-dimensional electrophoresis

For better understanding, the influence of the *P. pastoris* glycosylation on STEAP1 structure and aggregation, a bi-dimensional electrophoresis (2DE) was performed. Santos and coworkers were reported that the theoretical isoelectric point (pI) of STEAP1 is 9.28 [148].Two-dimensional (2D) gel electrophoresis analysis was performed according to the literature [149].

Samples (100 µL) were precipitated using 400uL methanol, 100 µL of chloroform and 300 µL of water and obtained pellet was solubilized using 7M Urea, 2 M thiourea, 4% (w/v) CHAPS, 40 mM

DTT, 0.5% (v/v) IPG buffer and bromophenol blue. After solubilization, 300 µg of protein were separated by 2-DE analysis using Ettan IPGphor 3 System (GE Healthcare) for isoelectric focusing and the Ettan DALTSix System (GE Healthcare) for SDS-PAGE. The isoelectric focusing was performed with a 24 cm Immobiline™ DryStrip (pH 3-10), which were rehydrated overnight (16 hours) at room temperature with 450 µL of the rehydration buffer (7 M Urea, 2 M thiourea, 2% (w/v) CHAPS, 40 mM DTT, 0.5% (v/v) IPG buffer and bromophenol blue). The isoelectric focusing was performed at 20 ºC in several stages: Step 1 (1 hour at 500V), Step 2 (1 hour at 1000V), Step 3 (4 hours at 10000V) and Step 4 (2 hours and 30 minutes at 10000V) for a total of 58.62 kVh. After focusing, the Immobiline™DryStrip were stored at -80 ºC. The individual strips were then washed in the re-equilibration buffer I (150 mM Tris-HCl, 6 M Urea, 30% (v/v) Glycerol, 2% (w/v) SDS and 0.5% (w/v) DTT, pH 8.8) for 15 minutes. Afterward, dry strips were washed in re-equilibration buffer II (150 mM Tris-HCl, 6 M urea, 30% (v/v) glycerol, 2% (w/v) SDS and 4.5% (w/v) iodoacetamide, pH 8.8) for 15 minutes. These procedures were performed to resolubilize proteins and reduce disulfide bonds. The second- dimension electrophoresis was performed using a 12.5% SDS-polyacrylamide gel. The gels were run at 17 W/gel until the dye front reached the bottom of the gel. The protein spots on analytical and preparative 2-DE gels were visualized by a Blue silver Colloidal Coomassie G-250.

2.9. STEAP1 Quantification

The Elisa Kit is a quantitive test to STEAP1 detection in human serum, plasma, tissue homogenate and others biological fluids [150]. It is based on a sandwich enzyme-linked immune-sorbent assay technology. This kit was applied according to the manufacturer instructions (M1-13586, Abbexa Lda). Briefly, a specific antibody to STEAP1 was pre-coated onto a 96-well plate. It was added 100 µL of a prepared standards/sample to each well. The plate was covered and incubated at 37ºC for 90 minutes. It was discarded the liquid without a wash. It was added 100 µL of a prepared solution of Biotin conjugated antibody specific to STEAP1 (used as detection antibody), sealed the plate and incubated at 37ºC for 60 minutes. After removing the cover, the plate was washed three times. Then, was added 100 µL of a SABC (Streptavidin- HRP conjugate) working solution into each well, incubated 30 minutes at 37ºC and washed again five times. Subsequently was attached 90 µL of TMB (3,3',5,5'-Tetramethylbenzidine) substrate into each well, covered and incubated at 37ºC in dark conditions for 15-20 minutes. When a blue gradient appears in the standard wells the reaction should be stopped, by the addition of 50 µL of a Stop solution. The optical density was measured spectrophotometrically at 450 nm in a microplate reader, and then the concentration of STEAP1 was calculated.

The more denoted characteristic of this test is the sensitivity (< 0.234 ng/mL) and the low detection limits ranged between 0.39 ng/mL – 25ng/mL. Depending on sample concentration was required a sample dilution of 1:10 000 and 1:15 000. The following calibration curve was used to quantify the cell lysates:

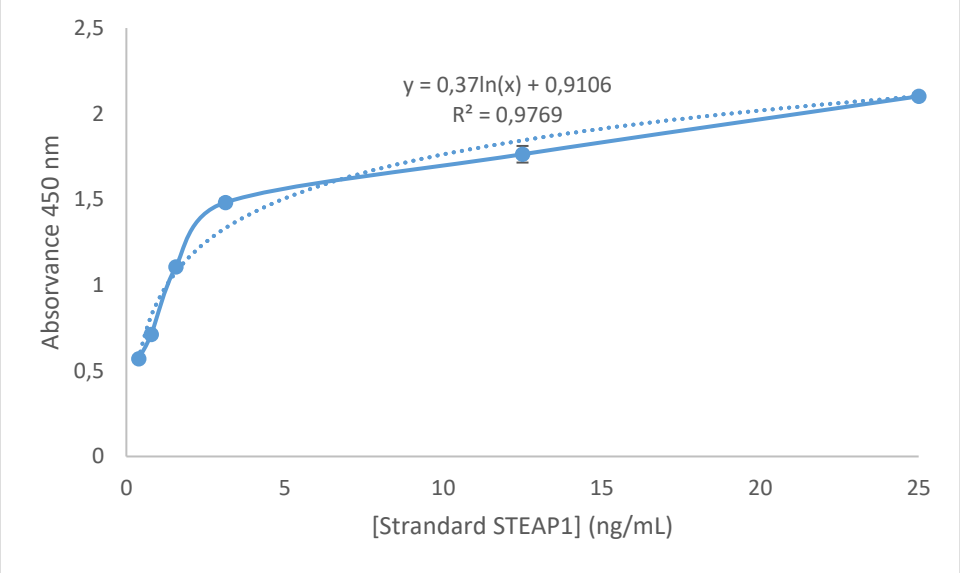

Figure 14. Typical standard ELISA curve, ranged between 0.39ng/mL to 25 ng/mL

Chapter IV – Results and Discussion

To perform structural and functional studies it is important to obtain high quantities of STEAP1 as close as conceivable to the native form. Using the yeast *P. pastoris,* as host, it can be possible to produce high quantities of a target protein in a short time. Therefore, the main aim of the work was the development of an adequate up-stream strategy to enhance the STEAP1 biosynthesis in mini-bioreactors *P. pastoris* X33 cultures. So, the proposal to enhance STEAP1 production was through the application of a fed-batch process, in order to increase the cell density and, consequently the protein production. Briefly, an initial glycerol batch fermentation was carried out, in order to know the length of this stage and establish the initial culture conditions. Next, a series of fed-batch fermentations with different feeding strategies were tested and analyzed to obtain the maximum of biomass levels and STEAP1 biosynthesis.

1. Setting up the batch phase

In the last years, our research group reported the optimization of several conditions for bioreactor fermentations [121]. Indeed, it was fixed several fermentation parameters, as DO set point at 20%, stirring at 500 rpm (at the begin), pH 4.7, temperature at 30ºC, BSM medium composition, and SMT composition [121,146,151,152]. Also, a constant glycerol and methanol feedings were fixed at 18,54 mL/L/H and 2.9 mL/L/H, respectively [121]. These parameters were the starting point for the strategy described in this study.

Since the optimization was performed in bench-top parallel mini-reactors, the stirring control is based on the DO concentration in medium and is related to the carbon source consumption and yeast growth. Therefore, the DO levels in the culture media were maintained at 20% by automatic adjustment of the agitation rate and the airflow. The agitation was constantly increased from 500 rpm to 950 rpm, followed by a constant increase of air-flow from 0.2 to 2 vvm (that start when maximum agitation is reached). The DO concentration is the most common parameter applied to decide when the fed-batch phase should start. Indeed, when occurs a sharp increase in the DO is a signal of the glycerol exhaustion and consequently the end of the batch phase [101,153].

The glycerol concentration in the medium is a critical parameter once that it is used as carbon and energy source. However, some studies proved that glycerol concentration higher than 40 g/L could inhibit the *P. pastoris* growth [101]. Initially, a typical batch run was performed and it was found that the glycerol levels decrease to the basal levels after 20 hours of the batch phase.

The initial glycerol concentration at the beginning was close to 40g/L (as presented in Figure 15) and then decrease over the fermentation cycle until basal concentrations, close to 2 g/L.

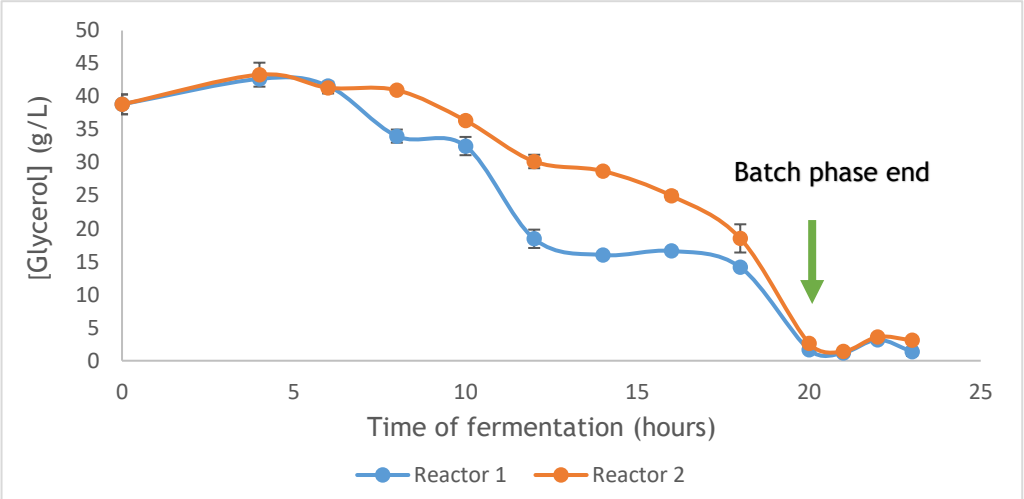

Figure 15. Residual glycerol concentration (g/L) measured by HLPC- RID during the batch fermentation (hours).

On the other hand, the biomass levels increase over the time until they reach a maximum of 25 g/L after 20 hours of the glycerol batch phase, as presented in Figure 16. Cos and coworkers previously reported a biomass dry weight close to 20g/L at the end of glycerol batch phase [101]. Although, other studies suggest a biomass concentration close to 28 g/L, being close to the values obtained in the work [109,124]. For this reason, the batch phase for the posterior fermentation was fixed close to 20 hours.

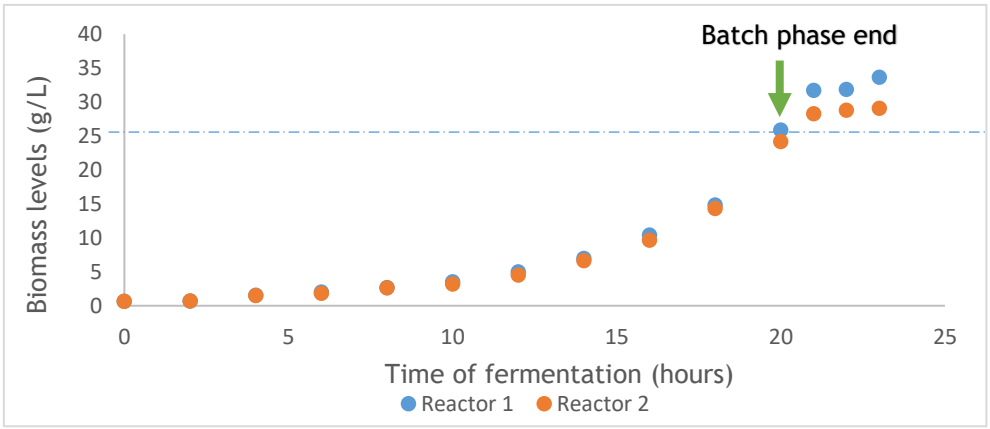

Figure 16. Biomass profile (g/L) over the glycerol batch phase (hours).

2. Optimization of the Fed-batch phases

Next, different glycerol feeding strategies were carried out, aiming to improve the biomass levels and adjust the *P. pastoris* cells to methanol induction, namely the expression of proteins involved in methanol metabolism.

This stage is composed of a glycerol fed-batch and a transition phase, which lasts for 3 hours. The glycerol fed-batch lasts for 2 hours with the purpose to control the *P. pichia* cells growth at limited rates. During this period, a 50% (v/v) glycerol solution was used to fed the culture, under different feeding strategies - constant, exponential, or stepwise.

The next stage is a transition phase that lasts 1 hours. During this stage, occurred a mixed feed with 50% (v/v) glycerol (for each feed profile described before) and 100% (v/v) methanol constant feeding fixed at 2.9 mL/L/H. During this hour arises a slowly de-repression of the AOX1 promoter. This behavior over the transition phase reveals more effective in comparison with shake flasks fermentations, once there is a slow change of *P. pastoris* phenotype for consequent methanol adaptation [153].

In this study, the flow rate for the constant glycerol feed was established at 18.54 mL/L/H, according to what was previously reported by our research group [121]. Therefore, for each feeding strategy being tested, the same volume of glycerol was added to the culture during a period of three hours. The time course profile of STEAP1 production for each glycerol feeding was performed during fixed intervals along the 60 hours of methanol induction with 100% (v/v) constant methanol feeding.

2.1. Constant feed profile

During the glycerol fed-batch and transition phase, a constant glycerol feed was tested with a fixed flow-rate at 18.54 mL/L/H. Following that, a methanol induction phase over 60 hours with a constant flow-rate was fixed at 2.9 mL/L/H. In agreement with the Figure 17, until the 20 hours of glycerol batch-phase, the biomass concentration enhances and the glycerol levels decrease. After the glycerol fed-batch phase, *P. pastoris cells* seem to enter in a stationary phase at 23 hours of fermentation. Then, at 20 hours of methanol induction was denoted a decrease of biomass growth until the end of fermentation, in total of 83 hours. The glycerol levels increase during the fed-batch process until a maxim value of 3.88 g/L at 2 hours of glycerol feed.

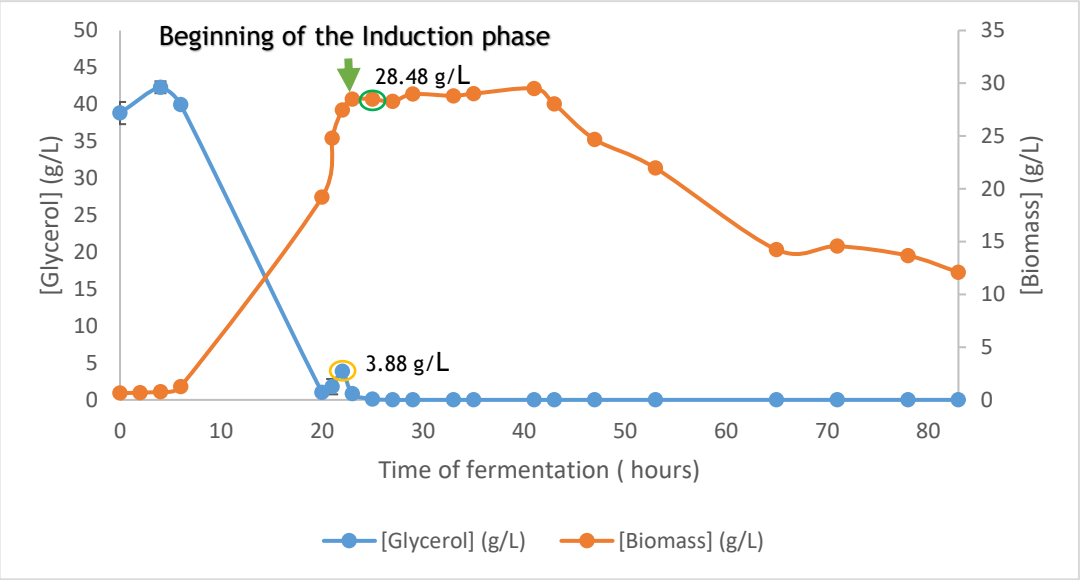

Figure 17. Glycerol concentration (g/L) and biomass profile (g/L) over 60 hours of methanol induction for the constant glycerol feed.

For quality control, samples were taken over 60 hours of methanol induction and lysed using the mechanical glass beads process. To better compare the STEAP1 production over the time, the same quantity of total protein - 50 µg - was analyzed by Western blot (WB). Using a specific antibody against STEAP1, a band was found at 48 kDa, as shown in Figure 18. Since the STEAP1 correct molecular weight is approximately 35 kDa [49,61]. Our results suggest the eventual existence of a different *N*-glycosylation pattern than the native, which could be responsible for an increase in the molecular weight. As demonstrated in the Figure 18, highest levels of STEAP1 were obtained at 2 hours of methanol induction, comparing the bands densitometry. Regarding the Figure 17, the glycerol was not detected at 2 hours of methanol induction and the biomass levels keep close to 28,48 g/L (final DO_{600nm} was 69.3). After 6 hours of methanol induction, STEAP1 expression seems to decrease as verified in previously work related with the STEAP1 expression in shake flasks.

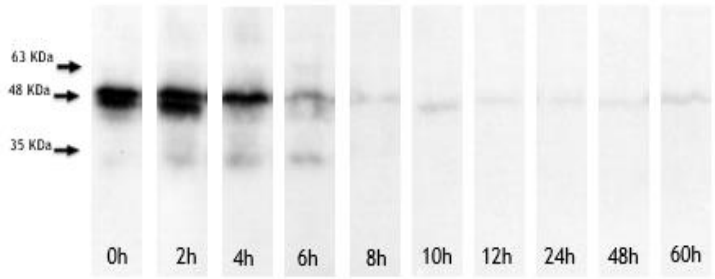

Figure 18. Western blot analysis of STEAP1 expression during a constant glycerol feed with 60 hours of methanol induction.

Also, it was obtained a high production at 0 hours of methanol induction. It was an unexpected result once that the induction time is too short to promote the STEAP1 biosynthesis. However, Bawa and coworkers suggest similar results, namely the production of the Human A2a adenosine receptor and the Green fluorescent protein, in pre-induction phases using *Pichia pastoris* cultures, as consequence of a mixed glycerol/methanol or glucose/methanol feeds [153].

2.2. Exponential feed profile

Characteristically, in an exponential feed, the flow-rate was increased exponentially. So, during the fed-batch phase, the flow rate of glycerol was 3.45 mL/L/H at the first hour, 9.48 mL/L/H in the second and 42.8 mL/L/H in the last hour.

The results in Figure 19 show that after 60 hours of induction with a constant methanol feed there is a spike in biomass production at 35 hours of fermentation (12 hours of induction) and then a decrease until the end of fermentation. Highest levels of STEAP1 were obtained at 5 and 8 hours of methanol induction as denoted in Figure 21. The DO_{600nm} for each duplicate at 5 hours of induction was 76.2 for reactor 1 and 81.9 for reactor 2, 31.27g/L and 33.58 g/L, respectively for biomass concentration. At 8 hours of methanol induction, the DO_{600nm} was 80.1 for reactor 1 and 83.6 for reactor 2. In this case, high biomass levels are not synonymous with high protein production.

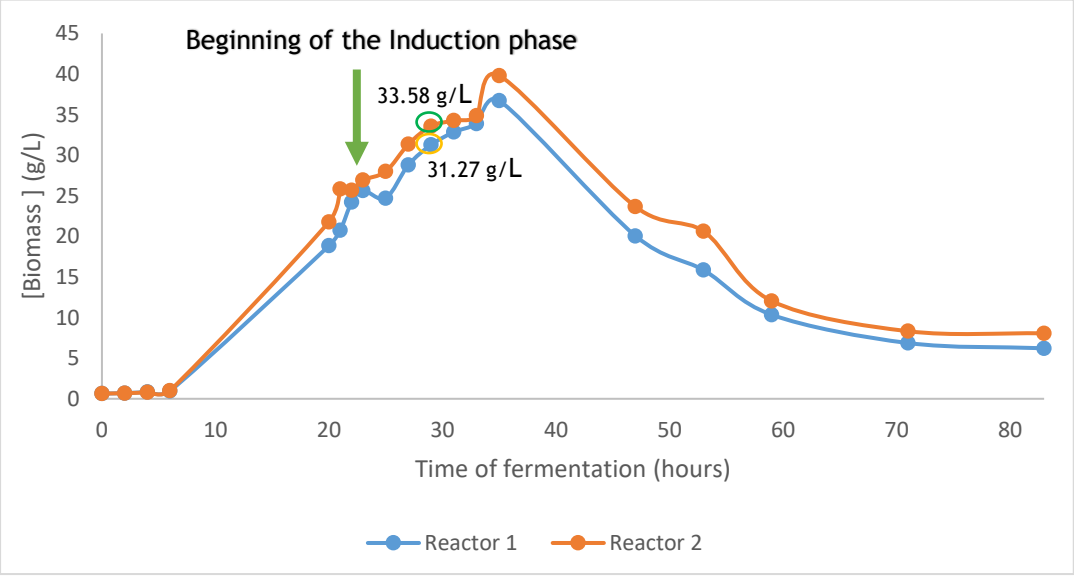

Figure 19. Biomass levels (g/L) for the reactor 1 and 2, over 60 hours of methanol induction for a typical exponential glycerol feed.

Concerning to the glycerol levels, higher concentrations were obtained at 2 hours of methanol induction (25 hours of fermentation, 8.28 g/L) and at the end of transition phase (23 hours of fermentation, 7.65 g/L) for the reactor 1 and 2, respectively. These differences may be due to the stressful condition that *P. pastoris* cells were exposed. The glycerol was detected until 8 or 10 hours of methanol induction, as demonstrated in Figure 20.

.

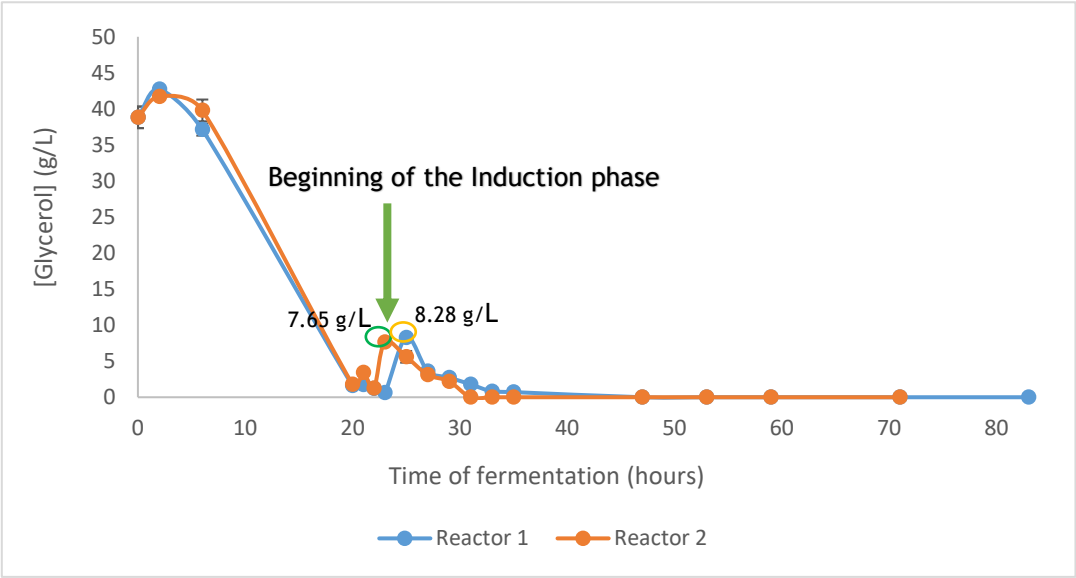

Figure 20. Glycerol concentration (g/L) in reactor 1 and 2, over 60 hours of methanol induction for the exponential glycerol feed.

As mentioned, based in the analysis of band densitometry, the higher STEAP1 obtained for a glycerol exponential feed was obtained at 5 and 8 hours of methanol induction. In these conditions, all the protein produced is in the correct molecular weight (~35 kDa) as demonstrated in the Figure 21.

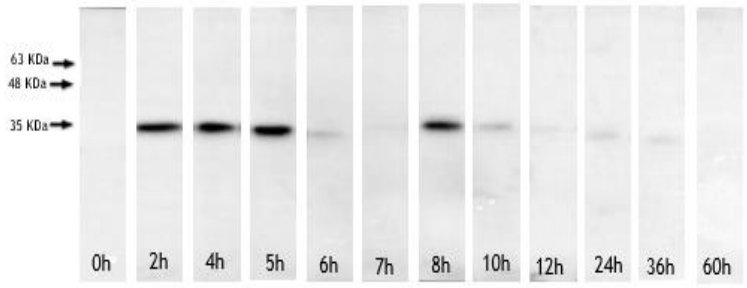

Figure 21. Western blot analysis of STEAP1 expression during an exponential glycerol feed with 60 hours of methanol induction.

2.3. Gradient feed profile

In the stepwise glycerol feed, the flow rate was gradually increased. So, the flow rate was 14.6 mL/L/H at the first hour, 18.6 mL/L/H in the second and 22.6 mL/L/H in the last hour. Both duplicate have an identical behavior during the glycerol fed-batch process, as shown in Figure 22. In this case, it was verified a growth during the fed batch phase. Unless constant and exponential feed, with this strategy there are several "biomass spikes" during the fermentation process at 2, 6 and 12 hours of induction. The DO_{600nm} spikes obtained were 86.7, 88.9, 86.3 and 71.8, 75.5 and 76.5 for the reactor 1 and 2, respectively. As denoted in Figure 24 high STEAP1 production at 10 hours of methanol induction. At this time, the DO_{600nm} for each duplicate was 81.7 for reactor 1 and 68.8 for reactor 2 that correspond at biomass level of 33.5 g/L and 28.2 g/L, respectively.

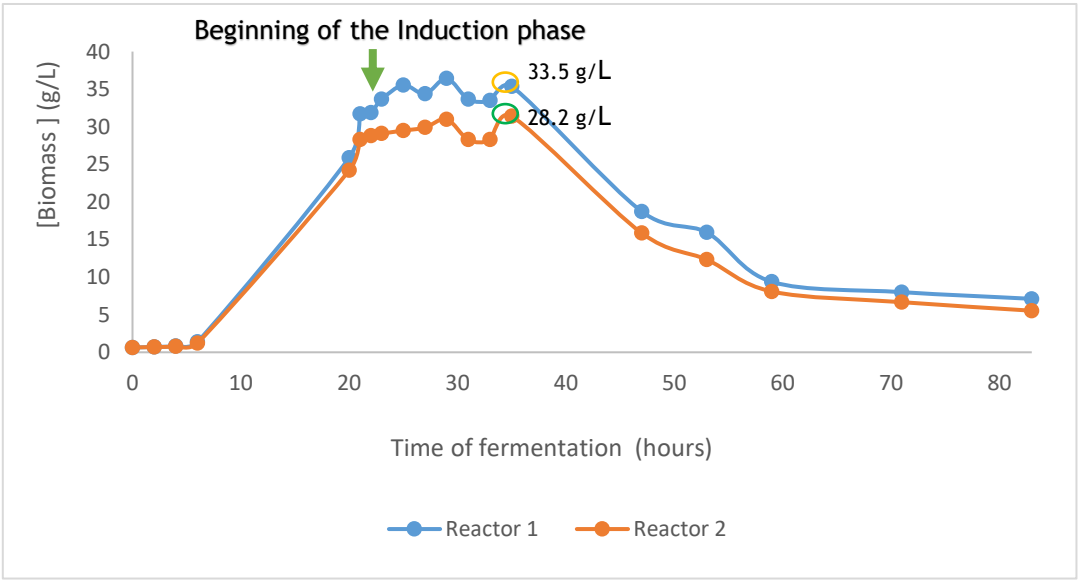

Figure 22. Biomass levels (g/L) over 60 hours of methanol induction for the gradient glycerol feed in reactor 1 and 2.

The glycerol concentration in reactor 2 increased more drastically during the fed-batch phase. The residual glycerol concentration reached its peak (6.7 g/L) at 2 hours of methanol inductions.

Regarding the reactor 1, the maximum value of glycerol in solution is 3.18 g/L at 2 hours of the glycerol fed-batch. The glycerol was detected in solution until the 4 hours of methanol induction, between 1.26 g/L to 1.33 g/L.

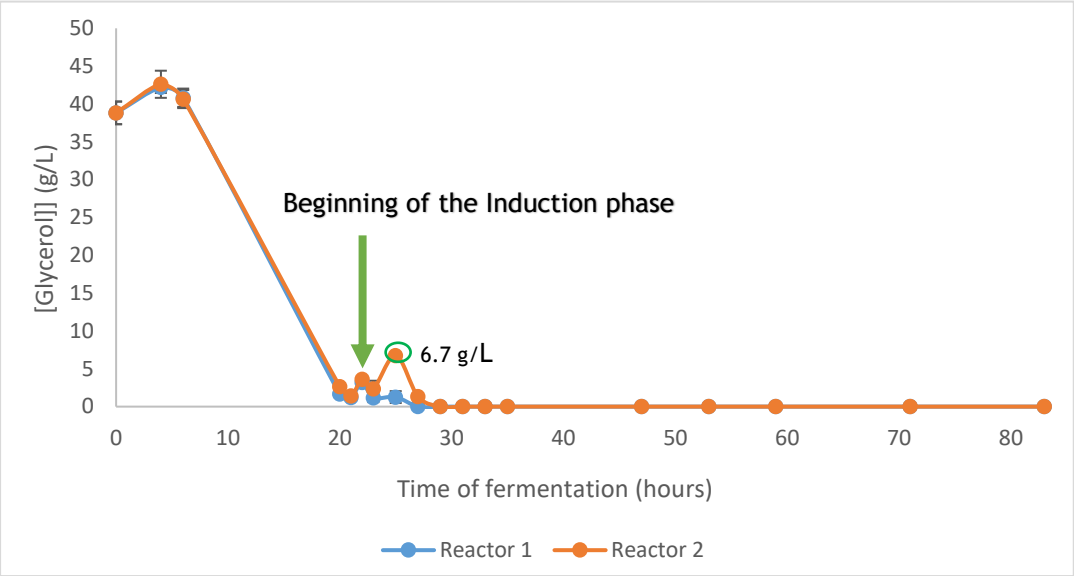

Figure 23. Glycerol concentration (g/L) in reactor 1 and 2, over 60 hours of methanol induction for a typical gradient glycerol feed.

As demonstrated in the Figure 24, it was obtained for the gradient glycerol feed a spike of STEAP1 production at 10 hours of methanol induction. In these conditions, the protein produced was at the correct molecular weight (~35kDa) but as well some proteins aggregates were detected at 63 kDa. Also, is denoted an immunoreactive band at 48 kDa, which may be due to an eventual glycosylation of STEAP1. There is STEAP1 production almost all hours tested since the 2 hours of methanol induction.

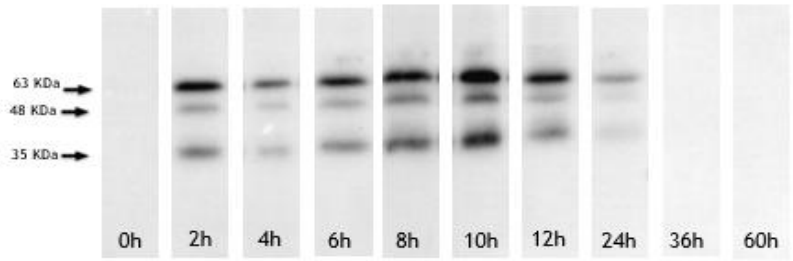

Figure 24. Western blot analysis of STEAP1 expression during a gradient glycerol feed with 60 hours of methanol induction.

2.4. Comparison of the three feeds

By comparing these three glycerol feedings strategies, it was possible to conclude that different fermentation conditions, affect *P. pastoris* metabolism in different ways, and consequently STEAP1 aggregation and/or PTMs (Figure 25). Based on bands immunoreactivity and density analyzed by WB, it was concluded that a gradient glycerol feed produces high quantities of STEAP1 at 10 hours of methanol induction. Nevertheless, some dimers are produced (~63kDa). With a constant glycerol feed, it was produced high amounts of STEAP1 with a higher molecular weight (~48kDa) at 2 hours of methanol induction. The different immunoreactive bands acquired by WB can be due to eventual modification in the STEAP1 structure by *N*-glycosylation. The exponential glycerol feed produces with 5 hours of methanol induction acceptable quantities of STEAP1 in the correct molecular weight (~35kDa). The replicates for exponential and gradient glycerol feed, and the SDS-PAGE of each glycerol feeding profile of STEAP1 expression were shown in Appendix 1 and 2, respectively.

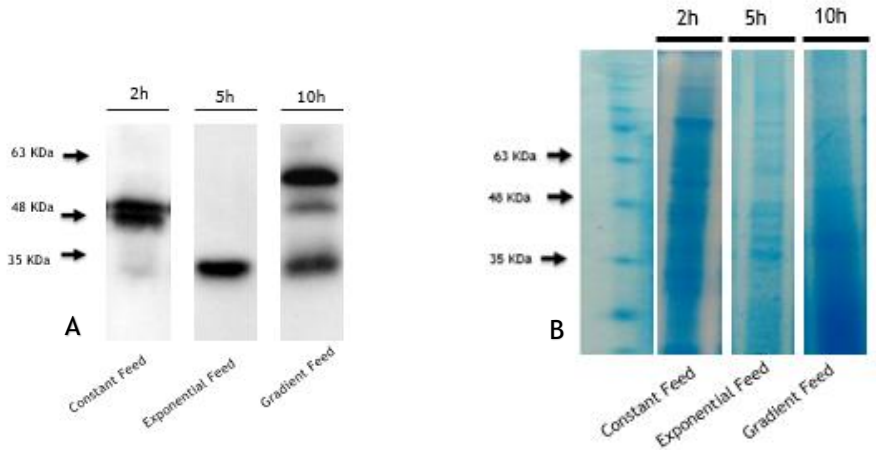

Figure 25. Analysis of the spikes of STEAP1 production with a glycerol constant (2h), exponential (5h) and gradient (10h) feed: A) Western blot, B) SDS-PAGE.

The medium biomass levels and $OD_{600\,nm}$ obtained for the feeds in the study ranged between 25-40 g/L and 46–82.1, respectively. Indeed, some authors suggest that biomass concentration (dry cells weight) at the beginning of the induction phase is a critical factor, once they recommend that the dry cell weight at the end of transition phase should be in the interval 30 – 50 g/L [101,122].

Comparing the biomass concentration at the end of fermentation process was 28.4, 30.5 and 30.75g/L for the constant, exponential, and gradient glycerol feed. These values seem to be involved in protein biosynthesis. However, the biomass peaks it is not necessarily related with a higher STEAP1 biosynthesis.

Relatively to the glycerol concentration in medium fermentation, it was shown that for exponential glycerol feed was ranged between 0.7- 7 g/L during the first 10 hours of induction. For the constant glycerol feed close to 0.15 g/L during the first two hours of induction. Finally, for the gradient glycerol feed ranged between 1.26-1.3 g/L for 4 hours of methanol, seen more closely in Figure 26. Therefore, residual glycerol concentration in solution seems do not repress STEAP1 expression. Also, it is supposed to be involved in STEAP1 stability, acting as chemical chaperone [101,133].

.

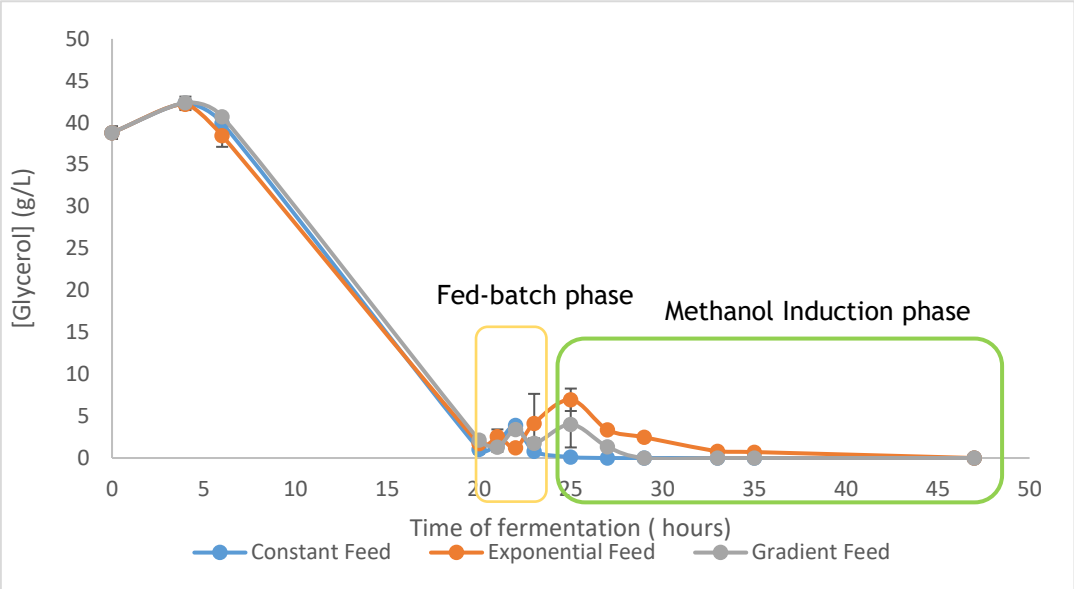

Figure 26. Residual glycerol concentration (g/L) in the different glycerol feeding tested.

Bawa and coworkers showed that a glycerol concentration of 3.0 g/L enhances the recombinant green fluorescent protein production in the pre-induction stage, suggesting the capacity of residual glycerol concentration to de-repress AOX expression. Also, it shows the important role in the support of P.pastoris growth [153].

Concerning the methanol levels, as shown in Figure 27, the beginning of measurements occurred at the methanol induction phase. Typically, methanol remains during the first hours of induction at low concentration. For the constant glycerol feed, the methanol concentration was maintained in residual values, close to 1.3 – 2.9 g/L during the first two hours of methanol induction. In the exponential feed was ranged between 3.75 - 5.06 g/L. For the gradient feed was maintained between 2.9 - 8.3 g/L during the first 10 hours of methanol induction. Briefly, as denoted in Figure 27 the methanol concentration stabilizes several hours during the three fermentation staategies and after approximately 30 hours of induction enhances to toxic values, close to 23.6 – 30.92 g/L.

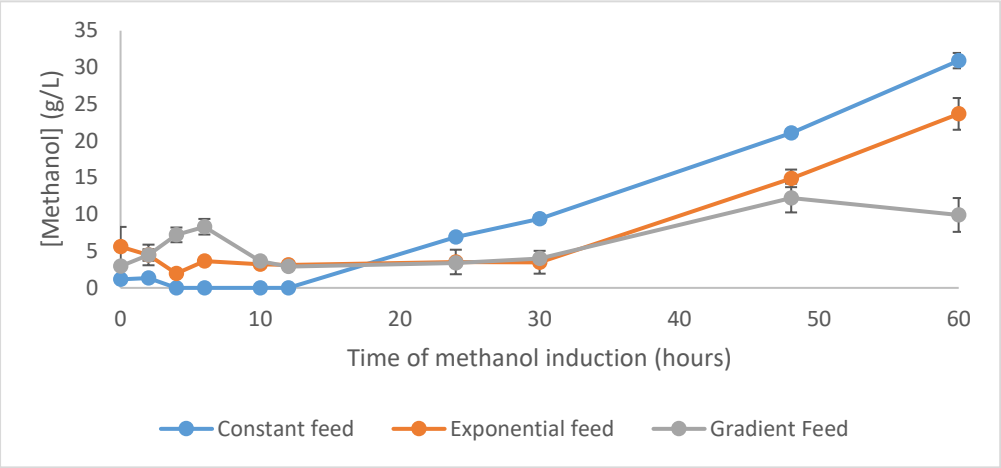

Figure 27. Residual methanol concentration (g/L) in the different glycerol feeding tested during the methanol induction.

As mentioned above, in the induction phase, methanol acts both as the carbon source and as an inducer of protein expression. Although an accumulation of methanol is toxic to the cells, a complete methanol depletion is undesirable, highlighting the importance of finding and maintain an optimal balance. Some authors reported an enhanced productivity when the residual methanol concentration is controlled at 0.4g/L, 3.7 g/L or between 4-30 g/L [101,154,155]. Parallelly, Cunha and coworkers showed that the specific methanol uptake may influence recombinant protein expression. It was denoted that the production rate of scFv antibody fragment increases linearly with lower specific methanol uptake rates as consequence of methanol concentration [128]. Also, it was reported that a residual methanol concentration ranged from 3.01-8.52 g/L enhance the production of some antibodies [153]. Trinh and coworkers have studied the effect of different methanol feeding strategies on the yield of recombinant endostatin. The higher efficiency of methanol utilization at the predetermined exponential rate suggests that this solvent is directed mainly towards energy generation and that only a small portion is directed to biomass production when used as sole carbon source [101,156]. So, it is suggested that a residual glycerol concentration in the first hours of induction could form a kind of mixed feed with the methanol. During this process, glycerol could be used as a carbon source and the methanol as an energy source for the next phases [101,157].

Typically, during the methanol adaptation (the transition phase), *Pichia pastoris* behavior is changed with different glycerol-methanol feed ratios. At this stage enhances the expression of enzymes involved in methanol pathways and in the citric acid cycle for posterior methanol uptake and metabolism. This is expected for low values of glycerol-methanol ratios [107,158].

As mentioned above, a good parameter to be applied for a fed-batch process evaluation is the growth rate of the strain under the different conditions tested. The specific growth rate (μ in h^{-1}) is a parameter for designing and compare an appropriate and specific upstream strategy.

Knowing that $N(t) = OD_{600nm} \times V_T$ and regarding the growth rate, μ (h^{-1}), it can be calculated by the equation (4):

$$\mu\,(t) = \frac{\ln(N_t) - \ln(N_0)}{t} \quad (4)$$

N_{ot} OD_{600nm} or dry cell weight (g/L)
N_0 OD_{600nm} or dry cell weight (g/L) at the beginning of the fermentation
t time (hours)

So, in this case, the growth rates obtained for each feeding strategy are depicted in Table 1.

Table 1. Specific growth rate of each glycerol feed during the glycerol fed-batch and methanol phase.

μ (h-1) in each carbon source

Glycerol feed	*Glycerol Fed-batch*	*Methanol induction*
Constant	0.149	0.011
Exponential	0.086	0.045
Gradient	0.083	0.008

Comparing the *P. pastoris* specific growth rate (Table 1) of each glycerol feed during the fed-batch the constant feed lead to the higher value, close to 0.149 h^{-1}. The medium value of each duplicate of the others feeds it was 0.086 h^{-1} and 0.083 h^{-1} for the exponential and gradient feed, respectively. It was described that 0.18 h^{-1} as the maximum specific growth rate of wild type *P. pastoris* growing on glycerol. It was reported that recombinant Mut^+ strains growth in excess of methanol at a wide range of μ from 0.001 h^{-1} to 0.14 h^{-1}, and Mut^S strains at 0.011 h^{-1} to 0.035 h^{-1} [122]. The results obtained to specific rate growth in the fed-batch phase were close to the values suggested by the literature, even though the *Pichia* cells in stressful fermentation conditions.

As for the specific growth rate during the methanol induction, the values obtained are not close to the minimum or the maximum value. Also, it was described that the specific growth rate in methanol is generally lower when *Pichia* produces heterologous protein because of the negative effect that these have on the microorganism growth [101]. In addition, the STEAP1 is a protein

related to carcinogenesis, it presence into *Pichia* cells may promote some influence in it growth.

It was suggested that higher specific growth rates mean a high biomass density and consequently high recombinant protein expression and yield [122] . However, the feed that presents more STEAP1 expression, the gradient glycerol feed ($\mu = 0.083\ h^{-1}$), corresponds to the lower specific growth obtained. Some authors suggested that this might be due to the lower growth rate producing lower biomass and therefore fewer extracellular proteases being present in medium cultivation [159].

Our results, therefore, suggest that the productivity is not solely reliant on methanol induction but also is important to study the impact on the specific productivity of pre-induction phase cultivation.

3. Optimization of fermentation conditions

Based on the previous results, it was chosen the bests glycerol feeding profiles to perform an improvement in STEAP1 productivity.

Thereby, starting from the beginning that the glycerol gradient feed produces high amounts of STEAP1 with some dimers, it was studied the different concentrations of Proline, Trehalose, and Histidine to improve the productivity. Likewise, the fermentation was stopped at 10 hours of methanol induction, the lysis process was carried out and analyzed by WB. It was suggested that a mixed chaperone solution is more advantageous, promoting several interactions between the host/chaperone or protein/chaperone [133]. Until now, DMSO reveals a good effect to promote protein folding but is not sufficient. Thereby, in this work, mixed solutions of DMSO and the compound described above were tested.

The change from a constant methanol feed to an exponential feed was described as a good option. Jahic and coworkers suggested that an exponential methanol feed during the induction phase enhances exponentially the AOX1 expression and consequently protein production [109]. In order to improve STEAP1 biosynthesis, it was studied an exponential methanol feeding during the induction phase for a gradient and exponential glycerol feed.

3.1. Chemical chaperones

3.1.1. Proline

Several studies showed a positive effect of proline on protein stabilization and as a supporter of *E. coli* growth under high osmolarities [143]. A similar supplementary effect of potassium ion was observed for the activities of proline uptake under high osmolarity, suggesting that proline acts at both respiration and uptake of some carbon sources, being suggested that it is efficient in concentrations ranging from 0.1 to 4 M. This reinforces the idea that proline may act as a possible chaperone that solubilizes the native state of an aggregation when interacting with the early aggregates of proteins and support host growth [133,143]. However, few studies have been done using proline as chaperones in *P. pastoris* cell cultures, the maximum concentration tested within this work was fixed on 1M proline. In fact, three different proline concentrations, 0.2M, 0.5M, and 1M were evaluated and it was observed that proline 1M is the most effective concentration, producing high quantities of monomeric STEAP1 and, hence with less aggregation, as shown in Figure 28.

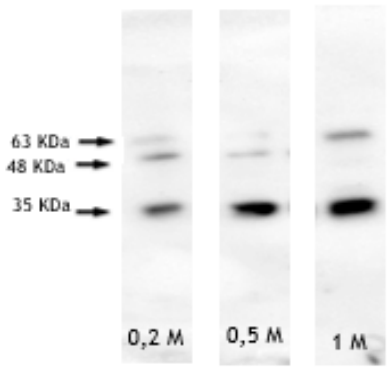

Figure 28. Western blot of the different proline concentrations tested: 0.1 M, 0.5 M, and 1 M, respectively.

According to the bands densitometry, as shown in Figure 28, low proline concentration could act as an insufficient carbon source, hence producing less amount of STEAP1. Otherwise, proline seems to act as both, carbon source and chemical chaperone at higher concentrations. As mentioned above, its functions and uptake in the cells seems to be associated with the presence of some ions. Thereby, proline efficiency could be explained due to the use of the SMT solution at the beginning of induction phase, promoting its uptake.

3.1.2. Histidine

It was described the use of histidine as a possible chaperone, acting as a physiological effector in metabolic regulation. It could form coordination complexes with metal ions of the proteins. Andre and coworkers reported the use of 0.04 mg/mL of histidine for enhancing functional production of G protein-coupled receptors into *P. pastoris* cultures [133,160]. Thus, two different histidine concentrations were studied, 0.04 mg/mL and 0.08 mg/mL. Comparing the two concentrations, 0.08 mg/mL seems to be the best option, as observed in Figure 29. Medium supplementation with 0.08 mg/mL seems to produce fewer dimmers aggregation (Figure 29, B2).

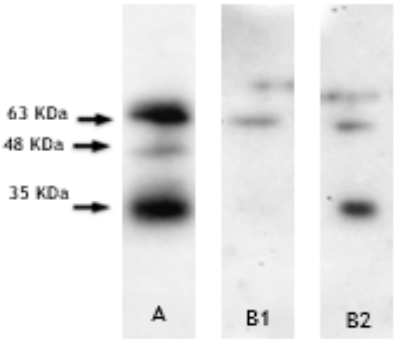

Figure 29. Western blot of the several histidine concentrations tested: A) 0.04mg/mL; B1 and B2) Comparation between 0.04 mg/mL and 0.08 mg/mL histidine, respectively.

It was reported that histidine may act as physiological "antioxidant"/ osmotolerant and protect the cells and proteins. Histidine would help for the recombinant protein production or protect the cells from toxic side effects of the recombinant protein. However, there has been a few reports about the effect of histidine on culture media formulation[137,160].

3.1.3. Trehalose

The disaccharide trehalose has a high affinity for water molecules and hence stabilizes partially unfolded protein molecules unspecifically and inhibits protein aggregation. Several authors related the use of trehalose as an endogenous osmoprotectant in *E. coli* cultures [161]. Also, it was studied the protective effect of trehalose during the heat shock in *S. cerevisiae* cells [162]. Moreover, it was also documented that trehalose acts as a chemical chaperone by suppressor of aggregation of denatured proteins [133,161–163]. Han and coworkers studied the *in vitro* protective effects of several osmolytes on yeast alcohol dehydrogenase conformational stability and aggregation. They studied the trehalose concentration between - 0.25, 0.5, 0.75 and 1.0 M and denoted that higher trehalose concentration provides the best results [164].

Besides, another study suggests that when the medium was supplemented with 0.5 M of trehalose reduce both the rate of reactivation and the yield of the renatured protein was reduced [163,164].

Therefore, we studied three different trehalose concentrations, 0.1 M, 0.25 M, and 0.5 M. The concentration of 0.1M showed the best results with fewer dimers produced, while that 0.25M produces STEAP1 degradation. The medium supplementation with 0.5 M of concentration produces fewer amounts of STEAP1 in comparison with the other concentrations tested, Figure 30.

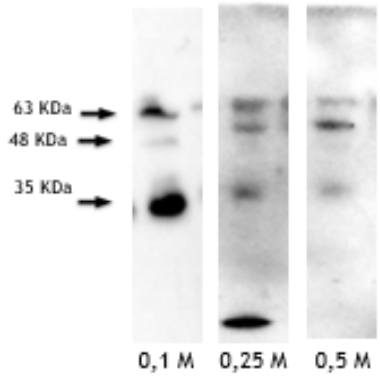

Figure 30. Western blot of the three trehalose concentrations tested: 0.1 M, 0.25 M and 0.5M, respectively.

It was further shown by the band densitometry analysis that trehalose seems to stabilize STEAP1 and attenuated the aggregation at low concentrations (0.1M). These results match with previous *in vitro* and *in vivo* studies, but further studies are needed [133,144,164].

3.1.4. Comparison of the 3 chaperones

A comparative WB was carried out in order to understand which of the chaperones in the study produces more amounts of STEAP1 in the correct molecular weight, Figure 31. Briefly, analyzing the bands densitometry all chaperones showed an improvement of STEAP 1 expression unless Trehalose at 0.25 M and 0.5 M. Proline seems to be the best choice, working both as chaperone and carbon source. Also, 0.1 M of trehalose and 0.08 mg/mL of histidine reveal an acceptable monomeric band in comparison with the original glycerol gradient feed. All the experimental point mentioned, which are in duplicated, are shown in Appendix 2.

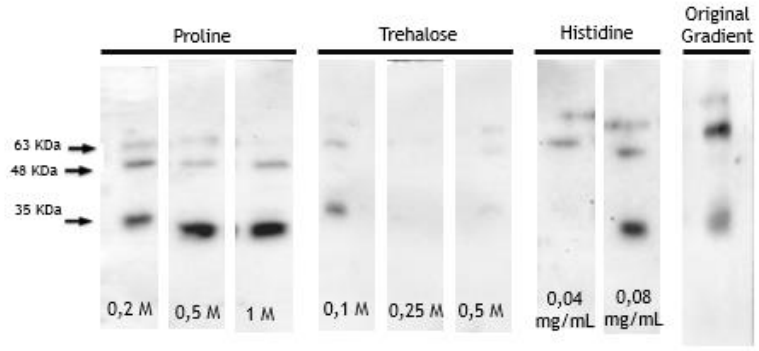

Figure 31. Comparison of WBs obtained in the original glycerol gradient feed and glycerol gradient feed supplemented with different concentrations of chaperones: Proline, Trehalose, and Histidine.

Also, the comparison by SDS-PAGE of the cell lysate shown that the application of chaperones decreases the presence of host proteins comparing with the original glycerol gradient feed, Figure 32.

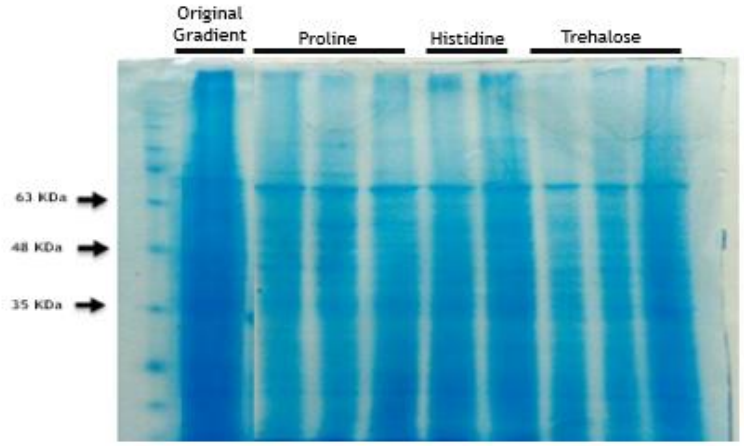

Figure 32. Comparison by SDS-PAGE of the original glycerol gradient feed and glycerol gradient feed supplemented with distinct concentrations of chaperones: Proline, Trehalose, and Histidine.

As demonstrated in Table 2, all the chemical chaperones tested, unless histidine at 0.08 mg/mL, showed higher optical densities in comparison with the original glycerol gradient feed, 81.7 and 68.8 for reactor 1 and 2, respectively.

Table 2. The relationship between DO_{600nm} and the different chaperone concentration tested.

Different chaperones concentration		*R1*	*R2*
Proline	0.2 M	*113.0*	*118.2*
	0.5 M	*90.3*	*92.9*
	1 M	*107.4*	*117.8*
Histidine	0.04 mg / mL	80.6	76.5
	0.08 mg/ mL	52.2	47.4
Trehalose	0.1 M	89.3	88.3
	0.25 M	*87.9*	*99.2*
	0.5 M	*79.4*	*78.1*

It was carried out a relative quantification of STEAP1 between the original gradient feed and the best chaperones concentration by densitometric analyses, Figure 31. In comparison with the original gradient glycerol feed, medium supplementation with 1M Proline showed the best results, enhancing the STEAP1 expression near 2.5 times. Histidine at 0.08 mg/mL and 0.1M Trehalose seem to produce almost the same STEAP1 quantity in analogy with the original feed tested, as shown in Figure 33.

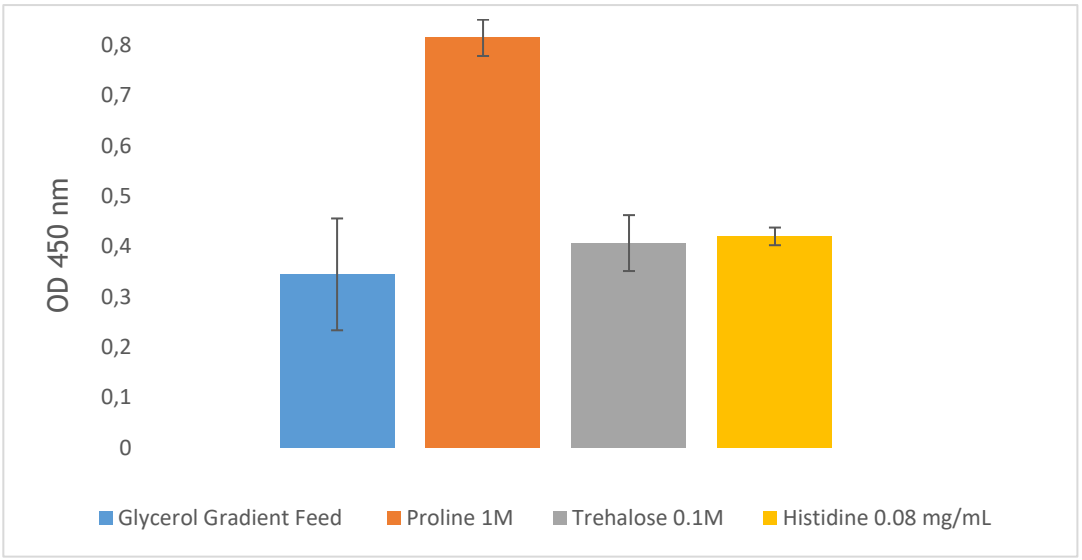

Figure 33. STEAP1 relative quantification for the original gradient glycerol feed and additional feeds supplemented with proline, trehalose and histidine.

3.2. Exponential Methanol Feeding

After the optimization of the glycerol fed-batch phase for increasing the STEAP1 production levels, it was evaluated the possibility of further increasing the STEAP1 protein levels in the induction phase by applying an exponential methanol feed. It was documented that a methanol exponential feed increases the production of several membrane proteins in P*ichia pastoris* cultures, through the exponential activity of the promotor AOX1[109,122]. Therefore, during an exponential feed, a constant specific growth rate (μ in h^{-1}) was required, and this value must be selected carefully. The *P. pastoris* X33 should grow in methanol with specific growth rate ranged between 0.001 h^{-1} (low methanol growth) and 0.14 h^{-1} (higher methanol growth) [122].

This strategy turns out to be unsuitable with μ close to the maximum value, since a small error in the flow rate calculation may lead to significant methanol accumulation. Lower specific growth rates close to 0.001 h^{-1} lead a much low methanol induction in comparison with constant feed studied previously. Despite the existing knowledge for AOX1 controlled product formation, process design at a low specific growth rate less than 0.04h^{-1} is particularly suitable for reaching high productivities [122]. Çalık and coworkers studied three different specific growth rates (0.02 h^{-1}, 0.03 $h^{-1,}$ and 0.04 h^{-1}) in recombinant human growth hormone production by *Pichia pastoris* mixed feeds. They denote highest growth hormone production, at μ = 0.03 h^{-1} as a consequence of the lower extracellular protease production and higher AOX activity[159].

Therefore, it was selected a μ = 0.03 h^{-1} and applied an exponential methanol feeding profile on the gradient and exponential glycerol feedings. The appropriate flow rate was calculated using the equations 1 and 2 [109,114].

As mentioned above, the peak of protein production for the gradient glycerol feed and constant methanol feed was at 10 hours of induction. Likewise, it was necessary to denote eventual other peaks of STEAP1 production, as shown in Figure 34. It was observed higher production at 8 hours of induction, this result has advantageous, allowed to reduce the induction time and the spare resources. A disadvantage associated was the presence of some STEAP1 degradations.

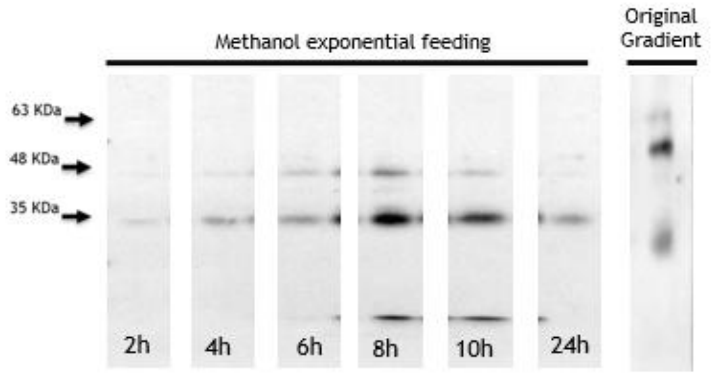

Figure 34. Western blot analysis of an exponential methanol feed and the original glycerol gradient feed (with a methanol constant flow-rate during the induction).

Comparatively, the spike of STEAP1 production for the exponential glycerol feed and constant methanol feed was fixed at 5 hours of induction. In this new fermentation conditions were a spike of production at 8 hours of exponential methanol induction. STEAP1 aggregates were produced in comparison with the original feed. While it was denoted no significant STEAP1 production at 6 hours of induction in the original feed (Figure 21) unless to the new exponential methanol feed (Figure 35). All the experimental point mentioned, which are in duplicated, are shown in Appendix 4.

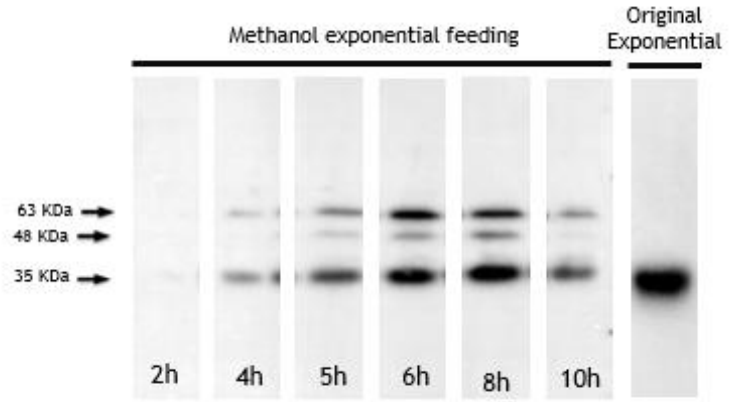

Figure 35. Western blot analysis of an exponential methanol feed and the original glycerol exponential feed (with a methanol constant flow-rate during the induction).

The DO_{600nm} of these cultures were increased in comparison with the initial feed tested, as shown in Table 3. For an exponential glycerol feed and a constant methanol feed with 5 hours of induction, the previous DO_{600nm} was 76.2 and 81.9 for reactor 1 and 2 respectively. For the gradient glycerol feed with a constant methanol feed (10 hours of induction), the initial DO_{600nm} obtained was 81.7 and 68.8 for reactor 1 and 2 respectively.

As mentioned above the production of dimers and the existence of degradation are disadvantageous for STEAP1 stability, which was been demonstrated here though the analysis of bands densitometry (Figures 34 and 35).

Table 3. The relationship between DO600nm and the exponential methanol feed during the induction phase.

	Exponential methanol feed			
	Gradient glycerol feed		***Exponential glycerol feed***	
Reactor	*R1*	*R2*	*R1*	*R2*
$DO_{600\ nm}$	*89.5*	*53.0*	*93.2*	*87.4*

The average of methanol concentration in each duplicated test showed that no methanol accumulation at toxic levels, as demonstrated in Figure 36. These values are closer than those obtained in the original conditions, 3.75 – 5.06 g/L for the exponential glycerol feed and 2.9 – 8.3 g/L for the gradient glycerol feed (Figure 27).

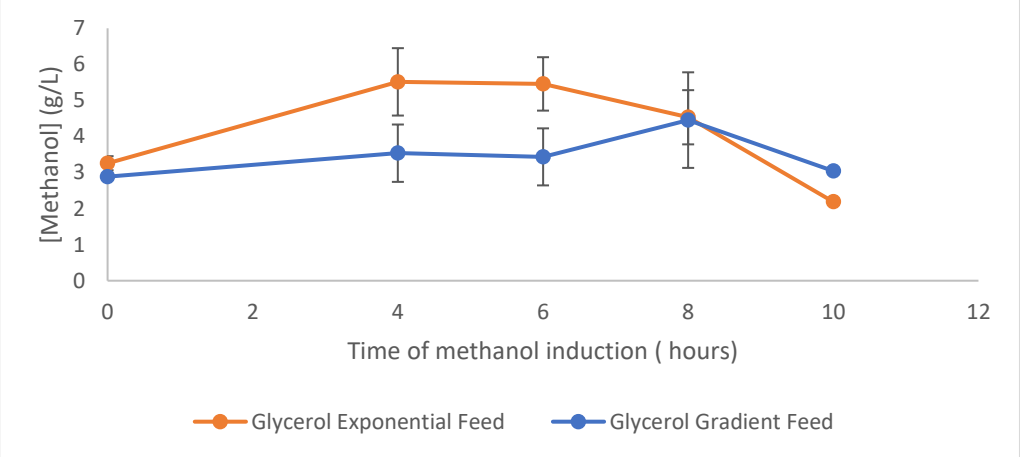

Figure 36. Residual methanol concentration (g/L) for the exponential and gradient glycerol feed in an exponential methanol feed during the induction.

4. Evaluation of *N*-glycosylation

Several fermentation parameters such as host, carbon source starvation, pH, and temperature affect the glycosylation profiles of recombinant proteins. The different feeds tested above could eventually lead to different STEAP1 glycosylation profiles. It was reported that the product quality can be improved by maintaining a high residual methanol concentration, growing cells at low rates, lowering the cultivation temperature or reducing the stirring rate and aeration [114,128,165]. Gomes and coworkers reported several putative STEAP1 post-translational modifications, which may increase its oncogenic function. It was denoted that different predicted *N*-glycosylation, glycation, phosphorylation and O-ß-GlcNAc sites in STEAP1 structure [78]. Once that *Pichia pastoris* may perform both *N*- and *O*- glycosylation and by the *in silico* analysis, the predicted *N*-glycosylation site in Asn143 was the most denoted. Thus, it was studied the eventual STEAP1 *N*-glycosylation modification with the enzyme PNGase F and by 2D-electrophoresis.

Kim and coworkers have reported that STEAP1 may form homodimers and heterodimers (with others STEAPs) and that the oligomeric state is partially resistant to the denaturing SDS–PAGE conditions [62]. Although, it was proposed the eventual STEAP1 aggregation in gradient glycerol feed due the PTM, our results show that after the PNGase F reaction no modifications on *N*-glycosylation profiles were found, as shown in Figure 37.

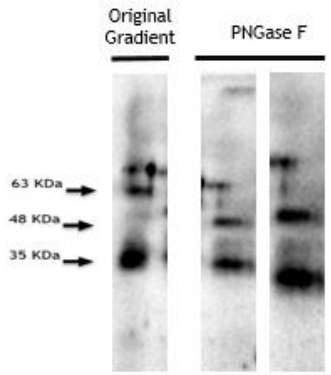

Figure 37. Western blot analysis of a cell lysate obtained from a glycerol gradient feed, non-treated (A) and treated (B) with 3 µL of PNGase F for 1 hour.

These results may be due to the high concentration and proteins diversity in the lysate that lack the reactions between the PNGase F and STEAP1 specifically. Despite that, it was tested the PNGase assay for each chaperone used (Figure 38).

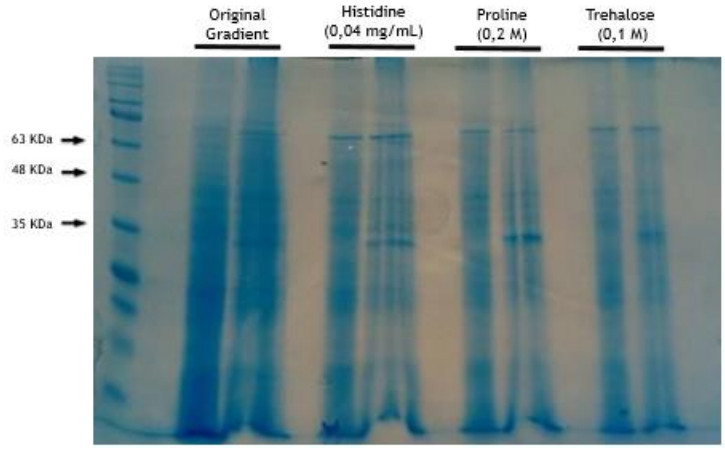

Figure 38. SDS-PAGE analysis of the cell lysate treated with the enzyme PNGase F, obtained from the original glycerol gradient feed supplemented with chaperones (0.04 mg/mL histidine, 0.2M proline, and 0.1 M trehalose).

Meanwhile, tests with different PNGase F volumes and reaction time were carried out with trehalose 0.1M lysates, as shown in Figure 39. An immunoreactive faint band appears to move from 63 kDa to 48 kDa. At the other side, the glycosylation profile is not modified with different PNGaseF volumes or time of reaction.

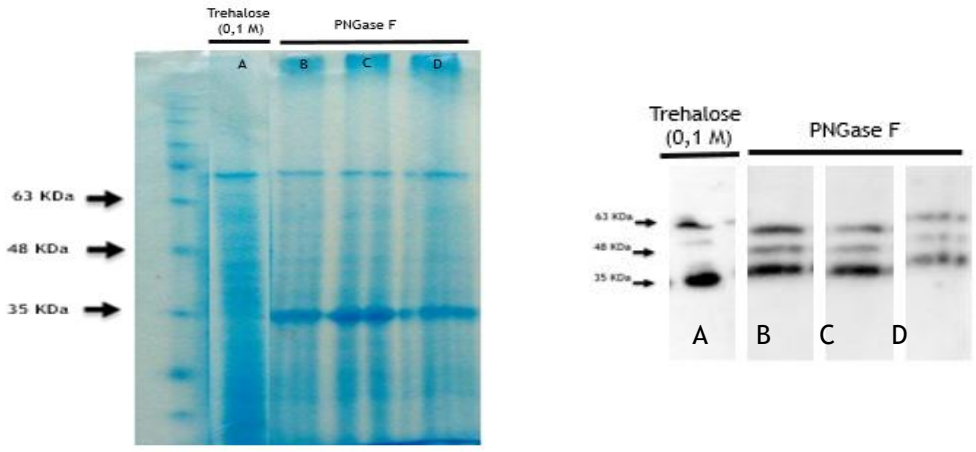

Figure 39. SDS-PAGE and Western blot analysis of the cell lysate treated with the enzyme PNGase F, obtained from the glycerol gradient feed supplemented with 0.1M of trehalose. A) original Trehalose 0.1M without PNGase F treatment; Trehalose 0.1M treated with B) 3 µL PNGase F for 1 hour; C) 5 µL PNGase F for 1 hour; D) 3 µL PNGase F for 2 hours.

Altogether, these results may suggest that the formation of STEAP1 dimers is not due the *N*-glycosylation interaction. Another reason is that the modifications are so strong that more quantities of PNGase F are needed or the extract understudy should be further purified.

So, a 2DE analysis was carried out in order to understand if there is glycosylation, through the isoelectric point change. The glycosylation is a strong modification in proteins structure since it is not undone during the samples denaturing treatment. It was used a sample from the original gradient glycerol feed as studied for PNGase F assay. Like this, it is possible to distinguish easily the eventual STEAP1 glycosylation once that exist different molecular weights in the lysate extract analyzed. Santos and coworkers reported a teoric isoelectric point for STEAP1 close to the 9.28, as obtained in this study [148]. Nevertheless, it was obtained an isolated spot, suggesting that there is no relationship between the dimers and the STEAP1 glycosylation for these fermentation conditions, as shown in Figures 37 and 40.

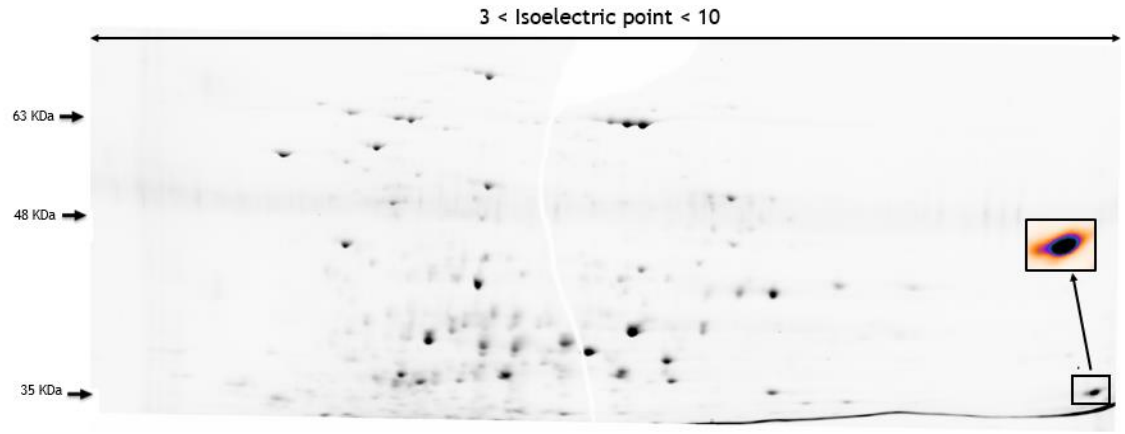

Figure 40. Description of Pichia pastoris X33 proteome by bi-dimensional electrophoresis obtained in a gradient glycerol and constant methanol feed during 10 hours of methanol induction.

Schenk and coworkers studied different glycosylation profiles of the recombinant avidin by mass spectroscopy. It was described that the most abundant forms found were the 9-10 mannose made by *P.pastoris,* which increase the protein weight a few kDa [114]. For this reason, it is important to study the PNGase F digestion in lysates of the constant glycerol feed that enhance the STEAP1 molecular weight only a few kDa. It was tested with the PNGase F assay in the constant feed and denoted a good result showed a diminution of glycosylation profile, as shown in Figure 41. However, more tests are needed.

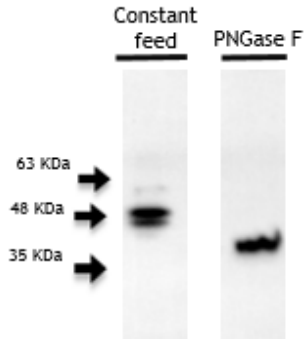

Figure 41. Western blot analysis of the cell lysate obtained from a constant glycerol and methanol feed, non-treated (A) and treated (B) with 3 µL PNGase F for 1 hour.

Given the circumstances, a glycerol constant feed seems to produce STEAP1 with *N*-glycosylation modification. On the other hand, the glycosylation does not seem to be responsible for the dimers formed during a gradient glycerol feed.

Chapter V - Conclusions and Future Perspectives

Nowadays, the rising and development of several human pathologies, such as cancer, and the lack of reliable treatments to them, has led to the necessity of developing new therapeutic strategies. Concerning this, the biosynthesis of membrane proteins and new biomolecules has been increased due to its role in the development and progression of PCa. Thereby, the enhancement of the protein production is essential for understanding its function and structure. Thus, in this study, several fermentation conditions were tested to increase STEAP1 expression in *P. pastoris* X33 strain in mini-bioreactor methanol induced culture. The scale-up of STEAP1 biosynthesis and the developing of a fed-batch suitable strategy were achieved with success.

Through the study of three glycerol flow-rates during the fed-batch phase different results were obtained. A gradient feed produces high quantities of STEAP1 with some dimers at 10 hours of methanol induction. Also, different chemical chaperones were tested, in order to decrease the dimers formed during these specific glycerol feed. Low concentration of Trehalose (~0.1M) and higher concentrations of Proline (0.5 and 1 M) and Histidine (0.08 mg/mL) revealed the best results. By the analysis with the enzyme PNGase F and confirmed by 2DE, these dimers are not a consequence of *N*-glycosylation. With a constant glycerol feed, the STEAP1 produced seems to be *N*-glycosylated. Contrariwise, the amounts of STEAP1 produced during an exponential glycerol feed are at the correct molecular weight (~35 kDa). As demonstrated, glycerol basal concentrations seem to promote STEAP1 stability, acting as chemical chaperone. Even so, the methanol concentration is not toxic to *P. pastoris* cells during the first hours of induction. Through the densitometry analysis, it was concluded that the exponential methanol feed tested during the induction phase, led to slightly increase in STEAP1 production, comparatively to the original conditions. However, it also produced STEAP1 degradation and dimers production. Although, these results leave an open door for future studies related to enhancing of STEAP1 production and the use of several chemical chaperones for its stabilization.

Summarizing, until now the best conditions for optimal protein production is a BMS medium with 20 hours of a glycerol-batch phase for *P. pastoris* growth. A gradient glycerol feed associated with a constant methanol feed supplemented with 6%(v/v) DMSO and Proline 1M, as a chemical chaperone, revealed an ideal fermentation strategy to enhance STEAP1 productivity and stability. These reactional conditions doubled the protein production when compared with the initial conditions.

Improvements can be made on the fermentation process. It is important to complement the study of the different chemical chaperones concentrations with the several fed-batch phases tested. Then it is important to study the influence of STEAP1 production into Pichia metabolism, for example by Flow Cytometry Assays.

As ongoing work, it is vital to perform STEAP1 purification and try to achieve different dimers recovery. Likewise, it would be of interest to develop a new method for STEAP1 quantification and eventually to study its PTMs, which may interfere with STEAP1 structure and oncogenic function.

Chapter VI – Bibliography

1. Verze P, Cai T, Lorenzetti S. The role of the prostate in male fertility, health and disease. Nat. Rev. Urol. Nature Publishing Group; 2016;8.

2. Marzo AM De, Platz EA, Sutcliffe S, Xu J, Grönberg H, Drake CG, et al. Inflammation in prostate carcinogenesis. Nat. Rev. Cancer. 2007;7:256–69.

3. Omabe M, Ezeani M. Infection, inflammation and prostate carcinogenesis. Infect. Genet. Evol. Elsevier B.V.; 2011;11:1195–8.

4. Vander A, Luciano D, Sherman J. Human Physiology: The Mechanisms of Body Function. 8th ed. McGraw-Hill, editor. New York; 2001.

5. Nieto CM, Rider LC, Cramer SD. Influence of stromal-epithelial interactions on androgen action. Endocr. Relat. Cancer. 2014;21:147–60.

6. Leach D, Buchanan G. Stromal Androgen Receptor in Prostate Cancer Development and Progression. Cancers (Basel). 2017;9:24.

7. Franklin RB, Milon B, Feng P, Costello LC. Zinc and zinc transporters in normal prostate function and the pathogenesis of prostate cancer. Front. Biosci. 2015;10:2230–9.

8. Kalinska M, Hoffert UM, Kantyka T, Potempa J. Kallikreins - the melting pot of activity and function. Biochimie. 2016;122:270–82.

9. Gilany K, Minai-Tehrani A, Savadi-Shiraz E, Rezadoost H, Lakpour N. Exploring the human seminal plasma proteome: An unexplored gold mine of biomarker for male Infertility and male reproduction disorder. J. Reprod. Infertil. 2015;16:61–71.

10. van Leenders GJLH, Schalken JA. Epithelial cell differentiation in the human prostate epithelium: implications for the pathogenesis and therapy of prostate cancer. Crit. Rev. Oncol. Hematol. 2003;46:3–10.

11. Heinlein CA, Chang C. Androgen Receptor in Prostate Cancer. Endocr. Rev. 2004;25:276–308.

12. Ferrero-Poüs M, Hersant AM, Pecking A, Brésard-Leroy M, Pichon M. Serum chromogranin A in advanced prostate cancer. BJU Int. 2001;88:790–6.

13. Sant' Agnese PA, Cockett ATK. Neuroendocrine Differentiation in Prostatic Malignancy. Am. Cancer Soc. 1996;78:357–61.

14. Debes JD, Tindall DJ. The role of androgens and the androgen receptor in prostate cancer. Cancer Lett. 2002;187:1–7.

15. Luo J, Solimini NL, Elledge SJ. Principles of Cancer Therapy: Oncogene and Non-oncogene Addiction. Cell. 2009;136:823–37.

16. Weisenthal LM. Cancer Cell Culture: Methods and Protocols. Methods Mol. Biol. Second Edi. 2011. p. 345–58.

17. Johansson N, Ahonen M, Kähäri VM. Matrix metalloproteinases in tumor invasion. Cell. Mol. Life Sci. 2000;57:5–15.

18. Bergers G, Benjamin LE. Tumorigenesis and the angiogenic switch. Nat. Rev. Cancer. 2003;3:401–10.

19. Hanahan D, Folkman J. Patterns and emerging mechanisms of the angiogenic switch during tumorigenesis. Cell. 1996;86:353–64.

20. Hanahan D, Weinberg RA. The hallmarks of Cancer. Cell. 2000;100:14.

21. Cushman S. Cancer. Robert H.B. Stilz HU, Bernstein PR, Buschauer A, Gether U, Lowe JA, editors. Biochem. Educ. Springer; 2007.

22. Hubert RS, Vivanco I, Chen E, Rastegar S, Leong K, Mitchell SC, et al. STEAP: A Prostate-specific cell-surface antigen highly expressed in human prostate tumors. Proc. Natl. Acad. Sci. U. S. A. 1999;96:14523–8.

23. Ramsay AK, McCracken SRC, Soofi M, Fleming J, Yu AX, Ahmad I, et al. ERK5 signalling in prostate cancer promotes an invasive phenotype. Br. J. Cancer. 2011;104:664–72.

24. Jemal A, Bray F, Center MM, Ferlay J, Ward E, Forman D. Global Cancer Statistics. CA CANCER J. Clin. 2011;61:69–90.

25. Miller KD, Siegel RL, Lin CC, Mariotto AB, Kramer JL, Rowland JH, et al. Cancer Treatment and Survivorship Statistics, 2016. CA CANCER J. Clin. 2016;66:271–89.

26. Pina F, Castro C, Ferro A, Bento MJ, Lunet N. Prostate cancer incidence and mortality in Portugal: trends, projections and regional differences. Eur. J. Cancer Prev. 2016;8.

27. Crawford DE. Epidemiology of Prostate Cancer. Urology. 2003;62:10.

28. Giovannucci E, Liu Y, Platz EA, Stampfer MJ, Willett WC. Risk factors for prostate cancer incidence and progression in the health professionals follow-up study. Int. J. Cancer. 2007;121:16.

29. Gann PH. Risk factors for Prostate Cancer. Rev. Urol. 2002;4:10.

30. Chan JM, Gann PH, Giovannucci EL. Role of Diet in Prostate Cancer Development and Progression. J. Clin. Oncol. 2005;23:8152–60.

31. Nelson PS, Montgomery B. Unconventional therapy for prostate cancer: Good, bad or questionable? Nat. Rev. Cancer. 2003;3:845–58.

32. Attard G, Parker C, Eeles RA, Schröder F, Tomlins SA, Tannock I, et al. Prostate Cancer. Lancet. Elsevier Ltd; 2015;6736:13.

33. Gurumurthy S, Vasudevan KM, Rangnekar VM. Regulation of apoptosis in prostate cancer. Cancer Metastasis Rev. 2002;20:225–43.

34. De Marzo AM, Marchi VL, Epstein JI, Nelson WG. Proliferative Inflammatory Atrophy of the Prostate. Am. J. Pathol. American Society for Investigative Pathology; 1999;155:1985–92.

35. Suzuki H, Ueda T, Ichikawa T, Ito H. Androgen receptor involvement in the progression of prostate cancer. Endocr. Relat. Cancer. 2003;10:209–16.

36. Vaz C V., Alves MG, Marques R, Moreira PI, Oliveira PF, Maia CJ, et al. Androgen-responsive and nonresponsive prostate cancer cells present a distinct glycolytic metabolism profile. Int. J. Biochem. Cell Biol. Elsevier Ltd; 2012;44:2077–84.

37. Soronen P, Laiti M, Törn S, Härkönen P, Patrikainen L, Li Y, et al. Sex steroid hormone metabolism and prostate cancer. J. Steroid Biochem. Mol. Biol. 2004;92:281–6.

38. Velonas VM, Woo HH, dos Remedios CG, Assinder SJ. Current Status of Biomarkers for Prostate Cancer. Int. J. Mol. Sci. 2013;14:11034–60.

39. Bickers B, Aukim-Hastie C. New molecular Biomarkers for the Prognosis and Management of Prostate Cancer - the post PSA Era. Anticancer Res. 2009;29:3289–98.

40. Bradford TJ, Tomlins SA, Wang X, Chinnaiyan AM. Molecular Markers of Prostate Cancer. Urol. Oncol. Semin. Orig. Investig. 2006;24:538–51.

41. Pentyala S, Whyard T, Pentyala S, Muller J, Pfail J, Parmar S, et al. Prostate cancer markers : An update (Review). Biomed. Reports. 2016;4:263–8.

42. Obort AS, Ajadi MB, Akinloye O. Prostate-Specific Antigen: Any Successor in Sight ? Rev Urol. 2013;15:97–107.

43. Humphrey PA. Gleason grading and prognostic factors in carcinoma of the prostate. Mod. Pathol. 2004;17:292–306.

44. Gleason DF. Histologic Grading of Prostate Cancer: A Perspective. Hum. Pathol. 1992;23:273–9.

45. Warde P, Mason M, Ding K, Kirkbride P, Brundage M, Cowan R, et al. Combined androgen deprivation therapy and radiation therapy for locally advanced prostate cancer: A randomised, phase 3 trial. Lancet. Elsevier; 2011;378:2104–11.

46. Nakada SY, Sant' Arnese PA, Moynes RA, Hiipakka RA, Liao S, Cockett ATK, et al. The Androgen Receptor Status of Neuroendocrine Cells in Human Benign and Malignant Prostatic Tissue. Cancer Res. 1993;53:1967–70.

47. Ichikawa T, Suzuki H, Ueda T, Komiya A, Imamoto T, Kojima S. Hormone treatment for prostate cancer : current issues and future directions. Cancer Chemother Pharmacol. 2005;56:58–63.

48. Holmes EH. PSMA specific antibodies and their diagnostic and therapeutic use. Expert Opin. Investig. Drugs. 2001;10:511–9.

49. Gomes IM, Maia CJ, Santos CR. STEAP Proteins: From Structure to Applications in Cancer Therapy. Mol. cancer Res. 2012;10:573–87.

50. Han KR, Seligson DB, Liu X, Horvath S, Shintaku PI, Thomas G V, et al. Prostate Stem Cell Antigen Expression is Associated With Gleason Score, Seminal Vesicle Invasion and Capsular Invasion in Prostate Cancer. J. Urol. 2004;171:1117–21.

51. Lam JS, Shintaku IP, Vessella RL, Jenkins RB, Horvath S, Said JW, et al. Prostate Stem Cell Antigen Is Overexpressed in Prostate Cancer Metastases. Clin. Cancer Res. 2005;11:2591–6.

52. Hu C-D, Choo R, Huang J. Neuroendocrine differentiation in prostate cancer: a mechanism of radioresistance and treatment failure. Front. Oncol. 2015;5:10.

53. Matei D-V, Renne G, Pimentel M, Sandri MT, Zorzino L, Botteri E, et al. Neuroendocrine differentiation in castration-resistant prostate cancer: a systematic diagnostic attempt. Clin. Genitourin. Cancer. 2012;10:164–73.

54. Gaiser MR, Daily K, Hoffmann J, Brune M, Enk A, Brownell I. Evaluating blood levels of neuron specific enolase, chromogranin A, and circulating tumor cells as Merkel cell carcinoma biomarkers. Oncotarget. 2015;6:26472–82.

55. Liancheng F, Yanqing W, Chenfei C, Jiahua P, X S, Zhixiang X, et al. Chromogranin A and neurone specific enolase variations during the first three months of abiraterone therapy predict outcomes in patients with metastatic castration-resistant prostate cancer. BJU Int. 2017;120:226–32.

56. Isgrò MA, Bottoni P, Scatena R. Neuron specific enolase as a Biomarker: Biochemical and Clinical Aspects. Adv. Cancer Biomarkers. 2015. p. 125–43.

57. Grunewald TGP, Diebold I, Esposito I, Plehm S, Hauer K, Thiel U, et al. STEAP1 is Associated with the Invasive and Oxidative Stress Phenotype of Ewing Tumors. Mol. Cancer Res. 2012;10:52–65.

58. Ohgami RS, Campagna DR, McDonald A, Fleming MD. The Steap proteins are metalloreductases. Blood. 2006;108:1388–94.

59. Alves PMS, Faure O, Graff-Dubois S, Cornet S, Bolonakis I, Gross D-A, et al. STEAP, a prostate tumor antigen, is a target of human CD8+ T cells. Cancer Immunol. Immunother. 2006;55:1515–23.

60. Hayashi S, Kumai T, Matsuda Y, Aoki N, Sato K, Kimura S, et al. Six-transmembrane epithelial antigen of the prostate and enhancer of zeste homolog 2 as immunotherapeutic targets for lung cancer. J. Transl. Med. 2011;9:14.

61. Grunewald TGP, Bach H, Cossarizza A, Matsumoto I. The STEAP protein family: Versatile oxidoreductases and targets for cancer immunotherapy with overlapping and distinct cellular functions. Biol. Cell. 2012;104:641–57.

62. Kim K, Mitra S, Wu G, Berka V, Song J, Yu Y, et al. Six-Transmembrane Epithelial Antigen of Prostate 1 (STEAP1) has a single b heme and is capable of reducing metal ion complexes and oxygen. Biochemistry. 2016;55:12.

63. Ohgami RS, Campagna DR, Greer EL, Antiochos B, McDonald A, Chen J, et al. Identification of a ferrireductase required for efficient transferrin- dependent iron uptake in erythroid cells. Nat Genet. 2005;37:14.

64. Korkmaz KS, Elbi C, Korkmaz CG, Loda M, Hager GL, Saatcioglu F. Molecular cloning and characterization of STAMP1, a highly prostate-specific six transmembrane protein that is overexpressed in prostate cancer. J. Biol. Chem. 2002;277:36689–96.

65. Porkka KP, Helenius MA, Visakorpi T. Cloning and characterization of a novel six-transmembrane protein STEAP2, expressed in normal and malignant prostate. Lab. Investig. 2002;82:1573–82.

66. Lespagnol A, Duflaut D, Beekman C, Blanc L, Fiucci G, Marine J-C, et al. Exosome secretion, including the DNA damage-induced p53-dependent secretory pathway, is severely compromised in TSAP6/Steap3-null mice. Cell Death Differ. 2008;15:1723–33.

67. Machlenkin A, Paz A, Haim EB, Goldberger O, Finkel E, Tirosh B, et al. Human CTL Epitopes Prostatic Acid Phosphatase-3 and Six-Transmembrane Epithelial Antigen of Prostate-3 as candidates for prostate cancer immunotherapy. Cancer Res. 2005;65:6435–42.

68. Korkmaz CG, Korkmaz KS, Kurys P, Elbi C, Wang L, Klokk TI, et al. Molecular cloning and characterization of STAMP2, an androgen-regulated six transmembrane protein that is overexpressed in Prostate Cancer. Oncogene. 2005;24:4934–45.

69. Challita-Eid PM, Morrison K, Etessami S, An Z, Morrison KJ, Perez-Villar JJ, et al. Monoclonal antibodies to six-transmembrane epithelial antigen of the prostate-1 inhibit intercellular communication In vitro and growth of human tumor xenografts In vivo. Cancer Res. 2007;67:5798–805.

70. Valenti MT, Carbonare LD, Donatelli L, Bertoldo F, Giovanazzi B, Caliari F, et al. STEAP mRNA detection in serum of patients with solid tumours. Cancer Lett. Elsevier Ireland Ltd; 2009;273:122–6.

71. Prevarskaya N, Skryma R, Bidaux G, Flourakis M, Shuba Y. Ion channels in death and differentiation of prostate cancer cells. Cell Death Differ. 2007;14:1295–304.

72. Smith P, Rhodes NP, Shortland a P, Fraser SP, Djamgoz MB, Ke Y, et al. Sodium channel protein expression enhances the invasiveness of rat and human prostate cancer cells. FEBS Lett. 1998;423:19–24.

73. Gomes IM, Arinto P, Lopes C, Santos CR, Maia CJ. STEAP1 is overexpressed in prostate cancer and prostatic intraepithelial neoplasia lesions, and it is positively associated with Gleason score. Urol. Oncol. Semin. Orig. Investig. Elsevier; 2014;32:7.

74. Maia CJB, Socorro S, Schmitt F, Santos CRA. STEAP1 is over-expressed in breast cancer and down-regulated by 17B-estradiol in MCF 7 cells and in the rat mammary gland. Endocrine. 2008;34:108–16.

75. Gomes IM, Santos CR, Socorro S, Maia CJ. Six transmembrane epithelial antigen of the prostate 1 is down-regulated by sex hormones in Prostate Cells. Prostate. 2013;73:605–13.

76. Herrmann VL, Wieland DE, Legler DF, Wittmann V, Groettrup M. The STEAP1 262-270 peptide encapsulated into PLGA microspheres elicits strong cytotoxic T cell immunity in HLA-A∗ 0201 transgenic mice - A new approach to immunotherapy against prostate carcinoma. Prostate. 2016;76:456–68.

77. Barroca-Ferreira J, Pais JP, Santos MM, Goncalves AM, Gomes IM, Sousa IM, et al. Targeting STEAP1 protein in human cancer: current trends and future challenges. Curr. Cancer Drug Targets. 2017;17:12.

78. Gomes IM, Santos CR, Maia CJ. Expression of STEAP1 and STEAP1B in prostate cell lines , and the putative regulation of STEAP1 by post-transcriptional and post-translational mechanisms. Genes Cancer. 2014;5:142–51.

79. Schwarz F, Aebi M. Mechanisms and principles of *N*-linked protein glycosylation. Curr. Opin. Struct. Biol. Elsevier Ltd; 2011;21:576–82.

80. Wang Z, Gucek M, Hart GW. Cross-talk between GlcNAcylation and phosphorylation: Site-specific phosphorylation dynamics in response to globally elevated *O*-GlcNAc. Proc. Natl. Acad. Sci. U. S. A. 2008;105:13793–8.

81. Fujimura T, Shinohara Y, Tissot B, Pang PC, Kurogochi M, Saito S, et al. Glycosylation status of haptoglobin in sera of patients with prostate cancer vs benign prostate disease or normal subjects. Int. J. Cancer. 2008;122:39–49.

82. Yang X-J. Multisite protein modification and intramolecular signaling. Oncogene. 2005;24:1653–62.

83. Kamigaito T, Okaneya T, Kawakubo M, Shimojo H, Nishizawa O, Nakayama J. Overexpression of *O*-GlcNAc by prostate cancer cells is significantly associated with poor prognosis of patients. Prostate Cancer Prostatic Dis. Nature Publishing Group; 2014;17:18–22.

84. Lin Cereghino J, Cregg JM. Heterologous protein expression in the methylotrophic yeast Pichia pastoris. FEMS Microbiol. Rev. Rev. 2000;24:45–66.

85. Porowińska D, Wujak M, Roszek K, Komoszyński M. Prokaryotic expression systems. Postepy Hig. Med. Dosw. 2013;67:119–29.

86. Liu L, Yang H, Shin HD, Chen RR, Li J, Du G, et al. How to achieve high-level expression of microbial enzymes: strategies and perspectives. Bioengineered. 2013;4:212–23.

87. Junge F, Schneider B, Reckel S, Schwarz D, Dötsch V, Bernhard F. Large-scale production of functional membrane proteins. Cell. Mol. Life Sci. 2008;65:1729–55.

88. Baumgarten T, Schlegel S, Wagner S, Löw M, Eriksson J, Bonde I, et al. Isolation and characterization of the E. coli membrane protein production strain Mutant56 (DE3). Sci. Rep. Nature Publishing Group; 2017;7:12.

89. Li W, Zhou X, Lu P. Bottlenecks in the expression and secretion of heterologous proteins in Bacillus subtilis. Res. Microbiol. 2004;155:605–10.

90. Ming YM, Wei ZW, Lin CY, Sheng GY. Development of a Bacillus subtilis expression system using the improved Pglv promoter. Microb. Cell Fact. 2010;9:55.

91. Jarvis DL. Baculovirus-Insect Cell Expression Systems. Methods Enzymol. 1st ed. Elsevier Inc.; 2009. p. 191–222.

92. Khan KH. Gene Expression in Mammalian Cells and its Applications. Adv. Pharm. Bull. 2013;3:257–63.

93. Lin-Cereghino GP, Lin-Cereghino J, Ilgen C, Cregg JM. Production of recombinant proteins in fermenter cultures of the yeast Pichia pastoris. Curr. Opin. Biotechecnology. 2002;13:329–32.

94. Darby R, Cartwright SP, Dilworth M, Bill R. Which Yeast Species Shall I Choose? Saccharomyces cerevisiae Versus Pichia pastoris (Review). Recomb. Protein Prod. Yeast Methods Protoc. 2012. p. 13.

95. Gellissen G. Heterologous protein production in methylotrophic yeasts. Appl. Microbiol. Biotechnol. 2000;54:741–50.

96. Curran BPG, Bugeja V. Basic investigations in Saccharomyces cerevisiae. Methods Mol. Biol. 2014;313:1–13.

97. Bonander N, Bill RM. Optimising Yeast as a Host for Recombinant Protein Production (Review). Recomb. Protein Prod. Yeast Methods Protoc. 2012. p. 1–9.

98. Bretthauer RK, Castellino FJ. Glycosylation of Pichia pastoris derived proteins. Biotechnol. Appl. Biochem. 1999;30:193–200.

99. Cregg JM, Vedvick TS, Raschke WC. Recent advances in the expression of foreign genes in Pichia pastoris. Biotechnology. (N. Y). 1993;11:905–10.

100. De Schutter K, Lin Y-C, Tiels P, Van Hecke A, Glinka S, Weber-Lehmann J, et al. Genome sequence of the recombinant protein production host Pichia pastoris. Nat. Biotechnol. 2009;27:561–9.

101. Cos O, Ramón R, Montesinos JL, Valero F. Operational strategies, monitoring and control of heterologous protein production in the methylotrophic yeast Pichia pastoris under different promoters: A review. Microb. Cell Fact. 2006;5:20.

102. Byrne B. Pichia pastoris as an expression host for membrane protein structural biology. Curr. Opin. Struct. Biol. 2015;32:9–17.

103. Gonçalves AM, Pedro AQ, Maia CJ, Fani S, Queiroz JA, Passarinha LA. Pichia pastoris: A recombinant microfactory for antibody and human membrane proteins. J. Microbiol. Biotechnol. 2013;23:587–601.

104. Cregg JM. Pichia Protocols. 2º. Human Press Inc., editor. Methods Mol. Biol. 2007.

105. Hartner FS, Glieder A. Regulation of methanol utilisation pathway genes in yeasts. Microb. Cell Fact. 2006;5:21.

106. Invitrogen LT. User manual - EasySelect™ Pichia Expression Kit. Cat. no. K1740-01. 2010.

107. Unrean P. Pathway analysis of Pichia pastoris to elucidate methanol metabolism and its regulation for production of recombinant proteins. Biotechnol. Prog. 2014;30:28–37.

108. Pedro AQ, Oppolzer D, Bonifácio MJ, Maia CJ, Queiroz JA, Passarinha LA. Evaluation of MutS and Mut+ Pichia pastoris strains for Membrane-Bound Catechol-*O*-Methyltransferase Biosynthesis. Appl. Biochem. Biotechnol. 2015;175:3840–55.

109. Jahic M, Veide A, Charoenrat T, Teeri T, Enfors SO. Process technology for production and recovery of heterologous proteins with Pichia pastoris. Biotechnol. Prog. 2006;22:1465–73.

110. Çelik E, Çalık P. Production of recombinant proteins by yeast cells. Biotechnol. Adv. 2012;30:1108–18.

111. Prielhofer R, Cartwright SP, Graf AB, Valli M, Bill RM, Mattanovich D, et al. Pichia pastoris regulates its gene-specific response to different carbon sources at the transcriptional, rather than the translational, level. BMC Genomics. 2015;16:17.

112. Zhou X-S, Zhang Y-X. Decrease of proteolytic degradation of recombinant hirudin produced by Pichia pastoris by controlling the specific growth rate. Biotechnol. Lett. 2002;24:1449–53.

113. Dai M, Yu C, Fang T, Fu L, Wang J, Zhang J, et al. Identification and functional characterization of glycosylation of recombinant human platelet-derived growth factor-BB in pichia pastoris. PLoS One. 2015;10:1–15.

114. Schenk J. , Balazs K., Jungo C. , Urfer J. WC, Zocchi A. , Marison Ian W. SU. Influence of Specific Growth Rate on Specific Productivity and Glycosylation of a Recombinant Avidin Produced by a Pichia pastoris Mut+ Strain. Biotechnol. Bioeng. 2007;99:368–77.

115. Zauner G, Kozak RP, Gardner RA, Fernandes DL, Deelder AM, Wuhrer M. Protein *O*-glycosylation analysis. Biol. Chem. 2012;393:687–708.

116. Hirose M, Kameyama S, Ohi H. Characterization of *N*-linked oligosaccharides attached to recombinant human antithrombin expressed in the yeast Pichia pastoris. Yeast. 2002;19:1191–202.

117. Han M, Wang X, Ding H, Jin M, Yu L, Wang J, et al. The role of *N*-glycosylation sites in the activity, stability, and expression of the recombinant elastase expressed by Pichia pastoris. Enzyme Microb. Technol. Elsevier Inc.; 2014;54:32–7.

118. Singh S, Gras A, Fiez-Vandal C, Martinez M, Wagner R, Byrne B. Large-Scale Production of Membrane Proteins in Pichia pastoris : The Production of G Protein-Coupled Receptors as a Case Study. Recomb. Protein Prod. Yeast Methods Protoc. 2012. p. 197–207.

119. Routledge SJ, Clare M. Setting Up a Bioreactor for Recombinant Protein Production in Yeast. Recomb. Protein Prod. Yeast Methods Protoc. 2012. p. 99–113.

120. Holmes WJ, Darby RA, Wilks MD, Smith R, Bill RM. Developing a scalable model of recombinant protein yield from Pichia pastoris: the influence of culture conditions, biomass and induction regime. Microb. Cell Fact. 2009;8:35.

121. Pedro AQ, Martins LM, Dias JML, Bonifácio MJ, Queiroz JA, Passarinha LA. An artificial neural network for membrane-bound catechol-*O*-methyltransferase biosynthesis with Pichia pastoris methanol-induced cultures. Microb. Cell Fact. BioMed Central; 2015;14:113.

122. Looser V, Bruhlmann B, Bumbak F, Stenger C, Costa M, Camattari A, et al. Cultivation strategies to enhance productivity of Pichia pastoris: A review. Biotechnol. Adv. Elsevier B.V.; 2014;33:1177–93.

123. Tolner B, Smith L, Begent RHJ, Chester K a. Production of recombinant protein in Pichia pastoris by fermentation. Nat. Protoc. 2006;1:1006–21.

124. Jahic M, Rotticci-Mulder J, Martinelle M, Hult K, Enfors SO. Modeling of growth and energy metabolism of Pichia pastoris producing a fusion protein. Bioprocess Biosyst. Eng. 2002;24:385–93.

125. Ramón R, Ferrer P, Valero F. Sorbitol co-feeding reduces metabolic burden caused by the overexpression of a Rhizopus oryzae lipase in Pichia pastoris. J. Biotechnol. 2007;130:39–46.

126. Routledge SJ, Hewitt CJ, Bora N, Bill RM, Holmes W, Darby R, et al. Antifoam addition to shake flask cultures of recombinant Pichia pastoris increases yield. Microb. Cell Fact. 2011;10:17.

127. Routledge SJ. Beyond de-foaming: the effects of antifoams on bioprocess productivity. Comput. Struct. Biotechnol. J. 2012;3:e201210014.

128. Cunha AE, Clemente JJ, Gomes R, Pinto F, Thomaz M, Miranda S, et al. Methanol induction optimization for scFv antibody fragment production in Pichia pastoris. Biotechnol. Bioeng. 2004;86:458–67.

129. Dragosits M, Stadlmann J, Graf A, Gasser B, Maurer M, Sauer M, et al. The response to unfolded protein is involved in osmotolerance of Pichia pastoris. BMC Genomics. 2010;11:16.

130. Zepeda AB, Figueroa CA, Abdalla DSP, Maranhão AQ, Ulloa PH, Jr AP, et al. Biomarkers to evaluate the effects of temperature and methanol on recombinant Pichia pastoris. Brazilian J. Microbiol. 2014;483:475–83.

131. Papp E, Csermely P. Chemical chaperones: Mechanisms of action and potential use. Handb. Exp. Pharmacol. 2006;172:405–16.

132. Rajan RS, Tsumoto K, Tokunaga M, Tokunaga H, Kita Y, Arakawa T. Chemical and pharmacological chaperones: application for recombinant protein production and protein folding diseases. Curr. Med. Chem. 2011;18:1–15.

133. Fahnert B. Using Folding Promoting Agents in Recombinant Protein Production: A Review. Recomb. Gene Expr. Rev. Protoc. 2012. p. 3–36.

134. Yancey PH, Clark ME, Hand SC, Bowlus RD, Somero GN. Living with water stress: evolution of osmolyte systems. Science (80-.). 1982;217:9.

135. Sadowska-Bartosz I, Pączka A, Mołoń M, Bartosz G. Dimethyl sulfoxide induces oxidative stress in the yeast Saccharomyces cerevisiae. FEMS Yeast Res. 2013;13:820–30.

136. Singh LR, Chen X, Kozich V, Kruger WD. Chemical chaperone rescue of mutant human cystathionine B-synthase. Mol. Genet. Metab. 2007;91:335–42.

137. Murakami K, Onoda Y, Kimura J, Masataka Y. Protection by histidine against oxidative inactivation of AMP Deaminase in yeast. Biochem. Mol. Biol. Int. 1997;42:1063–9.

138. Bennion BJ, Demarco ML, Daggett V, June R V, Re V, Recei M, et al. Accelerated Publications Preventing Misfolding of the Prion Protein by Trimethylamine N -Oxide †. 2004;43.

139. Chilson OP, Chilson AE. Perturbation of folding and reassociation of lactate dehydrogenase by proline and trimethylamine oxide. Eur. J. Biochem. 2003;270:4823–34.

140. Shiraki K, Kudou M, Fujiwara S, Imanaka T, Takagi M. Biophysical effect of amino acids on the prevention of protein aggregation. J. Biochem. 2002;132:591–5.

141. Arakawa T, Tsumoto K. The effects of arginine on refolding of aggregated proteins: Not facilitate refolding, but suppress aggregation. Biochem. Biophys. Res. Commun. 2003;304:148–52.

142. Yamaguchi H, Miyazaki M. Refolding techniques for recovering biologically active recombinant proteins from inclusion bodies. Biomolecules. 2014;4:235–51.

143. Nagata S, Sasaki H, Oshima A, Takeda S, Hashimoto Y, Ishida A. Effect of proline and K+ on the stimulation of cellular activities in Escherichia coli K-12 under high salinity. Biosci. Biotechnol. Biochem. 2005;69:740–6.

144. Jain NK, Roy I. Effect of trehalose on protein structure. Protein Sci. 2009;18:24–36.

145. Zou Q, Bennion BJ, Daggett V, Murphy KP. The molecular mechanism of stabilization of proteins by TMAO and its ability to counteract the effects of urea. J. Am. Chem. Soc. 2002;124:1192–202.

146. Brady CP, Shimp RL, Miles a P, Whitmore M, Stowers a W. High-level production and purification of P30P2MSP1(19), an important vaccine antigen for malaria, expressed in the methylotropic yeast Pichia pastoris. Protein Expr. Purif. 2001;23:468–75.

147. Silva F, Passarinha L, Sousa F, Queiroz JA, Domingues FC. Influence of growth conditions on plasmid DNA production. J. Microbiol. Biotechnol. 2009;19:1408–14.

148. Santos C, Socorro S, Maia C. STEAP1 (Six Transmembrane Epithelial Antigene of the Prostate 1). Atlas Genet. Cytogenet. Oncol. Haematol. 2011. p. 2009–11.

149. Dragosits M, Stadlmann J, Albiol J, Baumann K, Maurer M, Gasser B, et al. The effect of temperature on the proteome of recombinant *Pichia pastoris*. J. Proteome Res. 2009;8:1380–92.

150. Who. The enzyme-linked immunosorbent assay (ELISA). Bull. World Health Organ. 1976;54:129–39.

151. Cos O, Serrano A, Montesinos JL, Ferrer P, Cregg JM, Valero F. Combined effect of the

methanol utilization (Mut) phenotype and gene dosage on recombinant protein production in Pichia pastoris fed-batch cultures. J. Biotechnol. 2005;117:321–35.

152. Espírito Santo GM, Pedro AQ, Oppolzer D, Bonifácio MJ, Queiroz JA, Silva F, et al. Development of fed-batch profiles for efficient biosynthesis of catechol-*O*-methyltransferase. Biotechnol. Reports. Elsevier B.V.; 2014;3:34–41.

153. Bawa Z, Routledge SJ, Jamshad M, Clare M, Sarkar D, Dickerson I, et al. Functional recombinant protein is present in the pre-induction phases of Pichia pastoris cultures when grown in bioreactors , but not shake-flasks. Microb. Cell Fact. 2014;13:1–13.

154. Hellwig S, Emde F, Raven NPG, Henke M, Van Logt P Der, Fischer R. Analysis of single-chain antibody production in Pichia pastoris using on-line methanol control in fed-batch and mixed-feed fermentations. Biotechnol. Bioeng. 2001;74:344–52.

155. Zhang W, Bevins M a, Plantz B a, Smith L a. Modeling Pichia Pastoris growth on methanol and optimizing the production of a recombinant protein, the heavy-chain fragment C of botulinum Neurotoxic, serotype A. Biotechnol. Bioeng. 2000;0.

156. Trinh LB, Phue JN, Shiloach J. Effect of methanol feeding strategies on production and yield of recombinant mouse endostatin from Pichia pastoris. Biotechnol. Bioeng. 2003;82:438–44.

157. Zhang W, Hywood Potter KJ, Plantz BA, Schlegel VL, Smith LA, Meagher MM. Pichia pastoris fermentation with mixed-feeds of glycerol and methanol: growth kinetics and production improvement. J. Ind. Microbiol. Biotechnol. 2003;30:210–5.

158. Zhang W, Inan M, Meagher MM. Rational design and optimization of fed-batch and continuous fermentations. Methods Mol. Biol. 2007;389:43–64.

159. Çalik P, Inankur B, Soyaslan EŞ, Şahin M, Taşpinar H, Açik E, et al. Fermentation and oxygen transfer characteristics in recombinant human growth hormone production by Pichia pastoris in sorbitol batch and methanol fed-batch operation. J. Chem. Technol. Biotechnol. 2010;85:226–33.

160. André N, Cherouati N, Prual C, Steffan T, Zeder-Lutz G, Magnin T, et al. Enhancing functional production of G protein-coupled receptors in Pichia pastoris to levels required for structural studies via a single expression screen. Protein Sci. 2006;15:1115–26.

161. Miller EN, Ingram LO. Combined effect of betaine and trehalose on osmotic tolerance of Escherichia coli in mineral salts medium. Biotechnol. Lett. 2007;29:213–7.

162. Kaino T, Takagi H. Gene expression profiles and intracellular contents of stress protectants in Saccharomyces cerevisiae under ethanol and sorbitol stresses. Appl. Microbiol. Biotechnol. 2008;79:273–83.

163. Singer M a, Lindquist S. Multiple effects of trehalose on protein folding in vitro and in vivo. Mol. Cell. 1998;1:639–48.

164. Han H-Y, Yao Z-G, Gong C-L, Xu W-A. The protective effects of osmolytes on yeast alcohol dehydrogenase conformational stability and aggregation. Protein Pept. Lett. 2010;17:1058–66.

165. Hong F, Meinander NQ, Jönsson LJ. Fermentation strategies for improved heterologous expression of laccase in Pichia pastoris. Biotechnol. Bioeng. 2002;79:438–49.

Appendix

<u>Appendix 1</u>: Replicates of Exponential and Gradient feed profiles, respectively.

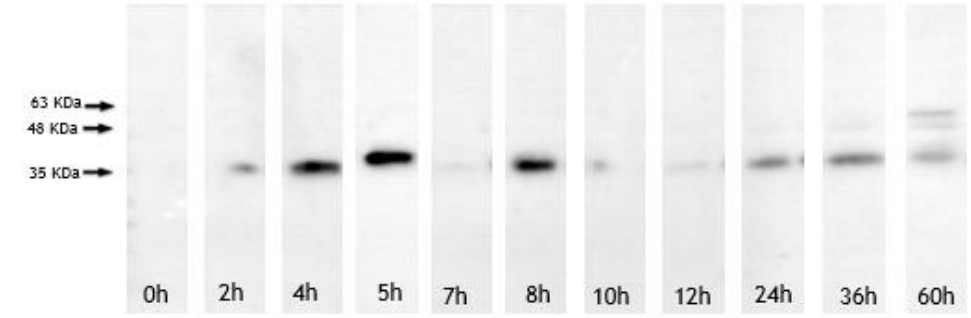

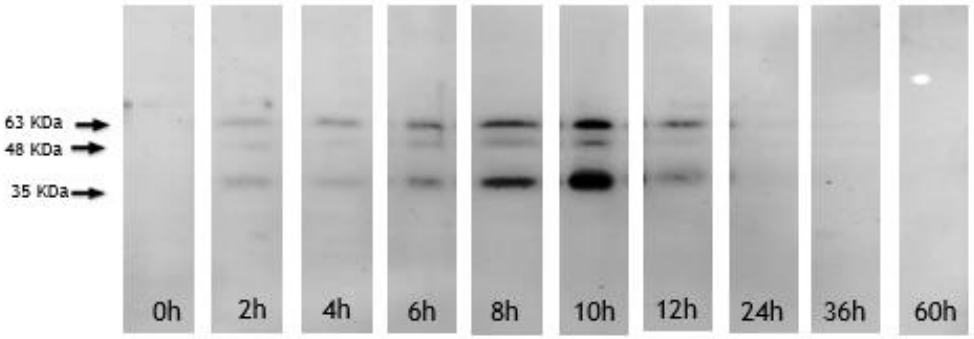

Appendix 2: **SDS-PAGE of the Constant, Exponential and Gradient glycerol feed profiles tested, respectively.**

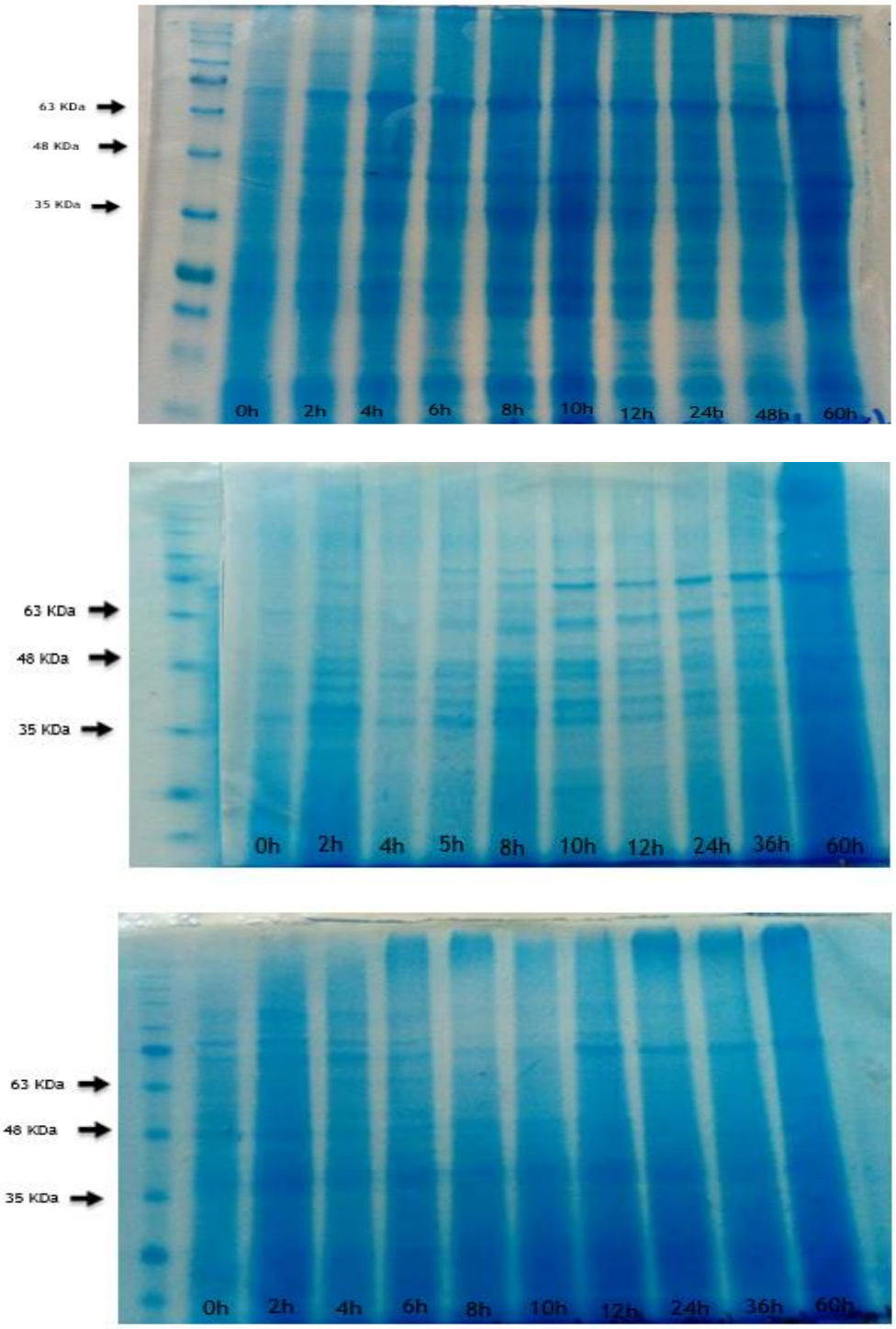

<u>Appendix 3:</u> Alteration of fermentation conditions (Replicate of the different concentrations of Proline, Histidine, and Trehalose, respectively.)

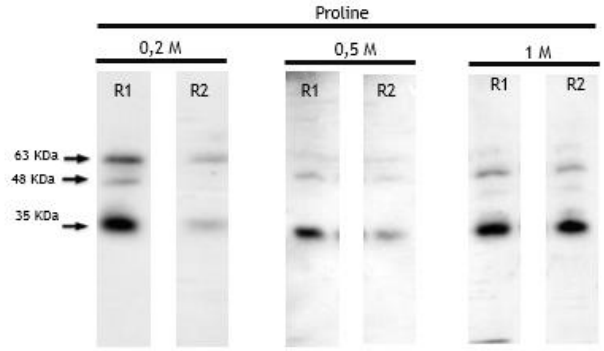

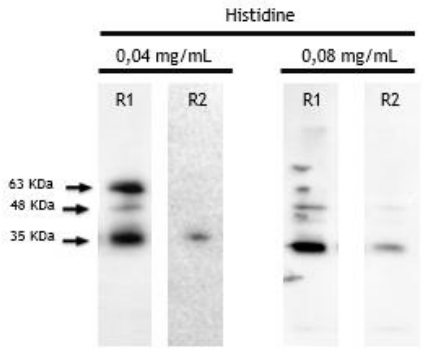

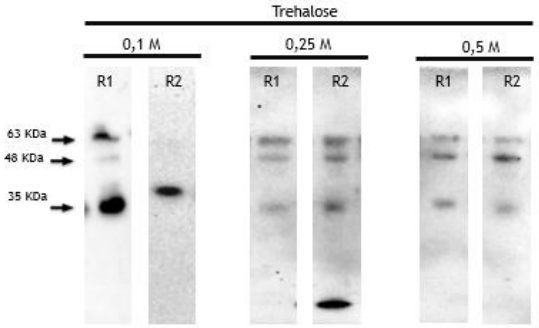

Appendix 4: **Alteration of fermentation conditions (Replicate of the exponential methanol feeding tested for exponential and gradient glycerol feed, respectively.)**

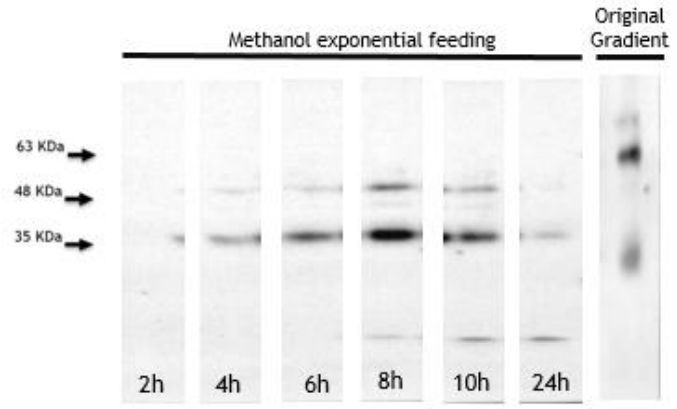

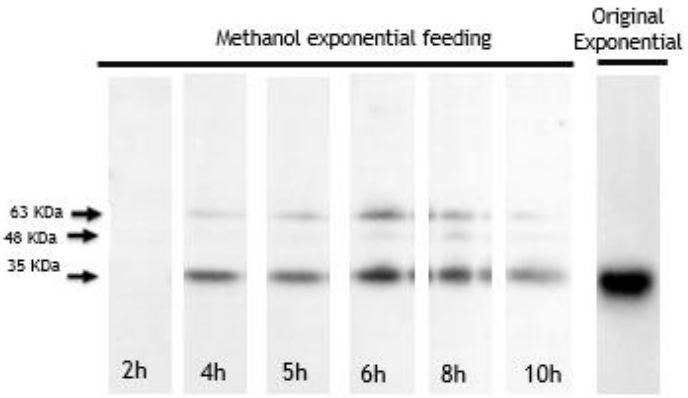

Appendix 5: **Poster presentation at** the II International Congress on Health Sciences

Research towards Innovation and entrepreneurship: Trends in Biotechnology for Biomedical Application, Covilhã (2017): Duarte DR, Pedro AQ, Maia CJ, Passarinha LA, Improvement of STEAP1 biosynthesis from Pichia Pastoris X33 cells under an optimized strategy.

CICS-UBI
Centro de Investigação em Ciências da Saúde
Health Sciences Research Centre

FACULDADE CIÊNCIAS DA SAÚDE

Improvement of STEAP1 biosynthesis from *Pichia pastoris* X33 cells under an optimized feeding strategy

Duarte D.R.[1], Pedro A.Q.[1,2], Maia C.J.[1], Passarinha L.A.[1]

[1] CICS-UBI – Health Sciences Research Centre, University of Beira Interior, Covilhã, Portugal; [2] CICECO – Aveiro Institute of Materials, Chemistry Department, University of Aveiro, 3810-193, Aveiro, Portugal.

Introduction

The Six-Transmembrane epithelial antigen of prostate 1 (STEAP1) is the first member of STEAP family(1 to 4) that share significant similarity although different functions[1,2]. STEAP1 is a 39 kDa protein, located in the plasmatic membrane, namely in tight or gap junctions[1-4]. Its structure and cellular location suggest that it may act as an ion channel, that contributes to metal homeostasis, stimulating cancer cell proliferation and tumor invasiveness [1-3]. STEAP1 is a immunogenic target since is overexpressed in several types of human cancer tissues, namely in all stages of prostate cancer [1-4].

Aim

The aim of this work is to perform the scale-up of STEAP1 biosynthesis from mini-bioreactor *P. pastoris* cultures.

This is achieved through the optimization of culture conditions under different glycerol feeding strategies (exponential, gradient and constant) in the fed-batch phase.

Methodology

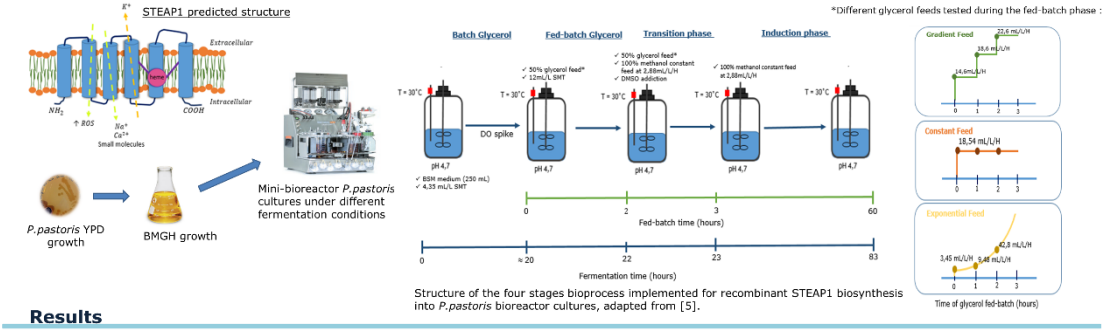

Structure of the four stages bioprocess implemented for recombinant STEAP1 biosynthesis into *P.pastoris* bioreactor cultures, adapted from [5].

Results

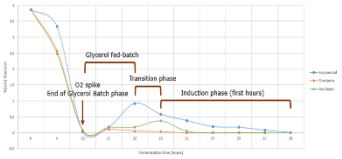

Figure 1 - Glycerol levels by HPLC-RID for each feed studied until full exhaustion.

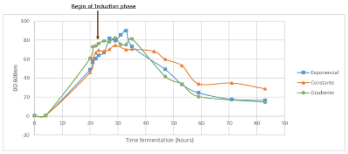

Figures 2 - OD_{600nm} over 60 hours of methanol induction in the different feeds tested.

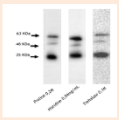

Figure 5- WB of STEAP1 production by testing different chaperones in the glycerol gradient feed.

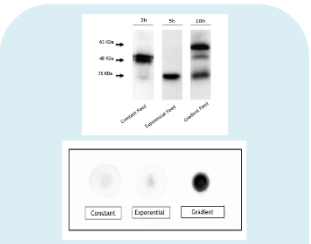

Figure 3 and 4 - WB and Dot Blot analysis of STEAP1 production by testing different glycerol feedings during the 3 hours of the fed-batch phase.

Conclusions

✓ High quantities of STEAP1 were obtained with exponential and gradient feeds of glycerol by 5 and 10 hours of methanol induction, respectively.

✓ Medium supplementation with Histidine, Trehalose and Proline enhances the biosynthesis of STEAP1 in the correct molecular weight and contributes to protein stabilization with less aggregation.

Abbreviations

BSM- Modified basal salts medium; DMSO- Dimethylsulfoxide; HPLC-RID- High-performance Liquid Chromatography coupled to a refractive index detection; *P.pastoris- Pichia pastoris X33*; SMT- Trace metal solution; STEAP1 – Six Transmembrane Epithelial Antigen of the Prostate 1; WB – Western Blot.

References

[1] Gomes IM et al, Mol. Cancer Res.,2012;10:573–87;[2] Grunewald TGP et al,Biol.Cell.,2012;104:641–57;[3] Ohgami RS et al,Blood, 2006;108:1388–94; [4] Barroca-FerreiraJ et al, Curr.Cancer Drug Targets, 2017;9;[5] Pedro AQ et al., Microb.Cell Fact.,2015;14:113.

FCT COMPETE 2020 PORTUGAL 2020

Poster presentation at the 9th Conference on Recombinant Protein Production, Croatia (2017): Barroca-Ferreira J, Pais JP, Santos MM, **Duarte DR**, Pedro AQ, Maia CJ, Passarinha LA, Evaluation of *Escherichia coli* and *Pichia pastoris* host in the biosynthesis of STEAP1: a membrane therapeutic target for prostate cancer.

CICS-UBI
Centro de Investigação em Ciências da Saúde
Health Sciences Research Centre

FACULDADE CIÊNCIAS DA SAÚDE

EVALUATION OF *ESCHERICHIA COLI* AND *PICHIA PASTORIS* HOSTS IN THE BIOSYNTHESIS OF STEAP1: A MEMBRANE THERAPEUTIC TARGET FOR PROSTATE CANCER

Barroca-Ferreira J.[1], Pais J.P.[1], Santos M.M.[1], Duarte D.R.[1], Pedro A.Q.[1,2], Maia C.J.[1], Passarinha L.A.[1]

[1] CICS-UBI – Health Sciences Research Centre, University of Beira Interior, Covilhã, Portugal; [2] CICECO – Aveiro Institute of Materials, Chemistry Department, University of Aveiro, 3810-193, Aveiro, Portugal.

Introduction

- STEAP1 is overexpressed in prostate cancer and it is preferentially located in tight or gap junctions [1]. Considering the transmembrane topology and cellular localization, STEAP1 may play an important role as a transport protein and/or in intercellular communication [2].
- An overexpression of STEAP1 enhances cancer cell proliferation and contributes to tumor progression and aggressiveness which strengths the usefulness of STEAP1 as therapeutic target [3, 4].
- Our goal was to implement a novel platform capable to produce high levels of $STEAP1_{1-142}$ and STEAP1 full length protein for further application in bio-interaction and structural studies.

Methodology

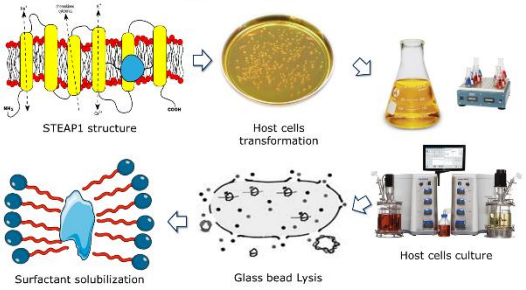

Results

$STEAP1_{1-142}$ in *E. coli* cells

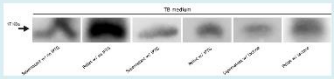

Figure 1. WB analysis of $STEAP1_{1-142}$ production in TB medium in presence of lactose and IPTG (1 mM). Control experiments were performed with non-induced cultures.

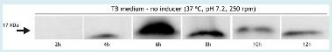

Figure 2. WB analysis of $STEAP1_{1-142}$ production in TB omitting the addition of an inducer, over 12h at 37ºC, pH 7.2 and 250 rpm operational settings.

STEAP1 full length in *E. coli* cells

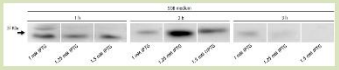

Figure 3. WB analysis of STEAP1 production in SOB medium in presence IPTG at different concentrations.

Figure 4. WB analysis of STEAP1 production in SOB medium in presence of 1.25 mM IPTG, evaluating the effect of several chaperone molecules at 37 ºC, pH 7.8 and 250 rpm.

STEAP1 full length in *P. pastoris* cells (Shake Flask)

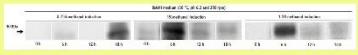

Figure 5. WB analysis of STEAP1 production in BMMH medium by testing different methanol concentrations, as inducer at 30ºC, pH 6.0 and 250 rpm operational settings.

STEAP1 full length in *P. pastoris* cells (Bioreactor)

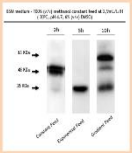

Figure 6. WB analysis of STEAP1 production in BSM medium by testing different glycerol feedings during the 3 hours of the fed-batch phase, with 100% (v/v) methanol at 2,9 mL/L/H, 30ºC, pH 4.7 and 6% (v/v) DMSO.

Conclusions

Best operating conditions for $STEAP1_{1-142}$ and STEAP1 biosynthesis in the different expression systems:

	Media formulation	Operational conditions	Inducer	Chaperone molecules	Surfactant
$STEAP1_{1-142}$ *(E. coli)*	TB (8 h fermentation period)	37 ºC pH 7.2 250 rpm	-----	-----	1 % (v/v) Triton X-100
$STEAP1_{full\ length}$ *(E. coli)*	SOB (7 h fermentation period)	37 ºC pH 7.8 250 rpm	1.25 mM IPTG (at 5 h fermentation)	1 % (v/v) DMSO	1 % (v/v) Triton X-100

	Media formulation	Operational conditions	Inducer	Chaperone molecules	Surfactant
$STEAP1_{full\ length}$ *(P. pastoris)* Shake flask	BMMH (6 h fermentation period)	30 ºC pH 6.0 250 rpm	1.25 % (v/v) Methanol	6 % (v/v) DMSO	1 % (v/v) SDS
$STEAP1_{full\ length}$ *(P. pastoris)* Bioreactor	BSM (28 h fermentation period)	30 ºC pH 4.7 *	100 % (v/v) Methanol**	6 % (v/v) DMSO	1 % (v/v) SDS

* 50%(v/v) glycerol exponential feed during the fed-batch phase.
** 100%(v/v) methanol constant feed at 2,9mL/L/H during 5h of induction.

Abbreviations

BMMH- Buffered Minimal Methanol; BSM- Modified basal salts medium; DMSO- Dimethylsulfoxide; *E.coli- Escherichia coli*; H – Hours; *P. pastoris- Pichia pastoris* X33; SOB – Super Optimal Broth; SOC – SOB with Catabolite Repression; STEAP1 – Six Transmembrane Epithelial Antigen of the Prostate 1; $STEAP1_{1-142}$ – STEAP1 first extracellular loop; TB – Terrific Broth; WB – Western Blot.

References

[1] Hubert RS *et al.*, Prod Natl Acad Sci, 1999, 10:14523-14528
[2] Yamamoto T *et al.*, Exp Cell Res, 2013, 319:2617-2626
[3] Gomes IM *et al.*, Urol Oncol, 2014, 32:23-29
[4] Gomes IM *et al.*, Protein Exp Purif, 2012, 62:1-8

FCT COMPETE 2020 PORTUGAL 2020